

A THEORY OF DROPWISE CONDENSATION

A THESIS SUBMITTED TO
THE GRADUATE SCHOOL OF NATURAL AND APPLIED SCIENCES
OF
MIDDLE EAST TECHNICAL UNIVERSITY

BY

HASAN FEHMİ TEKİN

IN PARTIAL FULFILLMENT OF THE REQUIREMENTS
FOR
THE DEGREE OF MASTER OF SCIENCE
IN
MECHANICAL ENGINEERING

DECEMBER 2005

Approval of the Graduate School of Natural and Applied Sciences

Prof. Dr. Canan ÖZGEN
Director

I certify that this thesis satisfies all the requirements as a thesis for the degree of Master of Science.

Prof. Dr. Kemal İDER
Head of the Department

This is to certify that we have read this thesis and that in our opinion it is fully adequate, in scope and quality, as a thesis for the degree of Master of Science.

Assoc. Prof. Dr. Cemil YAMALI
Supervisor

Examining Committee Members

Prof. Dr. Kahraman ALBAYRAK (METU,ME) _____

Assoc. Prof. Dr. Cemil YAMALI (METU,ME) _____

Asst. Prof. Dr. İlker TARI (METU,ME) _____

Asst. Prof. Dr. Tahsin ÇETİNKAYA(METU,ME) _____

Prof. Dr. Ercan ATAER (GAZİ UNV.,ME) _____

I hereby declare that all information in this document has been obtained and presented in accordance with academic rules and ethical conduct. I also declare that, as required by these rules and conduct, I have fully cited and referenced all material and results that are not original to this work.

Hasan Fehmi TEKİN

Signature:

ABSTRACT

A THEORY OF DROPWISE CONDENSATION

Tekin, Hasan Fehmi

M.S., Department of Mechanical Engineering

Supervisor: Assoc. Prof. Dr. Cemil Yamalı

December 2005, 167 pages

In this study, the effect of the substrate material on dropwise condensation was studied theoretically. Temperature distribution in the material was obtained by using the finite difference method for different substrate materials and drop radii and FORTRAN computer program was used for this purpose.

A computer program in Mathcad was also written to calculate heat transfer and heat flux for a single drop at various substrate materials and drop radii. After finding heat transfer and heat flux through droplets of various sizes, total dropwise condensation heat transfer and heat flux were calculated by integrating the heat transfer through droplets with respect to the size distribution of the droplet population. Substrate material effect in temperature distribution and heat transfer were presented as tables, graphs and were discussed. Average temperature at the base

of single droplet was obtained, then using the dropsize distribution the overall average temperature of the condenser surface in dropwise condensation was obtained for various substrate material. Finally overall average surface temperature and total dropwise condensation heat flux was used to calculate heat transfer coefficient in dropwise condensation as a function of thermal properties of the substrate material.

Major finding of this study is that the thermal conductivity of the substrate material effects to the dropwise condensation heat transfer coefficient and at low substrate thermal conductivity dropwise condensation heat transfer coefficient is lower.

Numerical results were compared with results in literature.

Keywords: Dropwise condensation, dropsize distribution, theoretical study, substrate material effect.

ÖZ

DAMLACIK YOĞUŞMASI TEORİSİ

Tekin, Hasan Fehmi

Yüksek Lisans, Makine Mühendisliği Bölümü

Tez Yöneticisi: Doç. Dr. Cemil Yamalı

Aralık 2005, 167 sayfa

Bu çalışmada yoğuşma yüzeyinin damlacık yoğuşması üzerindeki etkisi teorik olarak incelenmiştir. Malzemedeki sıcaklık dağılımı sonlu farklar metodu kullanılarak değişik yoğuşma yüzeyi malzemeleri ve damla yarıçapları için elde edilmiştir ve bu amaç için bilgisayar programı FORTRAN kullanılmıştır.

Tek bir damlacıktan geçen ısı transferi ve ısı akısını farklı yoğuşma yüzeyleri ve damla yarıçapları için hesaplamak amacıyla Mathcad'de de bir program yazılmıştır. Tek bir damla tabanındaki ortalama sıcaklık bulunmuş, daha sonra damlacık dağılımı kullanılarak farklı yoğuşma yüzeyi malzemeleri için damlacık yoğuşmasındaki yoğuşma yüzeyinin ortalama sıcaklığı elde edilmiştir. Isı transferi ve ısı akısını çeşitli boyutlardaki damlalar için bulduktan sonra, toplam damlacık yoğuşması ısı transferi ve ısı akısı damla dağılımına göre entegre edilerek hesaplanmıştır. Son olarak toplam yüzey sıcaklığı ve damlacık yoğuşması toplam ısı akısı; damlacık yoğuşmasındaki ısı transferi katsayısını yoğuşma yüzeyi

malzemesinin termal özellikleri fonksiyonu olarak hesaplamak amacıyla kullanılmıştır. Yoğuşma malzemesi yüzeyinin sıcaklık dağılımına ve ısı transferine olan etkisi tablolar, grafiklerle gösterilmiş ve yorumlanmıştır.

Bu çalışmanın en büyük sonucu yoğuşma yüzeyi malzemesinin damlacık yoğuşması ısı transferi katsayısına olan etkisi ve düşük termal iletkenli yoğuşma yüzeylerde damlacık yoğuşması ısı transferi katsayısının daha düşük olmasıdır.

Nümerik sonuçlar literatürdeki sonuçlarla karşılaştırılmıştır.

Anahtar Kelimeler: Damlacık yoğuşması, damlacık dağılımı, teorik çalışma, yoğuşma yüzeyi malzemesinin etkisi.

To my parents ,
who always support me in all aspects of my life

ACKNOWLEDGMENTS

I express my sincere appreciation to Assoc. Prof. Dr. Cemil Yamalı for his guidance, support, understanding and valuable contributions throughout the study. I am grateful to the jury members for their valuable contributions.

I express my deepest gratitude to my mother Hasine Tekin, my father M. Şükrü Tekin, my brothers and my sister, for their endurance and for their encouragements throughout my education life.

TABLE OF CONTENTS

PLAGIARISM	iii
ABSTRACT.....	iv
ÖZ	vi
ACKNOWLEDGMENT.....	ix
TABLE OF CONTENTS	x
LIST OF FIGURES	xiii
LIST OF TABLES	xvii
LIST OF SYMBOLS	xviii

CHAPTER

1. INTRODUCTION	1
1.1 Condensation.....	1
2. LITERATURE SURVEY	4
2.1 Dropsize Distribution	5
2.2 Heat Transfer Through the Droplet.....	9
2.3 The Effect of Surface Thermal Properties and Finish on Dropwise Condensation.....	10
2.4 Substrate Effect	11
2.5 Effect of Noncondensable Gases	22
2.6 Promoting Dropwise Condensation	24
3. MATHEMATICAL ANALYSIS	31
3.1 Mathematical Modeling of Dropwise Condensation with Substrate Material Effect	33
3.1.1 Temperature Distribution.....	33

3.1.2 Conduction Equations and Boundary Conditions Through a Single Droplet	36
3.1.3 Average Temperature Under the Droplet.....	51
3.1.4 Heat Transfer and Heat Flux	52
3.2 Finite Difference Solution of Dropwise Condensation with Substrate Material Effect	54
3.2.1 Temperature Distribution in the Substrate and Under the Droplet	54
3.2.2 Average Temperature Under the Droplet.....	62
3.2.3 Total Heat Transfer and Heat Flux in Dropwise Condensation.....	63
3.2.4 Dropwise Condensation Heat Transfer Coefficient	66
4. RESULTS AND DISCUSSIONS	67
4.1 Computation Results for the Temperature Distribution Under the Droplet and in the Substrate	67
4.1.1 Temperature Distribution Under a Single Droplet and Substrate Material	68
4.1.2 Average Temperature.....	74
4.2 Computation Results for the Heat Transfer in Dropwise Condensation Including the Substrate Effect.....	78
4.2.1 Effect of Droplet Radius on Heat Transfer and Heat Flux for a Single Droplet	79
4.2.2 Effect of Substrate Material on Heat Transfer and Heat Flux	80
4.3 Dropwise Condensation Heat Transfer Coefficient	90
4.4 Comparison of Numerical Results with the Results in the Literature.....	92
4.4.1 Comparison of Heat Transfer Coefficient.....	92
5. CONCLUSIONS	97
REFERENCES	98

APPENDICES

A. FORTRAN SOURCE PROGRAM.....	106
B. NONDIMENSIONAL RADIAL AND AXIAL DIRECTION.....	116
C. FORMULATION	118

D. MATHCAD SOURCE PROGRAM.....	120
E. RESULTS FOR TEMPERATURE DISTRIBUTIONS.....	126
F. RESULTS FOR HEAT TRANSFER AND HEAT FLUX	145

LIST OF FIGURES

FIGURE

1.1	Condensation on a vertical surface. (a) Dropwise. (b) Filmwise.	3
2.1	Comparison of drop distribution between random fractal model and photography	7
2.2	Effect of substrate material and pressure on heat transfer coefficient	13
2.3	Initial dropwise condensation on copper-nickel coated with No-Stick (left) and Nedox	26
2.4	Dependence of heat flux on coolant velocity. Different symbols denote different test runs. + x * z, unplated tubes; \bullet Δ \square \diamond , copper plated tubes	27
3.1	Droplet resting on a semi infinite substrate material	33
3.2	Thermal resistances associated with the drop	37
3.3	Physical model of thermal resistance R_c	42
3.4	Overall heat transfer coefficient under the droplet and bare area	46
3.5	Temperature nodes under the drop and in the substrate.....	56
4.1	Variation of nondimensional temperature as a function of nondimensional radial distance at nondimensional axial distance $\tilde{z} = 0$ for $B=0.001$	69
4.2	Variation of nondimensional temperature as a function of nondimensional radial distance at nondimensional axial distance $\tilde{z} = 0$ for $B=0.001$	70
4.3	Variation of nondimensional temperature as a function of nondimensional radial distance at nondimensional axial distance $\tilde{z} = 9.99 \times 10^{-5}$ for $B=0.001$	71
4.4	Variation of nondimensional temperature as a function of nondimensional radial distance at nondimensional axial distance $\tilde{z} = 9.99 \times 10^{-5}$ for $B=0.001$	72
4.5	Variation of average nondimensional condenser surface temperature at the drop base area as a function of drop radius for $A=100$	74

4.6	Variation of average nondimensional condenser surface temperature with B.	75
4.7	Variation of average nondimensional condenser surface temperature with A	76
4.8	Variation of dropwise condensation average nondimensional temperature with A	77
4.9	Variation of heat transfer with drop radius for A=1	79
4.10	Variation of heat flux with drop radius for A=1	80
4.11	Variation of Q_{nd} with A for B=0.001	81
4.12	Variation of Q with A for B=0.001	82
4.13	Variation of nondimensional resistance parameter with nondimensional drop radius for B=0.001 and A=1	83
4.14	Variation of heat transfer with A for $r=2.11 \times 10^{-4}$ m.....	84
4.15	Variation of heat flux with A for $r=2.11 \times 10^{-4}$ m.....	84
4.16	Variation of nondimensional heat transfer (Q_{nd}) with B and A	85
4.17	Variation of dimensional heat transfer (Q) with B and A.....	86
4.18	Variation of heat flux (Q'') with B and A	87
4.19	Variation of total dropwise condensation heat transfer (Q_{dc}) with A	88
4.20	Variation of total dropwise condensation heat flux (Q''_{dc}) with A	89
4.21	Variation of total dropwise condensation heat flux (Q''_{dc}) with A	90
4.22	Variation of dropwise condensation heat transfer coefficient with A.....	91
4.23	Comparison of heat transfer coefficients between the present study and Tanaka et. al [33]	93
4.24	Comparison of heat transfer coefficients between the present study and Tsuruta and Tanaka study [61]	94
4.25	Comparison of heat transfer coefficients between the present study and literature	95
4.26	Comparison of heat transfer coefficients between the present study and Yu Ting Wu et. al. study [17]	96
E.1	Variation of nondimensional temperature as a function of nondimensional radial distance at nondimensional axial distance $\tilde{z} = 0$ for B=0.01.....	130
E.2	Variation of nondimensional temperature as a function of nondimensional radial distance at nondimensional axial distance $\tilde{z} = 0$ for B=0.01.....	131

E.3	Variation of nondimensional temperature as a function of nondimensional radial distance at nondimensional axial distance $\tilde{z} = 0$ for $B=0.1$	132
E.4	Variation of nondimensional temperature as a function of nondimensional radial distance at nondimensional axial distance $\tilde{z} = 0$ for $B=0.1$	133
E.5	Variation of nondimensional temperature as a function of nondimensional radial distance at nondimensional axial distance $\tilde{z} = 0$ for $B=1$	134
E.6	Variation of nondimensional temperature as a function of nondimensional radial distance at nondimensional axial distance $\tilde{z} = 0$ for $B=1$	135
E.7	Variation of nondimensional temperature as a function of nondimensional radial distance at nondimensional axial distance $\tilde{z} = 0$ for $B=10$	136
E.8	Variation of nondimensional temperature as a function of nondimensional radial distance at nondimensional axial distance $\tilde{z} = 0$ for $B=10$	137
E.9	Variation of nondimensional temperature as a function of nondimensional radial distance at nondimensional axial distance $\tilde{z} = 0$ for $B=100$	138
E.10	Variation of nondimensional temperature as a function of nondimensional radial distance at nondimensional axial distance $\tilde{z} = 0$ for $B=100$	139
E.11	Variation of average nondimensional condenser surface temperature at the drop base area as a function of drop radius for $A=1$	143
E.12	Variation of average nondimensional condenser surface temperature at the drop base area as a function of drop radius for $A=0.01$	144
F.1	Variation of heat transfer with drop radius for $A=0.01$	148
F.2	Variation of heat flux with drop radius for $A=0.01$	149
F.3	Variation of heat transfer with drop radius for $A=100$	150
F.4	Variation of heat flux with drop radius for $A=100$	151
F.5	Variation of Q_{nd} with A for $B=0.01$	155
F.6	Variation of Q with A for $B=0.01$	156
F.7	Variation of Q_{nd} with A for $B=0.1$	157
F.8	Variation of Q with A for $B=0.1$	158
F.9	Variation of Q_{nd} with A for $B=1$	159
F.10	Variation of Q with A for $B=1$	160
F.11	Variation of Q_{nd} with A for $B=10$	161

F.12 Variation of Q with A for B=10.....	162
F.13 Variation of Q_{nd} with A for B=100.....	163
F.14 Variation of Q with A for B=100.....	164
F.15 Variation of heat transfer with A for $r=4.22 \times 10^{-6}$ m	166
F.16 Variation of heat flux with A for $r=4.22 \times 10^{-6}$ m	167

LIST OF TABLES

TABLE

2.1 Investigations into the surface thermal conductivity effect in dropwise condensation	16
2.2 Steam side heat transfer coefficients	26
2.3 Condensation mode criteria	30
4.1 Dropwise condensation average nondimensional temperature data	77
4.2 Variation of total dropwise condensation heat transfer (Q_{dc}) and total dropwise condensation heat flux (Q''_{dc}) data.....	88
4.3 Dropwise condensation heat transfer coefficient data	91
B.1 Variation of nondimensional radial distance rr_i	116
B.2 Variation of nondimensional axial distance z_j	117
E.1 Variation of temperature at $\tilde{z} = 0$ for $B=0.001$	126
E.2 Variation of temperature at $\tilde{z} = 9.99 \times 10^{-5}$ for $B=0.001$	128
E.3 The data of average temperature.....	140
F.1 The data and results of heat transfer and heat flux	145
F.2 The data and results of nondimensional heat transfer (Q_{nd})	152
F.3 Variation of nondimensional drop resistance for $B=0.001$ and $A=1$	165

LIST OF SYMBOLS

C_p	Specific heat at constant pressure	[J/(kgK)]
T_s	Surface temperature	
T_d	Temperature distribution in the droplet	
T_{in}	Initial temperature in the substrate material	
T_{dsur}	Surface temperature of droplet	
\tilde{T}_s	Nondimensional surface temperature	
\bar{z}	Axial direction	
\bar{r}	Radial direction	
h_i	Interfacial heat transfer coefficient	[W/(m ² K)]
h_{fg}	Latent heat of evaporation	[J/kg]
A	Nondimensional parameter	
B	Nondimensional parameter	
k_s	Substrate thermal conductivity	[W/(mK)]
k_d	Water thermal conductivity	[W/(mK)]
r	Drop radius	[m]
\tilde{r}	Nondimensional drop radius	
\tilde{z}	Nondimensional axial distance	
T	Temperature	[K]

\tilde{T}	Nondimensional temperature	
f_{co}	Fraction of area	
P_v	Vapor pressure	[N/m ²]
σ	Surface tension	
h	Heat transfer coefficient	[W/m ² K]
dt	Time	[sec]
γ	Condensation Coefficient	
F_r	Nondimensionless drop resistance	
ρ_s	Density of substrate	[kg/m ³]
ρ_l	Density of liquid	[kg/m ³]
Θ	Contact angle	[rad]
U	Overall heat transfer coefficient	[W/(m ² K)]
ΔT	Temperature difference	[K]
T_v	Vapor temperature	[K]
T_i	Temperature of liquid-vapor interface	[K]
Q_{num}	Numerical heat transfer	
Q_{nd}	Nondimensional heat transfer	
Q	Heat transfer rate	[W]
Q''	Heat flux	[W/m ² K]
R_i	Interfacial heat transfer resistance	[(m ² K)/W]
R_c	Condensate thermal resistance	[(m ² K)/W]
R_t	Total thermal resistance	[(m ² K)/W]
R_c^*	Constriction resistance	[(m ² K)/W]

\bar{A}	Area	[m ²]
G	Gas Constant	[J/kg.K]

Subscripts

dc	Dropwise condensation
ad	Average dropwise condensation
av	Average
max	Maximum
min	Minimum

CHAPTER 1

INTRODUCTION

1.1 Condensation

Condensation is defined as the phase change from the vapor state to the liquid or the solid state and occurs when the temperature of the vapor is reduced below its saturation temperature. Condensation is usually done by bringing the vapor into contact with a solid surface whose temperature is below the saturation temperature of the vapor. But condensation can also occur on the free surface of a liquid or even in a gas when the temperature of the liquid or the gas to which the vapor is exposed is below the saturation temperature.

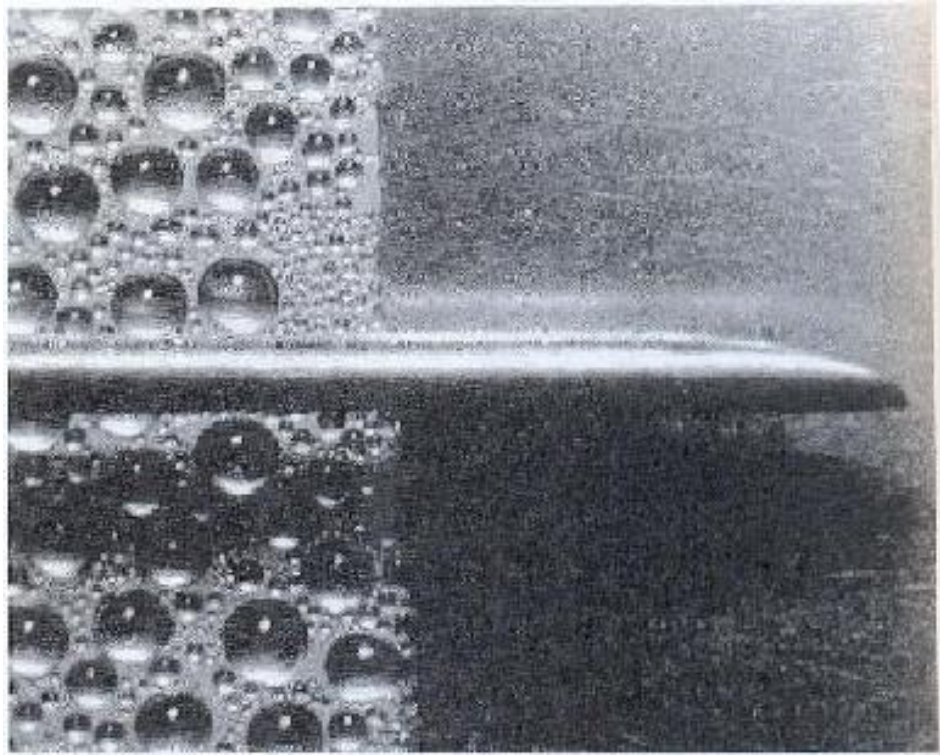
Condensation is classified into two groups; one is bulk condensation and the other is surface condensation. In bulk condensation vapor condenses in a gas phase. Formation of fog is an example of this type of condensation. Surface condensation occurs when the vapor contacts with a surface whose temperature is below the saturation temperature of the vapor. There are a lot of application with this type of condensation. Surface condensation is classified as filmwise condensation and dropwise condensation.

Filmwise condensation occurs when the liquid wets the surface and the condenser surface is blanket by a condensate film. Liquid film on the surface that slides down under the influence of gravity. The thickness of the liquid film increases in the flow direction as more vapor condenses on the film. This liquid film represents

a thermal resistance to heat transfer and a temperature gradient exists in the film. The analytical investigation of film condensation was first performed by Nusselt.

In dropwise condensation the condensed vapor forms droplets on the surface instead of continuous film and the surface is covered by several droplets of varying diameters. In dropwise condensation, the small droplets that form at the nucleation sites on the surface grow as a result of continued condensation, coalescence into large droplets and slide down when they reach a certain size, clearing the surface and exposing it to vapor. There is no liquid film in this case to resist heat transfer. As a result, with dropwise condensation heat transfer coefficients can be achieved that are more than 10 times larger than those associated with filmwise condensation. Large heat transfer coefficients enable designers to achieve a specified heat transfer rate with a smaller surface area and thus a smaller and less expensive condenser. Therefore, dropwise condensation is the preferred mode of condensation in heat transfer applications. However, it is very difficult to obtain dropwise condensation since it does not continue long time and converts to filmwise condensation after a while.

Dropwise condensation is achieved by adding a promoting chemical into the vapor, treating the surface with a promoter chemical or coating the surface with a polymer such as teflon or a noble metal such as gold, silver and platinum. The promoters used include various waxes and fatty acids such as oleic or lionic acids. They lose their effectiveness after a while, however because of fouling, oxidation and removal of the promoter from the surface. It is possible to sustain dropwise condensation for a long time by the combined effects of surface coating and periodic injection of the promoter into the vapor. However, any gain in heat transfer must be weighed against the cost associated with sustaining dropwise condensation. Another reason of losing the effectiveness of dropwise condensation is the accumulation of droplets on the condenser surface. Heat transfer rate sharply decreases because of the accumulated droplets. Therefore, most condensers are designed on the assumption that film condensation will take place on the surface.



(a)

(b)

Figure 1.1 Condensation on a vertical surface. (a) Dropwise. (b) Filmwise

CHAPTER 2

LITERATURE SURVEY

Considerable interest in dropwise condensation has been aroused since the discovery by Schmidt et al. [2] of this second “ideal” mode of condensation. The report by the above authors in 1930, that the heat transfer coefficient associated with the dropwise mode was substantially higher than that found in the presence of filmwise condensation and the potential industrial significance of this, have stimulated this interest.

A basic understanding of the mechanism of dropwise condensation requires a knowledge of how the drops form and grow. Jakob [3] proposed that very thin layer of steam or water rapidly develops on the surface, breaking into droplets after a certain thickness is reached; a new film immediately appears over the exposed area. This would explain the high heat transfer coefficients observed, since condensation would be taking place on a thin film having a low resistance to heat transfer. Jakob’s view was later supported by Baer and McKelvey [4] and by Welch and Westwater [5].

An opposing view was proposed by Tammann and Boehme [6] who observed that, upon repetitive condensation, drops appear to have the same arrangement on the surface, suggesting the existence of particular nucleation sites. This observation was substantiated by McCormick and Baer [7,8] whose experimental study of drop

formation and growth indicates that drops nucleate from randomly distributed sites and that these sites are probably pits and grooves in the surface.

Umur and Griffith [9] indicated that a film does not develop on the surface as the surface is cooled to below the vapor temperature. And also the film behind the drops rolling over the surface does not happen. Rolling drops leave behind them at most a monolayer. They concluded that no film greater than a monolayer in thickness exists on the area between the drops and that no net condensation takes place on this area.

In dropwise condensation, primary drops are first formed at nucleation sites. These grow by condensation until coalescence occurs between neighbours. The coalesced drops continue to grow and new ones to form and grow at sites exposed through coalescence. As the process continues, coalescences occur between drops of various sizes while the size of the largest drops present continues to increase. A situation is soon reached where the largest drops present appear more or less uniform in size and spacing. This situation persists as these largest drops grow and their number per area decreases until they reach a size at which the region is again swept.

In brief, most of the studies clearly show that formation of droplets occurs as a result of nucleation and no film formation between droplets takes place.

2.1 Dropsize Distribution

The rational solution of any heat transfer problem begins with the definition of the geometry. For dropwise condensation this means that the dropsize distribution must be specified.

In dropwise condensation high magnification visual observations of the condensation process show that there are drops of different size on the condenser surface with various diameters. Viewing any single spot on the surface, the drop size will vary in a steady and unsteady way, caused by condensation on the drops and by

coalescence. The surface temperature of the condenser change with the size of drops on it, causing fluctuations of the surface temperature.

P. Griffith and C. Graham [10] used a Polaroid microscope camera at a variety of magnifications to measure the drop distributions. They found 200×10^6 sites/cm² nucleation densities.

J. W. Rose and L. R. Glicksman [11] thought that while considerable progress has been made on the problem of calculating the heat transfer through a single drop of given size, the problem of the distribution of drop sizes is less well understood. In attempting to calculate the average heat transfer rate, different workers have dealt with the problem of the dropsize distribution in a variety of ways, Fatica and Katz [12] and Sugawara and Michiyoshi [13] assumed that on a given area all drops have the same size, are uniformly spaced and grow by condensation at their surfaces. Wenzel [14] assumed that drops grow in uniform square array and that coalescences occur between four neighbouring drops to form a larger drop in a new uniform square. Gose, Mucciardi and Baer [15] and more recently, Tanasawa and Tachibana [16] have attempted partially to model the drop growth and coalescence process by computer. The major problem here was the large time requirement to model the process adequately. In the study of J. W. Rose and L. R. Glicksman [11] the theoretical distribution of drop sizes relates to a particular small region of the condensing surface. Since falling drops sweep diverging tracks, the lower regions of the surface are swept more frequently and consequently largest generation of drops decreases with distance down the surface. In general, to determine the size distribution over a relatively large area, it would be necessary to determine the dependence of largest generation of drops on location and to integrate for the whole region. When considering larger areas it should also be noted that the theory does not include falling drops.

Yu-Ting Wu et al. [17] made a theoretical study in dropwise condensation. They insisted that dropwise condensation consists of the transient processes occurring repeatedly on the condensing surface. In the process, primary drops are

formed at nucleation sites, then coalescence occurs between neighboring drops with the drops growth. A new generation of drops is formed at sites exposed by coalescence. These again grow to be followed by a third generation and so on until a falling drop sweeps the entire field and the process restarts. They simulated random fractal model, dropsize and spatial distributions. They find the photographs of dropwise condensation taken at different instants or in different scales are similar and a whole photograph can be obtained by enlarging properly a local photograph. This characteristic indicates that dropwise condensation appears self-similar, which is one of the most important features of fractals. In addition, drop spatial distribution also possesses randomness. The random fractal model and a condensing photograph are given in Fig. 2.1.

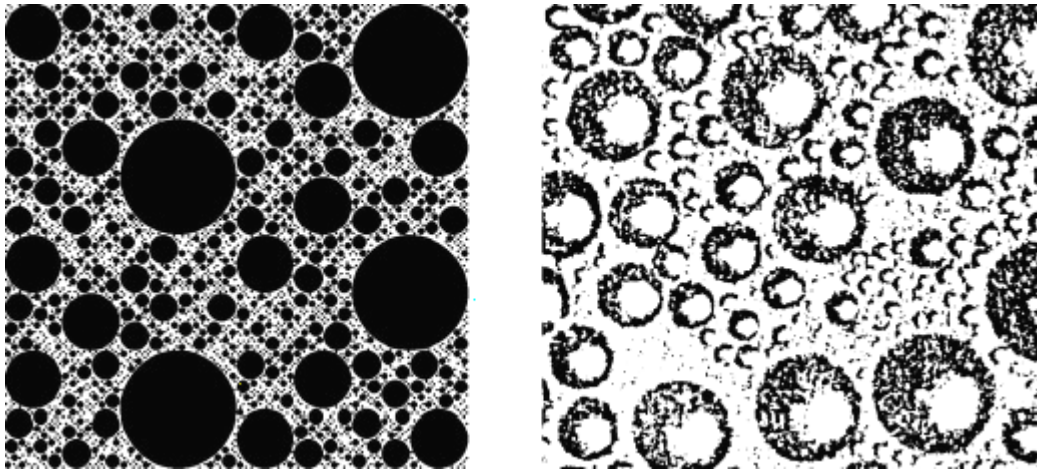


Figure 2.1 Comparison of drop distribution between random fractal model and photography (a- Drop distribution constructed by using the random fractal model. b- Close-up photography of condensing surface).

Le Fevre and Rose [18] proposed the following expression to calculate the fraction of surface covered by the droplets in the size range r to r_{\max} . They assumed a form for the time averaged distribution which had the correct behaviour for the limiting cases of very large and very small drops.

$$f_{co} \left(\frac{r}{r_{\max}} \right) = 1 - \left(\frac{r}{r_{\max}} \right)^n \quad (2.1)$$

This expression can be used for a surface swept by departing droplets as well as for unswept surfaces. The effect of sweeping can be introduced in to the expression above by choosing a suitable value for n. It is shown by Tanaka [19] that for an unswept surface the value of n is close to 1/3.

Rose and Glicksman [11] based on the results of Westwater and co-workers in which a high magnification cine film was used to observe the sequence of events resulting from sweeping of the condensing surface by departing drops, introduced a universal form for large drops that grow primarily by coalescence with small drops.

Maa and Wu [20] used the population balance model to derive the dropsize distribution of small drops which grow mainly by direct condensation based on the assumption of steady size distribution.

Later, Maa [21] used the population balance model to derive a dropsize distribution considering both small and large drops on the condensing surface. He solved the resulting equation numerically. The number of nucleation sites was varied so that the result would fit the experimental data.

Tanaka [22-24] based on photographs of a vertical condensing surface, argued that in the so called steady dropwise condensation, the surface is cleared of condensate periodically by falling drops. Those drops sweep the plate, exposing bare strips, on which transient condensation takes place without delay, until the area is swept clean again. Based on this, he attempted to describe the transient condensation by a set of simultaneous integrodifferential equation derived from statistical and geometrical considerations. The solution to these equations was expressed in terms of four-dimensional parameters, which were adjusted to fit the experimental data.

2.2 Heat Transfer Through the Droplet

Since condensation occurs on the droplets of varying sizes in the dropwise condensation, to find the total heat transfer rate, the amount of heat transfer through a single droplet as a function of its radius and the size distribution over the condensation surface should be known.

The number of variables which affect dropwise condensation heat transfer is quite large. Surface micro properties, system pressure, surface orientation, steam velocity, promoter, condenser thermal conductivity, noncondensable gas concentration, contact angle and departure radius all play important roles.

There are some important cases to find heat transfer through a single droplet. These cases are:

- a) Heat conduction through a single droplet.
- b) Heat conduction in the substrate material.
- c) The existence and the variation of the interfacial heat transfer coefficient at the vapor-liquid interface.
- d) Interference of heat conduction through a single droplet with the heat conduction in the neighboring droplets.

P. Griffith and C. Graham [10] evaluated the heat transfer through a single droplet and then to sum the heat transfer through all the drops on the surface using the droplet size distribution in their experimental analysis. The most important assumption in their study was that the bare spaces between the drops are completely inactive.

Fatica and Katz [12] proposed a model for heat transfer through an individual droplet during dropwise condensation. In this model it is assumed that the surface and base temperatures of the droplet are uniform and constant, equal to the vapor and

condenser temperatures, respectively. The majority of heat transfer actually takes place through a region very close to the periphery of the drop, the triple interface between the solid, liquid and vapor.

Sadhal and Plesset [31] studied effect of solid properties and contact angle in dropwise condensation and evaporation. They studied the effect of condenser material by solving the steady heat conduction equation for a geometry consisting of a droplet in the form of a spherical segment on a semi infinite solid.

Sadhal and Martin [62] used differential inequalities to find heat transfer through drop condensate. In their analysis the theory of differential inequalities was applied to obtain approximate solutions which are upper and lower bounds for the exact solutions of the temperature distributions in droplets of arbitrary contact angle $0 \leq \theta_0 \leq \pi/2$.

Tanner et. al. [25] indicated that; an increase in steam velocity past the condensing surface increases the heat transfer coefficient both by removing noncondensable gas and by altering the flow of condensate. And also they stated that steam side heat transfer coefficient decreases with decreasing pressure [26].

Experimental and theoretical results of the Hurst and Olson's studies [27] show that 83 to 98 percent of the calculated total heat transfer to a droplet comes in through the corner element where the hemispherical surface of the droplet intersected the condensing surface even for very small droplets. And in their investigation they showed that condensing surface temperatures in dropwise condensation can be predicted by assuming that all heat is transferred through a droplet by conduction.

2.3 The Effect of The Surface Thermal Properties and Finish on Dropwise Condensation

In order to make any rational correlation of the dropwise condensation heat transfer data it is necessary to have a clear picture of the physical processes involved.

When one looks a surface on which dropwise condensation is occurs, it is observed that drops form, grow, agglomerate and finally roll down or fall off.

Peter Griffith and Man Suk Lee [28] choose a horizontal surface facing down for this investigation because the experiments of Hampson show this geometry yielded a heat transfer coefficient that was independent of the condensing rate. It appears that the fraction of the surface which is covered with drops running down is heat flux dependent and this complication is eliminated with a horizontal surface facing down.

If the roughness and wetting effects are considered, according to results of their experiments, it was observed that the rougher the condensing surface, the lower the heat transfer coefficient. At the same time it was also observed for the rough lapped copper surface that only an imperfect type of drop condensing was initiated at the low heat load. As the heat load was increased, the contact angle of the drop was increased and the condensation was gradually changed to the good dropwise condensation. For the mirror finished surface it was also noticed that tiny scratches acted as favorable nucleation sites because they kept on producing the condensing drops. It appears that the primary effect of roughness is to decrease the apparent contact angle.

2.4 Substrate Material Effect

As far as the effect of substrate material properties are concerned the opinions differ. A group of scientist claim that thermal properties of substrate has an important effect on the rate of heat transfer, in dropwise condensation whereas others claim that substrate is not a factor in dropwise condensation.

Although many researchers have measured the heat transfer coefficients for various condensing surface materials with different thermal conductivity, the definite conclusion has not been obtained up to now. Tanner and colleagues compared the heat transfer coefficients of the dropwise condensation of steam at atmospheric

pressure on the copper and stainless steel surfaces [25,38]. Griffith and Lee experimented with dropwise condensation of the horizontal downward surfaces made of copper, zinc and stainless steel [28]. In addition, Wilkins and Bromely measured the heat transfer coefficients of five kinds of vertical pipes [56]. The above experimental results indicate that the experimental heat transfer coefficients decrease with the surface thermal conductivity. On the other hand, Aksan and Rose measured the heat transfer coefficients on copper and mild steel surfaces carefully and they obtained an opposing result that there was no significant difference between them [57]. Most of these researchers obtained the condensing surface temperature by extrapolation method using the temperature profile in the condenser block. Because the uncertainty in inferring the surface temperature from the extrapolation increases with decreasing surface thermal conductivity, many arguments have been made concerning the uncertainty of the experimental heat transfer coefficients together with some discussions on the effect of surface chemistry. Following them, Hanneman and Mikic [29] and Tsuruta and Tanaka [33] conducted the precise measurements of the surface temperature using a thin-film resistance thermometer deposited on the stainless steel surface and they obtained a lower heat transfer coefficient than that for the copper condensing surface.

Yu-Ting Wu, Chun-Xin Yang and Xiu-Gan Yuan [17] made theoretical study for the dropwise condensation heat transfer on the four kinds of surfaces; copper, zinc, carbon steel and stainless steel. The results indicate that the heat transfer coefficients are dependent on the surface thermal conductivity. The copper yields the highest heat transfer coefficient and it decreases markedly with the thermal conductivity in the order of zinc, steel and stainless steel. Dropwise condensation heat transfer coefficient increases with an increase in the thermal conductivity of the substrate material. It also found that the effect of thermal conductivity of the condenser material on dropwise condensation heat transfer increases with the system pressure, as shown in Figure 2.2. By this theoretical study it is confirmed that a decrease of the surface thermal conductivity raises the constriction resistance and reduces the heat transfer coefficient of dropwise condensation. When using low conductivity test plates, they find very small temperature differences between the

vapor and the surface. Under these circumstances, quite small errors in the surface temperature lead to large error in the vapor-side heat transfer coefficient. On the other hand, when they used high conductivity test plates, the temperature differences are high and the effect of the error on the heat transfer coefficient is very small. This is main reason for diversity of different experimental results.

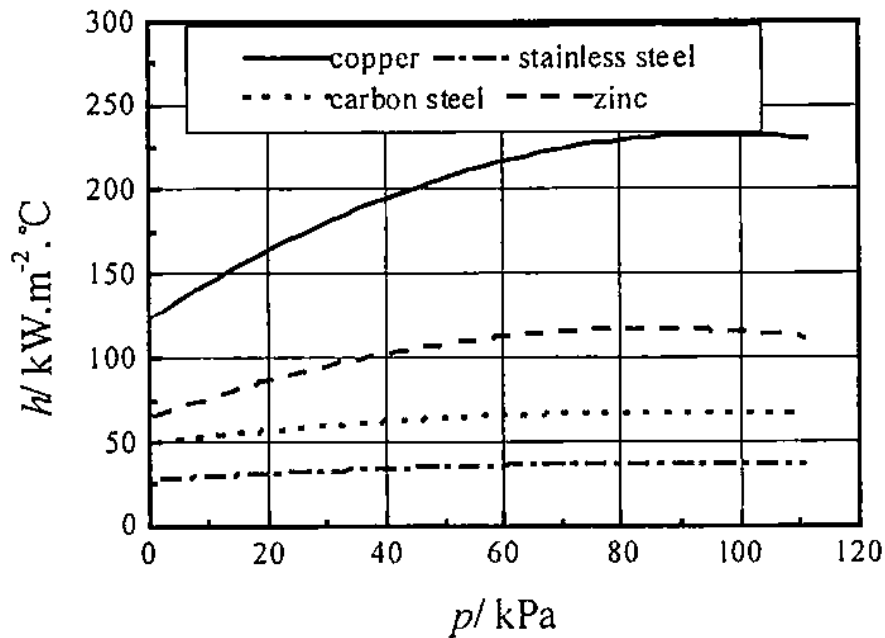


Figure 2.2 Effect of substrate material and pressure on heat transfer coefficient [17]

In dropwise condensation total resistance is expressed as the sum of two different thermal resistances in series. First, the surface to vapor resistance. The other resistance is called constriction resistance which is caused by the bending of the heat flux lines in the substrate. Constriction resistance was firstly recognized and studied by B. B. Mikic[30]. Heat flow through a material with a non-uniform heat flux over its surfaces is always associated with a thermal resistance known as a constriction resistance. The constriction resistance is caused physically by the heat flow redistribution in the material so that the flow could conform with the non-uniform heat flux at the surface. This resistance is significant only if the characteristic length representing non-uniform conditions over the surface is less than or equal to the

depth of the material where the constriction takes place. The most common example of the constriction resistance is the so called thermal contact resistance. Less common, but also very significant is constriction resistance in dropwise condensation where this type of the resistance for example could account for about 80 per cent of the total resistance in case of stainless steel as condensing surface. All studies related to the substrate effect consider that thermal conductivity of the substrate material is the only parameter governing the constriction resistance.

Mikic [57] consider the flow of heat through a solid. At the surface $z=0$, there is non-uniform heat transfer coefficient h . Far from the surface the temperature distribution is one dimensional. T_c represent the local surface temperature and T_0 constant temperature of the environment. The heat rate at the surface is then;

$$Q = \int_A h(T_0 - T_c) d\bar{A} \quad (2.2)$$

The surface temperature T_c would be non-uniform. The average flux over the heat transfer surface follows from (2-2) as

$$\frac{Q}{A} = T_0 h_{av} - \frac{1}{A} \int_A T_c h d\bar{A} = (T_0 - T_s) h_{av} - \frac{1}{A} \int_A (T_c - T_s) h d\bar{A} \quad (2.3)$$

Where $h_{av} = (1/A) \int h d\bar{A}$ and T_s is a constant hypothetical surface temperature obtained at $z=0$ by the extrapolation of the linear temperature profile existing far from the surface. Defining the total resistance from the surface to the environment as

$$R = \frac{T_0 - T_s}{Q/A} \quad (2.4)$$

It can be written from relation (2-3) the following

$$R = \frac{1}{h_{av}} + R_c^* \quad \text{where} \quad R_c^* = \frac{1}{Q} \int_A \frac{h}{h_{av}} (T_c - T_s) d\bar{A} \quad (2.5)$$

Equation (2-5) defines the constriction resistance R_c^* . It can be seen from relation (2-5) that $1/h_{av}$ is not the only resistance at the surface. The value of R_c^* is always positive since $(T_c - T_s)$ is higher for higher values of h/h_{av} . R_c^* goes to zero when $T_c \rightarrow T_s$ everywhere and that would be the case either for uniform h or an infinite conductivity of the surface material in the lateral direction.

R. J. Hannemann and B. B. Mikic [29] investigated experimentally surface thermal conductivity on dropwise condensation. For a gold coated stainless steel surface, they obtained heat transfer coefficient as $0.62 \times 10^5 \text{ W/m}^2\text{K}$, whereas for a gold coated copper surface heat transfer coefficient was found to be $1.5 \times 10^5 \text{ W/m}^2\text{K}$, almost 2.5 times the value obtained for the stainless steel (low conductivity surface). In their study, the single most significant experimental difficulty in condensation heat transfer research is due to the necessity of measuring accurately the temperature of the solid surface at which the phase change takes place. Since the surface conductances involved are very large, a slight error in the measurement of the fluid to surface temperature difference can lead to large errors in the computed heat transfer coefficients. The problems are most acute when thermal properties of the condensing surface are to be varied; low conductivity materials inherently lead to greater inaccuracies in almost any type of surface temperature measurement scheme.

Although most experimental studies on dropwise condensation have been performed using copper as a condensing surface material (due to its high conductivity and relative ease of promotion), at least four investigators have produced relevant direct data on the surface thermal conductivity dependence of the dropwise condensation heat transfer coefficient. The data summarized in Table 2.1.

Table 2.1 Investigations into the surface thermal conductivity effect in dropwise condensation

Investigators	Material	Thermal conductivity (W/mK)	Measured steamside coefficient (W/m ² K)	Condenser orientation
Tanner et al [38]	Copper	381	2.38×10^5	Vertical
	Stainless steel	17.3	0.45×10^5	Vertical
Griffith & Lee [28]	Copper	381	0.57×10^5	Horizontal
	Zinc	109	0.26×10^5	Facing
	Stainless steel	17.3	0.11×10^5	Down
Wilkins & Bromley [56]	Copper	393	2.27×10^5	Condensation on vertical tubes
	Gold	294	1.99×10^5	
	Admirally	121	1.59×10^5	
	Cu-Ni 90-10	50	1.25×10^5	
	Monel	27	0.55×10^5	
Aksan & Rose [57]	Copper	381	2.16×10^5	Vertical
	Steel	45	2.38×10^5	Vertical
Hanneman & Mikic [29]	Copper	395	1.50×10^5	Vertical
	Stainless steel	17.3	0.62×10^5	Vertical

In evaluating the results of these investigations, three main factors influencing the measurements must be considered: (1) the possible presence of significant noncondensable gas concentrations, (2) the accuracy with which the surface temperature was measured or inferred during condensation and (3) the effects of surface chemistry differences due to differences in promoters and surface microproperties.

Tanner et al. [38] obtained values for the heat transfer coefficient for atmospheric pressure dropwise condensation for both copper ($k=380$ W/mK) and stainless steel ($k=17$ W/mK) condensing specimens using the extrapolation method.

The conductance for the stainless steel surface was found to be a factor of five lower than for the copper surface.

Griffith and Lee [28] measured heat transfer coefficient for three different condensing surface materials with the condensing surface in the horizontal, facedown position. A modified extrapolation method was used, in which a thin condensing surface was soldered to a copper rod in which the temperature profile was measured. Conductances for stainless steel were again found to be a factor of five lower than those for copper. A uniform surface chemistry was obtained by standard promotion of the gold plated surfaces. Although noncondensable gases may have been present, the primary error in these data is thought to be due to extrapolation error.

Wilkins and Bromley [56] investigated a whole series of condenser materials, measuring the overall coefficient of heat transfer between vapor and cooling water for thin and thick walled condenser tubes. The steam side coefficient was then inferred from overall coefficient through knowledge of the coolant flowrate and material thermal conductivity. The results decrease systematically with conductivity with the conductance for Monel ($k=27$ W/mK) reported to be a factor of four lower than that for copper.

Aksan and Rose [57] measured conductances on copper and copper plated steel ($k=45$ W/mK) using the extrapolation method, obtaining results in opposition to those previously described. In fact, the conductance they report for copper is somewhat lower than that for the copper plated steel. The data were apparently flawed by neither noncondensable gas nor surface chemistry effects, but these authors estimated the possible error in their surface temperature measurements to be on the order of 0.6 K. A rough calculation shows that if this error were indeed present, the data point for steel could easily have been a factor of two lower than the copper data point.

Also, R. J. Hannemann and B. B. Mikic [59] made an analysis of the effect of surface thermal conductivity on the rate of heat transfer in dropwise condensation.

Due to the finite lateral thermal conductivity of the condensing surface material, the distribution of droplets of varying size over the surface during dropwise condensation and the resulting inhomogeneity of surface heat flux induces a thermal resistance in addition to the average droplet resistance. This resistance, the thermal constriction resistance, was studied analytically and the results compared to available data in the work described in the study. The analytical model, consisting of a synthesis of single drop constriction resistance results with known droplet distribution information, resulted in a correlation for the overall dropwise condensation constriction conductance as a function of the condensing surface thermal conductivity. In their study, calculating the overall thermal constriction resistance it is assumed that: (1) The droplet distribution is statistically stationary, with the macroscopic drop distribution being universal, (2) The droplet distribution is taken to be spatially random. Each drop is considered to be centered on a disc of surface area with which the droplet is associated, (3) The time response of the surface to changing heat transfer coefficients is sufficiently rapid and thermal storage effects sufficiently small that the steady state conduction equation in the condenser material is valid. The time for coalescence of macroscopic drops is assumed to be much smaller than the time between coalescences, so that steady state conduction can be assumed for calculating the droplet heat transfer resistance, (4) The constriction resistance due to pre-coalescence drops can be neglected.

In the study of Mikic [30], he noted that in the case of vertical position of the condensing surfaces constriction resistance was much lower. That should be expected, since for a given surface material the constriction resistance depends only on the distribution of large drops on the condensing surface and the latter strongly depends on the surface position. The heat transfer coefficient was also much higher for the vertical surfaces. That came not only due to the decrease in the constriction resistance but also due to a substantial decrease in thermal resistance excluding constriction resistance in the experiments done by Tanner et al., which was lower mainly because of the absence of noncondensibles in the condensing system. The fact that relative contribution of constriction resistances for the same material calculated from experimental results of Griffith and Lee, and Tanner et al., is the

same, is obviously accidental and no generalization should be made based on the fact that for the stainless steel surfaces constriction resistance was about 84 per cent of the total resistance and for copper about 20 per cent for both sets of experiments. The important conclusions that can be drawn from the above evaluations are:

1. The constriction resistance is present in dropwise condensation.
2. Its contribution to the overall resistance could be significant and therefore cannot be left out from any dropwise condensation model.

Hannemann [60] indicated that the constriction of the heat flow lines near the surface due to non-uniformity of the surface temperature leads to the conclusion that the resulting thermal resistance depends also upon the condensing surface thickness.

Sadhal and Plesset [31] analyzed the effect of condenser material is dealt with by solving the steady heat conduction equation for a geometry consisting of a droplet in the form of a spherical segment on a semi-infinite solid. In their models they assumed that the influence on a droplet due to surrounding droplets is negligible. And they concluded that the importance of the material properties of the solid and of the droplet contact angle for condensing droplets.

T. Tsuruta and H. Tanaka [61] made a theoretical study on the constriction resistance in dropwise condensation. The effect of the thermal conductivity of the condenser material on dropwise condensation heat transfer was studied. By taking account of the contribution of the droplet resistance in the individual drop size class to the thermal resistance in transient dropwise condensation, a fundamental differential equation describing the constriction resistance caused by the inhomogeneity of surface heat flux is derived. It is found from the non-dimensionalized fundamental equation that the constriction resistance can be determined by a Biot number defined by the interfacial heat transfer coefficient, the departing drop radius and the surface thermal conductivity, in addition to a few characteristic parameters. And they concluded that heat transfer coefficient of

dropwise condensation decreases with decreasing surface thermal conductivity due to increasing constriction resistance.

Peter Griffith and Man Suk Lee [28] emphasized surface thermal conductivity in their study. They point out that if equations and boundary conditions written, it is apparent that surface thermal conductivity could enter into the condensing heat transfer coefficient as well as the thermal conductivity of the condensate itself. If the surface thermal conductivity is very large, the surface temperature approaches uniformity at a value close to the saturation temperature of the condensate. This tends to give a high heat transfer coefficient. For low surface thermal conductivity, only a very local cooling occurs in the vicinity of the triple interfaces and a large proportion of the surface is well below saturation temperature. This gives a low heat transfer coefficient. In their experiment they used horizontal downward-facing condensing surfaces of copper, zinc and stainless steel. All three surfaces were gold plated so as to obtain identical surface chemistries as well as readily promotable surfaces. The promoter used was oleic acid. In the case of the zinc and stainless steel surfaces thin disks of these materials were respectively soft-soldered and silver-soldered to thicker copper disks in which the temperature distributions were measured. The steam side heat transfer coefficients were found to be independent of heat flux and to have values of about $57 \text{ kW/m}^2\text{K}$, $26 \text{ kW/m}^2\text{K}$ and $11 \text{ kW/m}^2\text{K}$ for copper, zinc and stainless steel respectively. These results suggest a systematic dependence of the steam side heat transfer coefficient on the thermal conductivity of the plate material, whose approximate values were 381 W/mK , 109 W/mK and 17.3 W/mK for copper, zinc and stainless steel respectively. These authors reported heat transfer coefficients in the approximate ratios 5:2.2:1 for copper, zinc and stainless steel, respectively. So, it is by no means obvious that the dropwise condensation heat transfer coefficient should be a function of the thermal conductivity of the bulk material underlying the promoter. How this comes about can be seen most easily by considering the heat transfer through and around a drop. Near the triple interface, the conduction path is very short and the local heat transfer coefficient is very large. On bare surface the heat transfer coefficient is virtually zero. On the surface near the middle of a drop, the conduction path through the liquid is quite long and the heat

transfer coefficient is very low. One finds then, on the surface, a local heat transfer coefficient which is a strong function of position. This gives rise to a crowding of heat flux in certain spots as one gets close to the surface. Locally, this crowding results in an additional temperature drop, the magnitude of which is a function of the thermal conductivity of the bulk material. The way the heat transfer coefficient is defined makes the dropwise condensation heat transfer coefficient then a function of the thermal conductivity of the base material. An effect such as this can occur any time the local heat transfer coefficient is not constant over the area.

Tanner et al [38] made measurements on vertical copper and stainless steel surfaces using montanic acid as promoter. The surface temperature and heat flux were found from observed temperature distributions in the plates. The maximum heat flux obtained in the case of the stainless steel was about 30kW/m^2 . They report that the steam side coefficient for the stainless steel plate was lower than that for the copper plate by a factor of about 5 at the highest heat flux and by an even greater amount lower heat fluxes.

J. W. Rose [32] indicated that for dropwise condensation of steam on tubes of different materials, the vapour-side heat transfer coefficient depended strongly on the tube material as well as on the wall thickness. It was suggested that this dependence was due to the thermal properties of the tube material along the lines of a theoretical treatment, which considered the heat transfer resistance arising from the non-uniformity of heat flux near the condensing surface.

T. Tsuruta, H. Tanaka and S. Togashi [33] studied the effect of thermal properties of the condenser material on dropwise condensation heat transfer. They indicated in their experimental analysis that the heat transfer coefficient dependent upon the surface thermal conductivity. They used quartz glass, stainless steel and carbon steel as the condenser material. The heat transfer coefficient for steam is measured very carefully and precisely using thin film resistance thermometers deposited on the condensing surface. All tests are conducted in a pressure range from 10 kPa down to 1 kPa to minimize the effect of nucleation site density on the heat

transfer. In the experimental data it was shown that the heat transfer coefficients agree satisfactorily with the predictions by the previously developed constriction resistance theory. The copper surface yields the highest heat transfer coefficient and it decreases markedly with the thermal conductivity in the order of carbon steel, stainless steel, quart glass. And they considered that the constriction resistance theory can describe fairly well the effect of the surface thermal conductivity on the heat transfer coefficient. It is then confirmed that a decrease of the surface thermal conductivity raises the constriction resistance and reduces the heat transfer coefficient of dropwise condensation.

J. W. Rose [34] stated the importance of constriction resistance in dropwise condensation. He indicated that the effective vapor-to-surface heat transfer coefficient should depend on the conductivity of the surface material.

2.5 Effect of Noncondensable Gases

Noncondensable gases in the working fluid have some undesirable effects during condensation. They reduce the heat transfer rate and make temperature measurements quite difficult, since large fluctuations in the temperature of the condensation surface takes place. The source of this gas is usually air leake in a vacuum apparatus or dissolved gases in feed water.

Both filmwise and dropwise condensation are affected by non-condensable gases present in the vapor, but it is the most significant for the case of dropwise condensation. Noncondensable gases carried to the condenser surface by the condensing vapor accumulate and cause a reduction in heat transfer coefficient by reducing the vapor partial pressure. This reduction might be large enough to offset the gains of dropwise condensation. Therefore, the removal of non-condensable gases may become necessary to improve the heat transfer coefficient. On the other hand, in certain applications such as the production of liquified petroleum gases, liquid

nitrogen and liquid oxygen, condensation must take place in the presence of non-condensables, because of the nature of the specific process.

The first study about the effect of non-condensable gases on heat transfer in dropwise condensation was done by Othmer [35]. He concluded that with an increase in the amount of non-condensable gases, in filmwise condensation of steam-air mixtures on a horizontal tube, causes a significant decrease in heat transfer coefficient. It was concluded that the non-condensable gases which reach the tube surface remain there and become an obstacle to condensation.

Le Fevre and J. W. Rose [36] used a special venting technique after a series of experiments to obviate the effects of the non-condensable gases. They removed temperature fluctuations and also they got new steady temperatures which was higher than the old peak temperatures. E. Citakoğlu and J. W. Rose [37] also studied effects of local venting. They indicated that the errors, caused by such gas concentrations remain in steam after prolonged boiling, may be eliminated by venting. However, care must be taken regarding the position of the vent and the venting rate, so as to ensure that the venting is sufficient to reduce the local gas concentration to an insignificant level without, at the same time, causing errors through disturbance of the condensate.

In their several experiments Tanner et. al. found that the addition of nitrogen or carbon dioxide to the inlet steam caused a marked reduction in heat transfer by introducing a diffusional resistance but produced no lasting effect [25]. Oxygen, in addition to creating a diffusional resistance, produced on copper surfaces a permanent decrease from the development of areas of filmwise condensation, which was attributed to the growth of an oxide layer. Removal of this layer by carbon dioxide attack restored dropwise condensation [38].

2.6 Promoting Dropwise Condensation

Because of high heat transfer coefficient, dropwise condensation is preferred to filmwise condensation in industrial applications. However, it is very difficult to obtain dropwise condensation since it does not continue long time and converts to filmwise condensation after a while. So this can be achieved by promoting dropwise condensation.

Dropwise condensation can be promoted by;

- a) Applying a suitable chemical such as oleic acid or montan wax to the condenser surface
- b) Injecting nonwetting chemicals called promoters into the vapor which are deposited on the condenser surface
- c) Using a low-surface energy polymer or noble metal coating generally gold

Producing dropwise condensation by chemical promoters have a disadvantage that it has a limited life. For providing continuous dropwise condensation, promoter must be injected repeatedly into the condenser at certain intervals of time. Otherwise, it eventually reverts to the filmwise mode as the promoter is washed away. Another factor contributing to the failure of the promoter is the accumulation of fouling matter that may be present in vapor; the promoter becomes submerged beneath the fouling matter. Considerable excess of fatty acid in the system had to be avoided because it would be gradually accumulate on the surface, causing poor dropwise condensation. A large excess of oleic acid usually resulted in a gelatinous emulsion on the surface which cut down the heat transmission greatly [12].

The use of permanent coatings of the noble metals only gold and silver have been shown consistently to produce excellent dropwise condensation since the surface energy of these noble metals is relatively high. Also gold has the ability to attract and retain organics which render the surface hydrophobic. For this reason gold is referred to as a self-promoter.

Coating the condenser surface with a low surface energy polymer or a noble metal is very important. If the coating is too thin, it wears away in a short period of time. On the other hand if it is too thick the thermal resistance introduced circumvents the gains of dropwise condensation. So, selecting the correct thickness is very important for the effective use of this procedure.

Hurst and Olson [27] coated the copper surface with a promoter to insure dropwise condensation in their experiments. Benzyl mercaptan was chosen for this because it had contact angles near 90 deg when water vapor condensing, so that condensate droplets were very nearly hemispherical.

P. Griffith and M. S. Lee [28] coated copper, zinc and stainless steel surfaces with 0.005 in thick in order to secure identical chemical and mechanical surface conditions. The reason for selecting gold as the plating material was first to eliminate any adverse effects due to surface oxidation and second to have a minimum temperature drop across its thickness.

J. W. Rose et. al. [39] coated several substrates with different polymer coatings to increase steam side heat transfer coefficient. The results for these coatings is shown in Table 2.2. It is clearly seen in Table 2.2 that Nedox produced the best thermal performance. Nedox is a commercially available coating developed by the General Magnaplate Corporation for use as a corrosion resistant mold release. Fig 2.3 is an example of dropwise condensation on copper-nickel coated with No-stick (left) and Nedox.

Table 2.2 Steam side heat transfer coefficients [39]

Coating Type	$h_o / (\text{kW}/\text{m}^2.\text{K})$
Uncoated	10 ± 0.5
No-Stik	4 ± 0.5
Nedox	86 ± 13
NRL C-6 Fluoroepoxy	20 ± 1
NRL Fluoroacrylic	53 ± 7
Parylene-N, 0.5 μm	67 ± 10
Parylene-N, 1.0 μm	52 ± 8

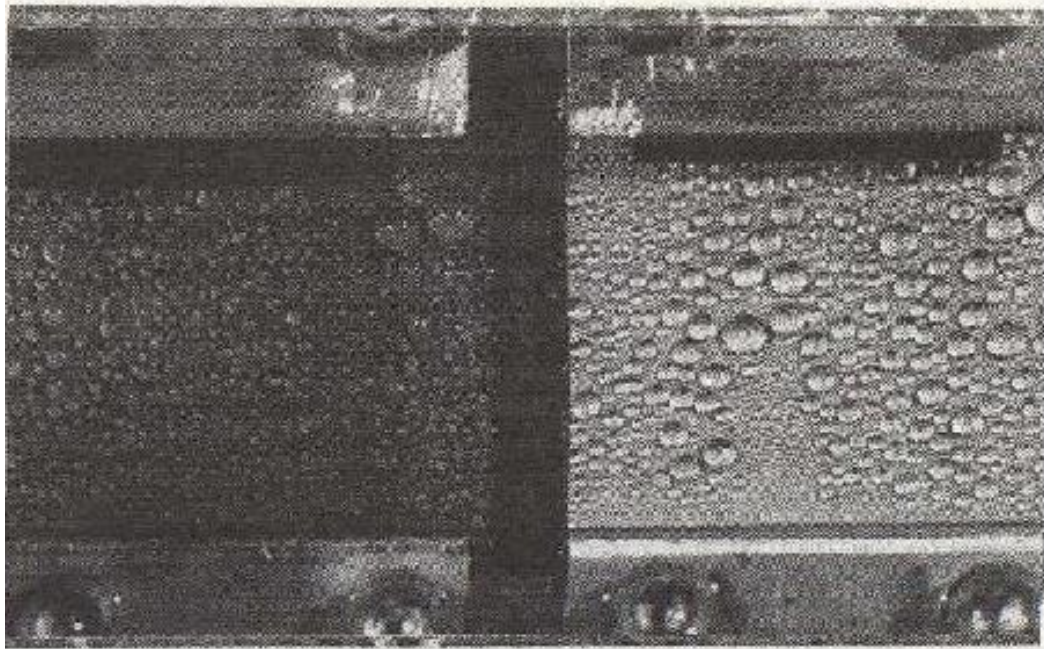


Figure 2.3 Initial dropwise condensation on copper-nickel coated with No-Stick (left) and Nedox [39]

J. W. Rose [32] made an experimental study to show the important of promoting surface with a metal. In the experiment; brass, aluminum and stainless steel tubes had been copper plated to a thickness of $9 \pm 1 \mu\text{m}$. According to the results

for the brass and copper plated brass surfaces were essentially the same, but the observed heat fluxes for the aluminum and stainless steel tubes were substantially higher when copper plated than when unplated. Figure 2.4 shows the results of this experiment.

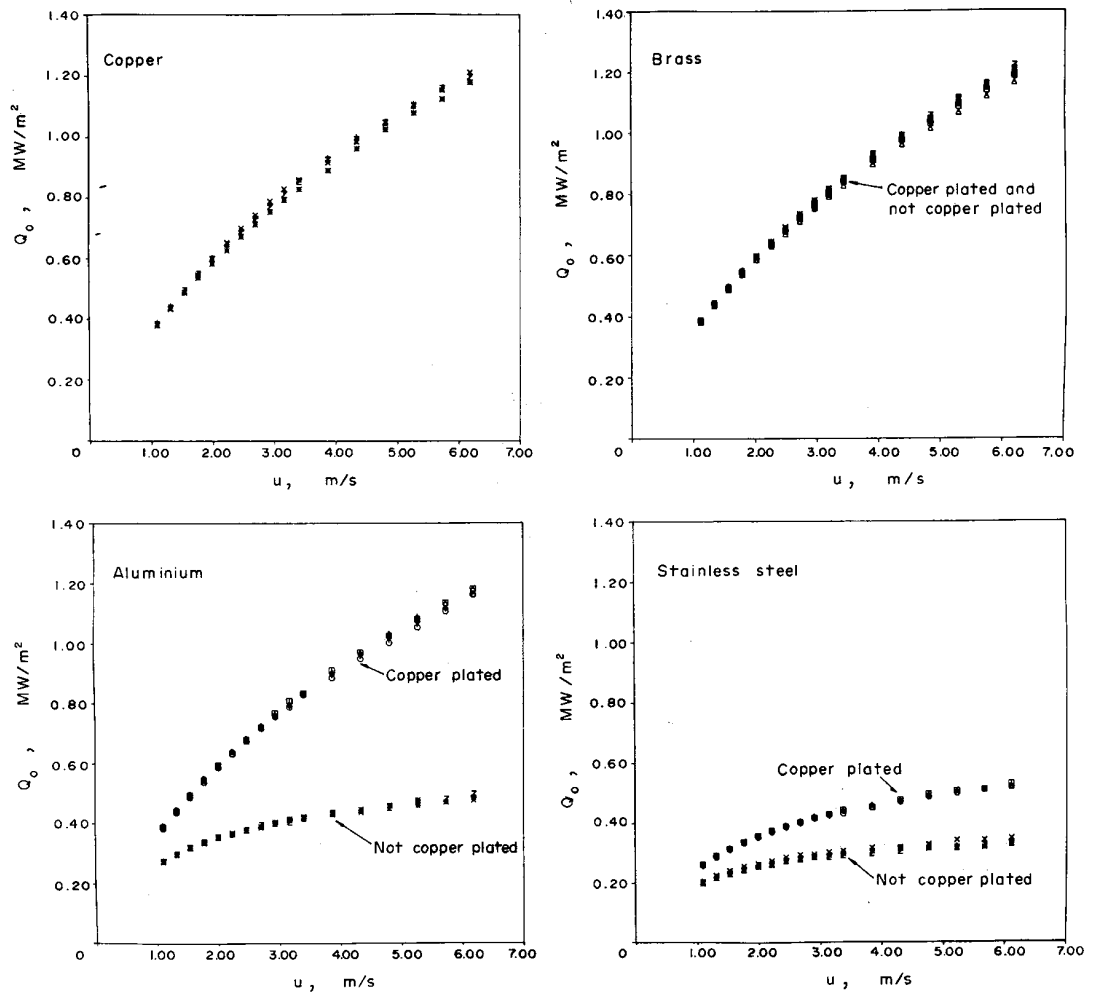


Figure 2.4 Dependence of heat flux on coolant velocity. Different symbols denote different test runs. + x * z, unplated tubes; o Δ □ ◇, copper plated tubes [32]

Zhang et al. [40,41] used various surface processing methods including mechanical polish, ion plating, and ion plating and ion-beam mixing technology, to modify the micro structure of the metal surface layer in order to form a amorphous-state surface layer, which has low surface free energy. The Cu–Cr surface prepared by

ion plating and ion-beam mixing combination technique maintained dropwise condensation for 8500 h. Zhao et al. [42] studied the effects of different ion-implanted elements and processing conditions on the dropwise condensation heat transfer characteristics. It was found that the processing condition for different implanted elements had considerable impact on the dropwise condensation heat transfer.

Song et al. [43] investigated condensation heat transfer characteristics of steam on brass tubes having chromium surfaces prepared with three kinds of surface processing techniques, i.e. ion plating, electroplating, and ion plating with ion-beam mixing. The ion-plated tubes were sorted into three sets for experimental tests. The first set of tubes was used to conduct experiments in the laboratory immediately after the surface was treated. This kind of surface maintained dropwise condensation for 50 h. The tubes of the second set were installed in a large scale steam–water heat exchanger in a power station which operated for one and half years. Then, one of the tubes was taken from the heat exchanger and used in condensation experiments in the laboratory. Film condensation only was obtained. The third set of tubes which had been exposed to the air for about 2 years also failed to promote dropwise condensation. The chromium surfaces prepared by ion plating technique were of very high purity due to the vacuum operation for surface processing. The freshly treated surface gives rise to dropwise condensation of steam due to the organic substances adsorbed from the environment. One electroplated chromium surface maintained dropwise condensation in the laboratory even after the surface was exposed to the air for 1 year. As noted earlier by Finnicum and Westwater [44] dropwise condensation on electroplated chromium surfaces is due to impurities from the surface processing technique rather than the metal itself. The ion plating with ion-beam mixing technology transforms the chromium surface layer into an amorphous state which possesses low surface free energy, hence, resulting in dropwise condensation.

For metal organic compound films, the main problems concerned are the cost for surface film preparation on an industrial scale and the durability of the dropwise promoting surface. Zhao et al. [45-49] have successfully applied one of this kind of surface film in a practical condenser in the integral heating system in Dalian Power

Station in China. The surface film was prepared by the patented Activated Reactive-Magnetron Sputtering Ion Plating technique [50,51]. The condenser is 800 mm of diameter and 3500 mm high with 800 brass tubes each having 16 mm i.d. and 3000 mm long. An overall heat transfer coefficient between 6000 and 8000 W/m²K with 2-3 m/s cooling water velocity has been maintained since its installation October 1989, to the present. The dropwise condenser was used to replace the old film one, which has 1600 brass tubes. The tubes used in the film condenser have the same dimensions with the treated ones.

For liquids with high surface free energy (or surface tension) such as water and ethanol, metal organic compound surface layers, which have good adhesion with the substrate, would be expected to maintain dropwise condensation mode for a long period of time to meet the requirements of industrial applications. However, for most organic vapours, which are widely used in petrochemical processes, a polymer film on the metal substrate may be the only approach for promoting dropwise condensation. The difficulties for the polymer lie in its much lower thermal conductivity and poor adhesion with metal substrates. The different thermal expansivities of metal and polymer film, and the weak binding effect between the two materials lead to the polymer film peeling after a period of time. In the laboratory test, dropwise condensation of steam on a copper tube with 10mm o.d. and 100mm long, which was coated with a PTFE polymer film has been maintained for about 1000 h so far [52].

Contact angle has sometimes been used to predetermine the condensation mode on a specific solid surface. However, the contact angle measured at room temperature and in equilibrium with an air environment has been proven not to be useful for determining the wettability of systems where mass transfer takes place.

Ma [53] put forward a surface free energy criterion, i.e. the surface free energy difference between the condensate liquid at the condensation temperature and the solid surface, defined as $\Delta\gamma_{l-s}$ (γ_l and γ_s denote the surface free energies of liquid and solid, respectively) to predict whether filmwise or dropwise condensation of a

vapour will occur on a solid surface. In a conservative manner, the critical surface free energy difference was considered to be 0.0333 J/m² according to an empirical correlation between contact angle and surface free energy difference [54]. The surface free energy of a solid depends only on its composition and chemical structure and can be calculated from the measured contact angles at room temperature [55] for low surface-free-energy solid surfaces like polymer films. Consequently, it is more convenient and accurate to use the surface free energy rather than the contact angle to predict condensation mode because the surface free energy criterion is not affected by the measuring temperature of the contact angles. The new surface free energy difference criteria and comparison with contact angle method are shown in Table 2.3.

Table 2.3 Condensation mode criteria [53]

Surface free energy difference criterion	Contact angle method	Condensation mode
$\Delta\gamma \leq 0$	–	Filmwise
$0 \leq \Delta\gamma < 0.0333$	$0^\circ \leq \theta < 90^\circ$	Mixed condensation
$\Delta\gamma \geq 0.0333$	$\theta \geq 90^\circ$	Dropwise

CHAPTER 3

MATHEMATICAL ANALYSIS

In this chapter, heat transfer in dropwise condensation is modeled including the effect of substrate material. Differential equations are obtained for temperature distribution in the substrate and the droplet. Since analytical solution of the differential equation system is quite complicated by the known methods, no attempt is made to solve these equations analytically. Instead of solving the differential equations of the drop and the substrate simultaneously, the diffusion equation of the droplet is replaced by the equivalent thermal resistances and these resistances are used as boundary condition for the diffusion equation for the substrate material. Temperature distribution in the substrate material is obtained with finite difference method and the calculations are performed for different substrate materials and for various drop radii by using the FORTRAN computer program developed. Heat transfer and heat flux are calculated through a single droplet with the use of temperature distribution, then total heat transfer and flux is obtained by integrating the heat transfer through a single drop for the entire drop population. Finally heat transfer coefficient for dropwise condensation is determined by using the total heat flux and average surface temperature of the drop to substrate interface.

Previous analytical and theoretical models of dropwise condensation used expressions for the heat transfer through single droplets of specific sizes and then the total heat transfer is determined by integrating over the distribution of sizes. Such an analysis will also be followed here.

Following assumptions are made in the analysis of this study :

- The vapor is at uniform temperature.
- Heat transfer from vapor to substrate is carried out only by condensation.
- Substrate material, although it has a finite thickness in typical applications, will be assumed to be a semi-infinite body since its thickness is considerably large for the majority of the droplets on the surface of condensation.
- The area between the droplets can be considered as thermally insulated. Because the small amount of heat transfer by convection is negligible compared to the high rate of heat transfer on the surface of the drop.

Previous studies result in two important conclusions;

i. The majority of the heat transfer in a drop takes place within a narrow region close to the perimeter of the drop, due to the very small thermal resistance existing there.

ii. The majority of the heat transfer in dropwise condensation takes place through droplets of very small sizes, because of their small thermal resistances and large numbers.

3.1 Mathematical Modeling of Dropwise Condensation with Substrate Material Effect

3.1.1 Temperature Distribution

The most important phenomena in dropwise condensation is the heat conduction through the droplet and the substrate which results in the heat transfer and also the formation of the specially shaped isotherms in both substances.

Overall heat flux in dropwise condensation depends on the growth of a single droplet and hence, it is necessary to find the droplet temperature distribution and also the substrate material temperature distribution.

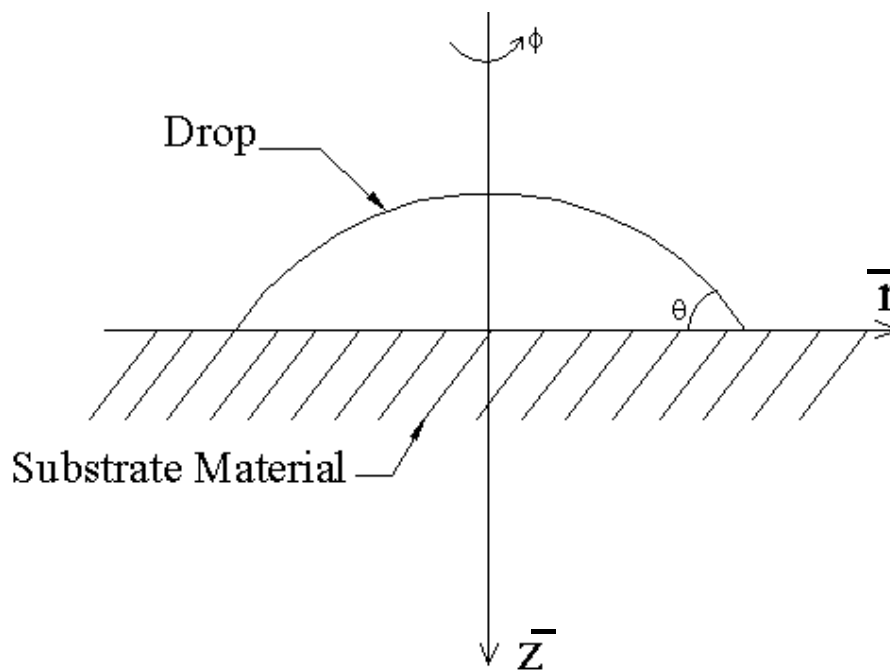


Figure 3.1 Droplet resting on a semi infinite substrate material

The governing differential equation for diffusion of heat in cylindrical coordinates for substrate material:

$$\frac{1}{\bar{r}} \frac{\partial}{\partial \bar{r}} \left(k_s \bar{r} \frac{\partial T_s}{\partial \bar{r}} \right) + \frac{1}{\bar{r}^2} \frac{\partial}{\partial f} \left(k_s \frac{\partial T_s}{\partial f} \right) + \frac{\partial}{\partial \bar{z}} \left(k_s \frac{\partial T_s}{\partial \bar{z}} \right) + q^* = r_s C \frac{\partial T_s}{\partial t} \quad (3.1)$$

where:

T_s : Temperature distribution in the substrate

\bar{z} : Axial direction (Figure 3.1)

k_s : Thermal conductivity of substrate material, constant

r_s : Density of substrate

C : Specific heat

Since there is no heat generation q^* is taken as zero.

$$T_s \Big|_{t=0} = T_{in}$$

T_{in} : Initial temperature in the substrate material

With constant thermal conductivity, no heat generation and symmetry, Eq. (3.1) is reduced to;

$$\frac{1}{\bar{r}} \frac{\partial T_s}{\partial \bar{r}} + \frac{\partial^2 T_s}{\partial \bar{r}^2} + \frac{\partial^2 T_s}{\partial \bar{z}^2} = \frac{rC}{k_s} \frac{\partial T_s}{\partial t} \quad (3.2)$$

The governing differential equation in cylindrical coordinates for droplet;

$$\frac{1}{\bar{r}} \frac{\partial}{\partial \bar{r}} \left(k_d \bar{r} \frac{\partial T_d}{\partial \bar{r}} \right) + \frac{1}{\bar{r}^2} \frac{\partial}{\partial f} \left(k_d \frac{\partial T_d}{\partial f} \right) + \frac{\partial}{\partial \bar{z}} \left(k_d \frac{\partial T_d}{\partial \bar{z}} \right) + q^* = r_d C \frac{\partial T_d}{\partial t} \quad (3.3)$$

where:

T_d : Temperature distribution in the droplet

\bar{r} : Radial direction (Figure 3.1)

k_d : Thermal conductivity of droplet, constant

Since there is no heat generation q^* is taken as zero.

$$T_d|_{t=0} = T_i$$

With constant thermal conductivity, no heat generation, symmetry, steady state, Eq. (3.3) is reduced to;

$$\frac{1}{\bar{r}} \frac{\partial T_s}{\partial \bar{r}} + \frac{\partial^2 T_s}{\partial \bar{r}^2} + \frac{\partial^2 T_s}{\partial \bar{z}^2} = \frac{rC}{k_s} \frac{\partial T_s}{\partial t} \quad (3.4)$$

On the surface of the droplets heat conduction rate can be equated to the heat convected at the interface.

$$-k \frac{\partial T_d}{\partial n} \Big|_{dropsurface} = h(T_{dsur} - T_v)$$

where n is the direction perpendicular to the drop surface.

T_{dsur} : Surface temperature of droplet

Simultaneous solution of differential Equations (3.2) and (3.4) with the boundary conditions gives the temperature distribution in the substrate and the droplet.

One of the major objects of this study is to determine the temperature distribution in the droplet and substrate combination described and formulized above. It is found in the literature that similar studies are made on this subject previously. The studies of Sadhal and Plesset [31], Sadhal and Martin [62] on drop conduction are explained in the previous chapter. However, since the conduction analysis made by Sadhal and Plesset[31] and Sadhal and Martin[62] to calculate the heat transfer through droplets is applicable only under limited conditions they are not sufficient and appropriate to make heat flux calculations for dropwise condensation in general.

In their studies Hurst and Olson [27] met with similar difficulties in solving the differential equations that they obtained and they evade the difficulty by using finite element method and they could obtain solutions only for limited cases.

For that reason, in this study temperature distribution in the substrate will be obtained for the most general situation by numerical methods also.

3.1.2 Conduction Equations and Boundary Conditions Through a Single Droplet

In the previous section, it was mentioned that analytical solution of the differential equation system is complicated and difficult. Therefore, in this study differential equation system is not solved. Instead of solving the differential equation system, total resistance from the drop surface to the drop-substrate interface is taken into consideration. That is, drop on the surface of substrate material removed then resistance R_i associated with interfacial heat transfer coefficient on the droplet surface and thermal resistance caused from drop conductance R_c , are placed instead Fig (3.2). In this approach, it is assumed that heat flow lines in the drop cross section becomes approximately a piece of circle which has the center on the edge of the droplet. For that reason, in this approach heat flow lines becomes the torus surfaces which are centered at the droplet edge and the heat flow takes place from the interface between the drop and the vapor to the interface between the drop and the

substrate. Total resistance can be found with the summation of these resistances. Lastly, heat transfer through a single droplet can be obtained by the use of boundary conditions obtained from the total resistance and conduction equation.

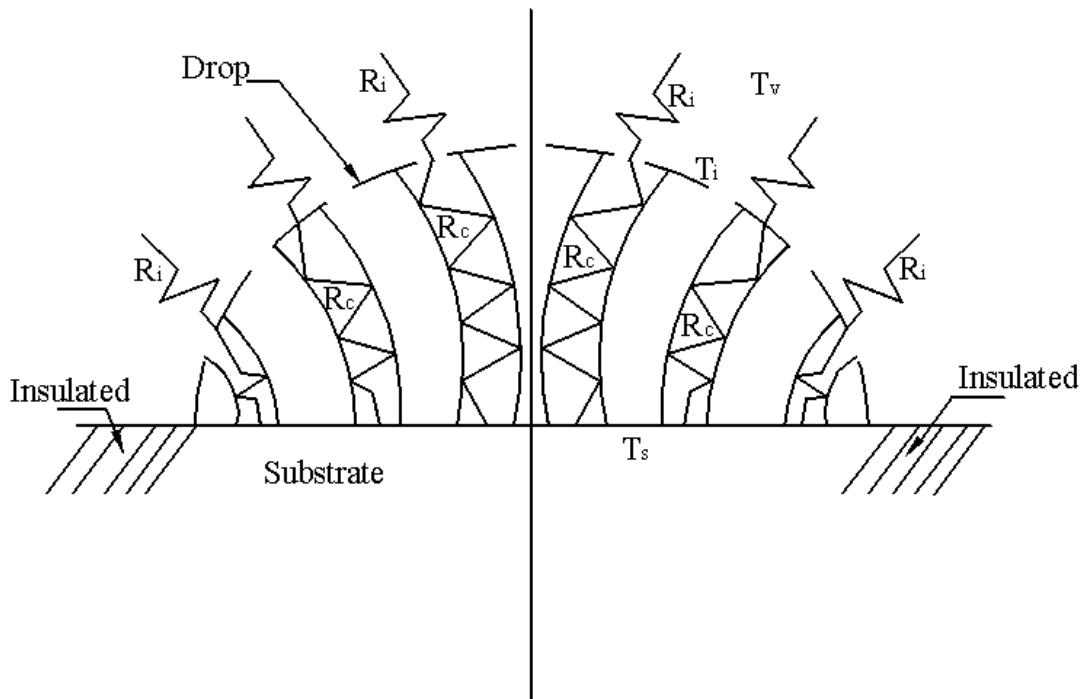


Figure 3.2 Thermal resistances associated with the drop

The major portion of heat transfer in dropwise condensation takes place near the edge of the droplet. While R_i remains constant at the surface of the drop, R_c decreases to the edge of the droplet. That is, there is much lower resistance to the heat transfer near the edge of the droplet.

In recent, studies of the mathematical modeling of dropwise condensation the surface temperature of the droplet is assumed to be equal to the temperature of the surrounding vapor. In this model, since the surface temperature of the drop is taken constant and interfacial thermal resistance is neglected calculation of the temperature distribution in the drop becomes much simpler. Nevertheless, in this approach the isotherm on the drop surface and the isotherm on the drop base which

have different temperature values meet at the edge of the drop and at the edge of the drop the anomaly of existence of two different temperatures takes place. To avoid this anomaly the edge elements of the drop is not taken into consideration in heat transfer calculations which results in a large error since most of the heat transfer through the droplet takes place here. In the study, the conduction model for individual droplet will also consider the thermal resistance due to the interfacial heat transfer coefficient.

Schrage's equation for interphase mass transfer under nonequilibrium conditions is modified by means of the Kelvin-Helmholtz equation and Clausius-Clapeyron relation.

Mass transfer through the interface is given under nonequilibrium conditions by,

$$w = \left(\frac{2g}{2-g} \right) \left(\frac{1}{2pg} \right)^{1/2} \left[\frac{P_v}{T_v^{1/2}} - \frac{P_i^{**}}{T_i^{1/2}} \right] \quad (3.5)$$

where

- γ : Condensation coefficient
- ω : Net rate of condensation per unit interfacial area
- P_i^{**} : Equilibrium pressure corresponding to the temperature of liquid-vapor interface
- P_v : Vapor pressure
- T_v : Vapor temperature
- T_i : Temperature of liquid vapor interface

Using Kelvin-Helmoltzs equation

$$\ln \frac{P_r^{**}}{P_i^*} = \frac{2sn_l}{rGT_i} \quad (3.6)$$

where

- P_r^{**} : Equilibrium pressure corresponding to the drop radius r
 P_i^* : Saturation pressure corresponding to temperature of liquid vapor interface temperature T_i
 σ : Surface tension
 v_l : Specific volume of liquid
 T_i : Temperature of liquid vapor interface
 G : Gas constant

By using the property of $P_r^{**} = P_i^{**}$ at interface, Eq. (3.5) becomes;

$$w = \left(\frac{2g}{2-g} \right) \left(\frac{1}{2pg} \right)^{1/2} \frac{P_v}{T_v^{1/2}} \left[1 - \frac{P_i^*}{P_v} e^{\frac{2sn_l}{rGT_i} \frac{T_v^{1/2}}{T_i^{1/2}}} \right] \quad (3.7)$$

From the Clasius-Clapeyron relation;

$$\ln \frac{P_i^*}{P_v^*} = -\frac{h_{fg}}{GT_i} \left(1 - \frac{T_i}{T_v} \right) \quad (3.8)$$

- P_v^* : Saturation pressure corresponding to vapor temperature

If it is assumed that the vapor is saturated, P_v in Eq. (3.7) becomes the saturation pressure P_v^* .

$$P_v = P_v^* \quad (3.9)$$

Substituting Eq. (3.9) and Eq. (3.8) into Eq. (3.7)

$$w = \left(\frac{2g}{2-g} \right) \left(\frac{1}{2pg} \right)^{1/2} \frac{P_v}{T_v^{1/2}} \left[1 - e^{-\frac{2sn_l}{rGT_i}} e^{-\frac{h_{fg}}{GT_i} \left(1 - \frac{T_i}{T_v} \right) \frac{T_v^{1/2}}{T_i^{1/2}}} \right] \quad (3.10)$$

From Eq. (3.6) and Eq. (3.8)

$$\ln \frac{P_i^*}{P_v^*} = -\frac{h_{fg}}{GT_i} \left(1 - \frac{T_i}{T_v} \right) = -\frac{2sn_l}{r^* GT_i} \quad (3.11)$$

$$h_i = \frac{wh_{fg}}{T_v - T_i} \quad (3.12)$$

Then, interface heat transfer coefficient becomes;

$$h_i = \frac{h_{fg}}{T_v - T_i} \left(\frac{2g}{2-g} \right) \left(\frac{1}{2pg} \right)^{1/2} \frac{P_v}{T_v^{1/2}} \left[1 - \frac{T_v^{1/2}}{T_i^{1/2}} \exp \left[-\frac{h_{fg}}{GT_i} \left(1 - \frac{T_i}{T_v} \right) \left(1 - \frac{R^*}{R} \right) \right] \right] \quad (3.13)$$

Using the approximation $T_v^{3/2} T_i = T_v^{5/2}$, expanding the exponential function in expression (3.13) and neglecting small terms, an expression for interfacial heat transfer coefficient becomes;

$$h_i = \left(\frac{2g}{2-g} \right) \left(\frac{1}{2p} \right)^{1/2} \frac{h_{fg}^2 P_v}{G^{3/2} T_v^{5/2}} \left(1 - \frac{R^*}{R} \right) \quad (3.14)$$

$$R^* = \frac{2T_{sat}S}{h_{fg} r_l \Delta T}$$

where

ρ_l : Liquid density

ΔT : Difference between vapor and interface temperature

R^* : Critical radius for formation of the droplet

R : The radius of curvature of the interface at the point of interest

Eq.(3.14) has been used in several drop conduction models. In this equation last term accounts for the effect of the curvature of the interface. In this study it can be neglected.

The heat transfer is determined by the effects of curvature, interfacial mass transfer between liquid and vapor phases, conduction through the drop, noncondensibles in the vapor and non-uniform conduction in the material forming the condensing surface. The effects of noncondensibles, non-uniform conduction in the material and effects of curvature have been omitted in this study.

In this way, the flow of heat from vapor to solid is controlled by two resistances, namely the interfacial resistance and conduction resistance through the drop. These resistances is shown in Figure 3.2.

Thermal resistance associated with the interfacial heat transfer coefficient for a hemispherical drop can be expressed as;

$$R_i = \frac{1}{h_i} \tag{3.15}$$

$$b = q - a$$

where

θ : contact angle between drop and surface

$$\widehat{APB} = a$$

Angle of arc AP is $2a$

So the angle of \widehat{AOP} become equal to the angle of arc by the geometrical property.

$$\widehat{AOP} = 2a$$

The length of AP is equal to KP. In the triangle \widehat{AOP} line OM, which is drawn perpendicular to the line AP, become bisector and intersect AP into the two equal pieces.

$$\widehat{AOM} = \widehat{MOP} = a$$

$$AM = \left(\frac{r - x}{2} \right)$$

In the triangle \widehat{OMP} ;

$$\sin a = \frac{AM}{R} = \frac{\left(\frac{r - x}{2} \right)}{R}$$

$$a = \sin^{-1} \left(\frac{\left(\frac{r-x}{2} \right)}{R} \right)$$

$$z + q = 90 \quad D\hat{P}O = z \quad \text{So; } D\hat{O}P = q$$

In the triangle $D\hat{O}P$;

$$\sin q = \frac{r}{R} \quad \Rightarrow \quad R = \frac{r}{\sin q}$$

$$a = \sin^{-1} \left(\frac{\left(\frac{r-x}{2} \right)}{\frac{r}{\sin q}} \right) = \sin^{-1} \left[\left(\frac{r-x}{2} \right) \frac{\sin q}{r} \right] \quad (3.18)$$

$$R_c = \frac{(r-x)}{k} [q - a] \quad (3.19)$$

Substituting Eq. (3.18) into the Eq. (3.19)

$$R_c = \frac{(r-x)}{k} \left[q - a \sin \left(\left(\frac{r-x}{2} \right) \frac{\sin q}{r} \right) \right] \quad (3.20)$$

Modifying R_c according to nondimensional length;

$$\tilde{r} = \frac{x}{r} \quad (3.21)$$

$$1 = \frac{r}{r} \quad (3.22)$$

\tilde{r} : Nondimensional drop radius

Substituting Eq. (3.21) and Eq. (3.22) into the Eq. (3.17) and Eq. (3.18)

$$\mathbf{l} = (r1 - \tilde{r}r)\mathbf{b} = r(1 - \tilde{r})\mathbf{b}$$

$$a = \sin^{-1} \left(\frac{\left(\frac{r1 - \tilde{r}r}{2} \right)}{\frac{r1}{\sin q}} \right) = \sin^{-1} \left[r \left(\frac{1 - \tilde{r}}{2} \right) \frac{\sin q}{r} \right] = \sin^{-1} \left[\left(\frac{1 - \tilde{r}}{2} \right) \sin q \right]$$

So R_c becomes;

$$R_c = \frac{r(1 - \tilde{r})}{k} \left[q - a \sin \left(\frac{(1 - \tilde{r})}{\left(\frac{2}{\sin q} \right)} \right) \right] \quad (3.23)$$

Total thermal resistance can be expressed as;

$$R_t = R_i + R_c$$

$$R_t = \frac{1}{h_i} + \frac{r(1 - \tilde{r})}{k} \left[q - a \sin \left(\frac{(1 - \tilde{r})}{\left(\frac{2}{\sin q} \right)} \right) \right] \quad (3.24)$$

Overall heat transfer coefficient which is equal to the inverse of the total thermal resistance becomes;

$$U = \frac{1}{R_t}$$

$$U = \frac{1}{\frac{1}{h_i} + \frac{r(1-\tilde{r})}{k_d} \left[q - a \sin \left(\frac{(1-\tilde{r})}{\left(\frac{2}{\sin q}\right)} \right) \right]} \quad (3.25)$$

The transformed form of the differential equation and the boundary condition system which is obtained after replacing the droplet by the thermal resistances is shown in Figure 3.4. In the figure r and T_s represent the radius and condenser surface temperature, respectively.

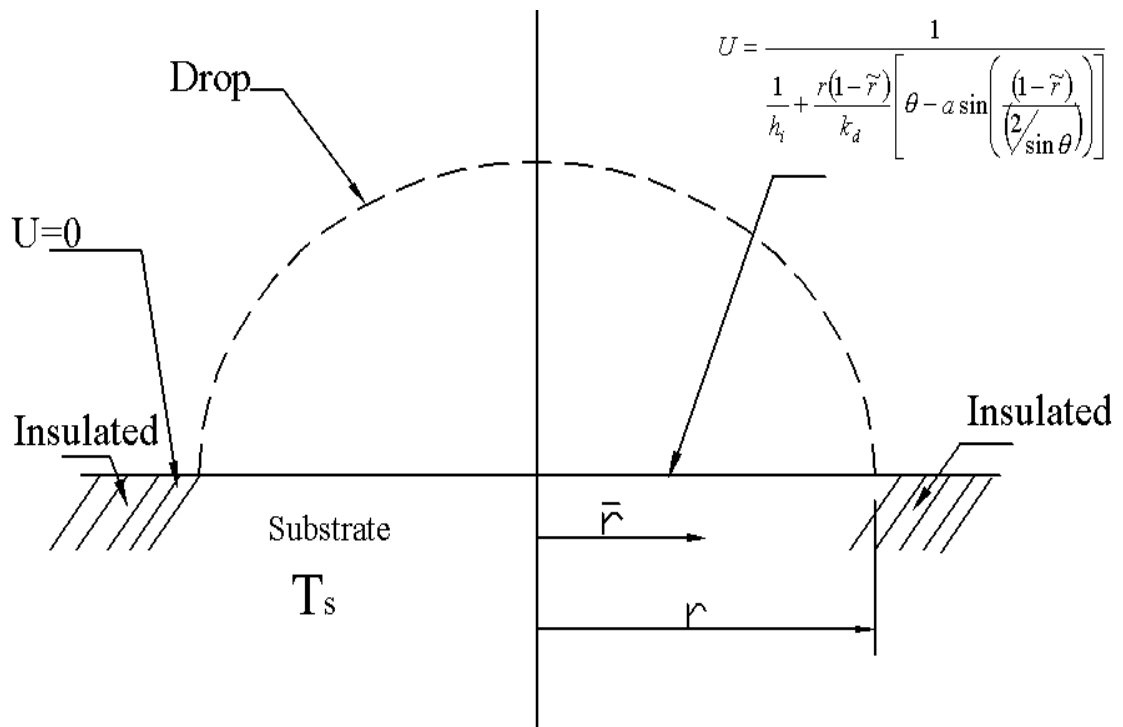


Figure 3.4 Overall heat transfer coefficient under the droplet and bare area

Differential equation for the substrate material is;

$$\frac{1}{\bar{r}} \frac{\partial T_s}{\partial \bar{r}} + \frac{\partial^2 T_s}{\partial \bar{r}^2} + \frac{\partial^2 T_s}{\partial \bar{z}^2} = \frac{rC}{k_s} \frac{\partial T_s}{\partial t}$$

At steady state, differential equation reduces to;

$$\frac{1}{\bar{r}} \frac{\partial T_s}{\partial \bar{r}} + \frac{\partial^2 T_s}{\partial \bar{r}^2} + \frac{\partial^2 T_s}{\partial \bar{z}^2} = 0 \quad (3.26)$$

On the surface of the substrate material heat conduction rate can be equated to heat convection represented by the overall heat transfer coefficient U.

$$-k_s \left. \frac{\partial T}{\partial \bar{z}} \right|_{\bar{z}=0} = U(T_s|_{\bar{z}=0} - T_v) \quad (3.27)$$

where

$$U = \frac{1}{\frac{1}{h_i} + \frac{r(1-\tilde{r})}{k_d} \left[q - a \sin \left(\frac{(1-\tilde{r})}{\left(\frac{2}{\sin q} \right)} \right) \right]} \quad \text{for } \bar{r} \leq r \quad (3.28)$$

$$U = 0 \quad \text{for } \bar{r} > r \quad (3.29)$$

r is the radius of the drop

At large distance in z direction in the substrate;

$$T_s|_{\bar{z} \rightarrow \infty} = T_0 \quad (3.30)$$

After obtaining the differential equation and the boundary conditions, these equations and boundary conditions are written in nondimensional form as follows

The nondimensionalized differential equation;

$$r^2 \left(\frac{1}{\bar{r}} \frac{\partial T_s}{\partial \bar{r}} + \frac{\partial^2 T_s}{\partial \bar{r}^2} + \frac{\partial^2 T_s}{\partial \bar{z}^2} \right) = 0$$

$$\frac{1}{\left(\frac{\bar{r}}{r}\right)} \frac{\partial T_s}{\partial \left(\frac{\bar{r}}{r}\right)} + \frac{\partial^2 T_s}{\partial \left(\frac{\bar{r}^2}{r^2}\right)} + \frac{\partial^2 T_s}{\partial \left(\frac{\bar{z}^2}{r^2}\right)} = 0$$

$$\frac{1}{\tilde{r}} \frac{\partial T_s}{\partial \tilde{r}} + \frac{\partial^2 T_s}{\partial \tilde{r}^2} + \frac{\partial^2 T_s}{\partial \tilde{z}^2} = 0$$

$$\frac{1}{\frac{T - T_0}{T_v - T_0}} \left(\frac{1}{\tilde{r}} \frac{\partial T_s}{\partial \tilde{r}} + \frac{\partial^2 T_s}{\partial \tilde{r}^2} + \frac{\partial^2 T_s}{\partial \tilde{z}^2} \right) = 0$$

$$\frac{1}{\tilde{r}} \frac{\partial \tilde{T}_s}{\partial \tilde{r}} + \frac{\partial^2 \tilde{T}_s}{\partial \tilde{r}^2} + \frac{\partial^2 \tilde{T}_s}{\partial \tilde{z}^2} = 0 \tag{3.31}$$

where

\tilde{T}_s : nondimensional surface temperature

Nondimensionalized boundary condition at condenser surface;

$$-k_s \frac{\partial T}{\partial \bar{z}} \Big|_{z=0} = \left(\frac{1}{\frac{1}{h_i} + \frac{r(1-\tilde{r})}{k_d} \left[q - a \sin \left(\frac{(1-\tilde{r})}{(2/\sin q)} \right) \right]} \right) (T_s|_{z=0} - T_v) \quad (3.32)$$

$$\frac{\partial \tilde{T}_s}{\partial \left(\frac{\tilde{z}}{r} \right)} = \frac{1}{r} \left(\frac{1}{\frac{1}{h_i} + \frac{r(1-\tilde{r})}{k_d} \left[q - a \sin \left(\frac{(1-\tilde{r})}{(2/\sin q)} \right) \right]} \right) (1 - \tilde{T}_s)$$

$$\frac{\partial \tilde{T}_s}{\partial \tilde{z}} \Big|_{\tilde{z}=0} = \left(\frac{1}{\frac{k_s}{r \times h_i} + (1-\tilde{r}) \left[q - a \sin \left(\frac{(1-\tilde{r})}{(2/\sin q)} \right) \right] \frac{k_s}{k_d}} \right) (1 - \tilde{T}_s|_{\tilde{z}=0}) \quad (3.33)$$

Defining nondimensional parameters $A = k_s/k_d$ and $B = k_s/(h_i r)$ in the Eq.(3.33);

$$\left. \frac{\partial \tilde{T}_s}{\partial \tilde{z}} \right|_{\tilde{z}=0} = \left(\frac{1}{B + (1 - \tilde{r}) \left[q - a \sin \left(\frac{(1 - \tilde{r})}{\left(\frac{2}{\sin q} \right)} \right) \right]} \right) \left(1 - \tilde{T}_s \Big|_{\tilde{z}=0} \right) \quad (3.34)$$

Nondimensional overall heat transfer coefficient is obtained as follows;

$$\frac{rU}{k_s} = \frac{1}{\frac{k_s}{h_i r} + \frac{k_s}{k_d} (1 - \tilde{r}) \left[q - a \sin \left(\frac{(1 - \tilde{r})}{\left(\frac{2}{\sin q} \right)} \right) \right]} \quad (3.35)$$

Nondimensional overall heat transfer coefficient is called as nondimensional drop resistance parameter F_r .

$$F_r = \frac{1}{\frac{k_s}{h_i r} + \frac{k_s}{k_d} (1 - \tilde{r}) \left[q - a \sin \left(\frac{(1 - \tilde{r})}{\left(\frac{2}{\sin q} \right)} \right) \right]} \quad (3.36)$$

or

$$F_r = \frac{1}{B + (1 - \tilde{r}) \left[q - a \sin \left(\frac{(1 - \tilde{r})}{\left(\frac{2}{\sin q} \right)} \right) \right]} A \quad (3.37)$$

Consequently the problem is reduced to the following form;

$$\frac{1}{\tilde{r}} \frac{\partial \tilde{T}_s}{\partial \tilde{r}} + \frac{\partial^2 \tilde{T}_s}{\partial \tilde{r}^2} + \frac{\partial^2 \tilde{T}_s}{\partial \tilde{z}^2} = 0$$

with the boundary conditions;

$$\tilde{T}_s \Big|_{\tilde{z} \rightarrow \infty} = 0$$

$$\frac{\partial \tilde{T}_s}{\partial \tilde{z}} \Big|_{\tilde{z}=0} = \left(\frac{1}{B + (1 - \tilde{r}) \left[q - a \sin \left(\frac{(1 - \tilde{r})}{\left(\frac{2}{\sin q} \right)} \right) \right]} \right) \left(1 - \tilde{T}_s \Big|_{\tilde{z}=0} \right)$$

or

$$\frac{\partial \tilde{T}_s}{\partial \tilde{z}} \Big|_{\tilde{z}=0} = F_r \left(1 - \tilde{T}_s \Big|_{\tilde{z}=0} \right) \quad (3.38)$$

with the boundary conditions;

$$F_r = \frac{1}{B + (1 - \tilde{r}) \left[q - a \sin \left(\frac{(1 - \tilde{r})}{\left(\frac{2}{\sin q} \right)} \right) \right]} \quad \text{for} \quad \tilde{r} \leq 1 \quad (3.39)$$

$$F_r = 0 \quad \text{for} \quad \tilde{r} > 1 \quad (3.40)$$

3.1.3 Average Temperature Under the Droplet

Temperature distribution in the substrate can be obtained by solving the differential equation with its boundary conditions given in the previous section. Then, the average nondimensional temperature under the droplet is obtained as follows.

$$\tilde{T}_{av} = \frac{1}{\pi \tilde{r}^2} \int_{\tilde{r}=0}^{\tilde{r}=1} \tilde{T}_s 2\pi \tilde{r} d\tilde{r} \quad (3.41)$$

Fraction of area occupied by droplets is given by;

$$f_{co}(r) = 1 - \left(\frac{r}{r_{\max}} \right)^n$$

$$d[f_{co}(r)] = d \left[1 - \left(\frac{r}{r_{\max}} \right)^n \right]$$

$$df_{co}(r) = n \left(\frac{r}{r_{\max}} \right)^{n-1} \frac{dr}{r_{\max}} \quad (3.42)$$

Consequently average nondimensional condenser surface temperature in dropwise condensation is obtained by integrating average nondimensional temperature of drop to substrate interface over the size distribution of the drops in dropwise condensation.

$$\tilde{T}_{ad} = \int_{r_{\min}}^{r_{\max}} \tilde{T}_{av} df_{co} \quad (3.43)$$

3.1.4 Heat Transfer and Heat Flux

Heat transfer through a single droplet is given by;

$$Q = \int_{\bar{r}=0}^{\bar{r}=r} -k \frac{\partial T}{\partial \bar{z}} \Big|_{\bar{z}=0} 2\pi \bar{r} d\bar{r} \quad (3.44)$$

or

$$Q = \int_{\bar{r}=0}^{\bar{r}=r} U(T_v - T_s|_{\bar{z}=0}) 2p \bar{r} d\bar{r} \quad (3.45)$$

Nondimensional heat transfer is obtained as follows;

$$\frac{1}{k_s \Delta T} \left(\frac{Q}{r} \right) = \left(\int_{\bar{r}=0}^{\bar{r}=r} U r (T_v - T_s|_{\bar{z}=0}) 2p \frac{\bar{r}}{r} d \frac{\bar{r}}{r} \right) \frac{1}{k_s \Delta T}$$

$$\frac{Q}{k_s r \Delta T} = \int_{\bar{r}=0}^{\bar{r}=r} \frac{U r}{k_s} \frac{(T_v - T_s|_{\bar{z}=0})}{\Delta T} 2p \frac{\bar{r}}{r} d \frac{\bar{r}}{r}$$

$$Q_{nd} = \int_{\tilde{r}=0}^{\tilde{r}=1} F_r (1 - \tilde{T}_s|_{\tilde{z}=0}) 2p \tilde{r} d\tilde{r} \quad (3.46)$$

and

$$Q_{nd} = \frac{Q}{k_s r \Delta T}$$

where $\Delta T = T_v - T_0$

Total heat transfer is obtained by integrating heat transfer through the droplet over the size distributions of the drops in dropwise condensation.

$$Q_{dc} = \int_{r_{\min}}^{r_{\max}} Q df_{co} \quad (3.47)$$

or

$$Q_{dc} = \int_{r_{\min}}^{r_{\max}} Q n \left(\frac{r}{r_{\max}} \right)^{n-1} \frac{dr}{r_{\max}} \quad (3.48)$$

Then, total heat flux becomes;

$$Q''_{dc} = \int_{r_{\min}}^{r_{\max}} \frac{Q}{pr^2} \times n \left(\frac{r}{r_{\max}} \right)^{n-1} \frac{dr}{r_{\max}} \quad (3.49)$$

3.2 Finite Difference Solution of Dropwise Condensation with Substrate Material Effect

3.2.1 Temperature Distribution in the Substrate and Under the Droplet

In order to obtain the temperature distribution in the substrate under the droplet a computer code (FORTRAN program), which is given in Appendix A, is used. In the program thermal conductivity of the substrate material and the radius of the droplet is chosen and entered as the main data in addition to other thermal and geometric parameters. Nodal points for temperatures nodes in the substrate and under the droplet is shown in Figure 3.5. In a drop profile substrate material is divided into 1830 nodes. Nondimensional temperatures are equal to zero in the substrate and unity in the condensing vapor. Consequently, nondimensional temperature distribution in the substrate under the newly formed small droplets and the larger droplets that forms as a result of coalescences should be zero. For that reason, the nodal points that represents the initial nondimensional temperature distribution in the substrate are given the value zero and by using the time marching technique steady state temperature in the droplets are obtained. Nodal equations are obtained by discretizing the substrate under the droplet and applying the conservation of the thermal energy for each node. Equations are differed according to special nodes (4, 5, 6, 7, 8, 9, 10, 11, 12, 13). Substrate material is divided into 61 section on radial (r) and 30 section on axial (z) direction. For all conditions nondimensional drop radius is taken as unity which is represented by node 31.

In the program there are two nondimensional parameter that effect temperature distribution and heat transfer. These parameters are as shown before A and B.

$$A = \frac{k_s}{k_d} \quad (3.50)$$

$$B = \frac{k_s}{h_i r} \quad (3.51)$$

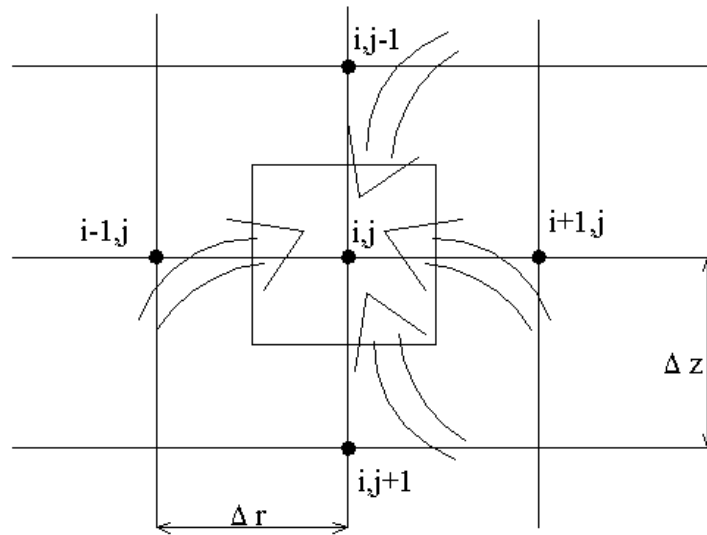
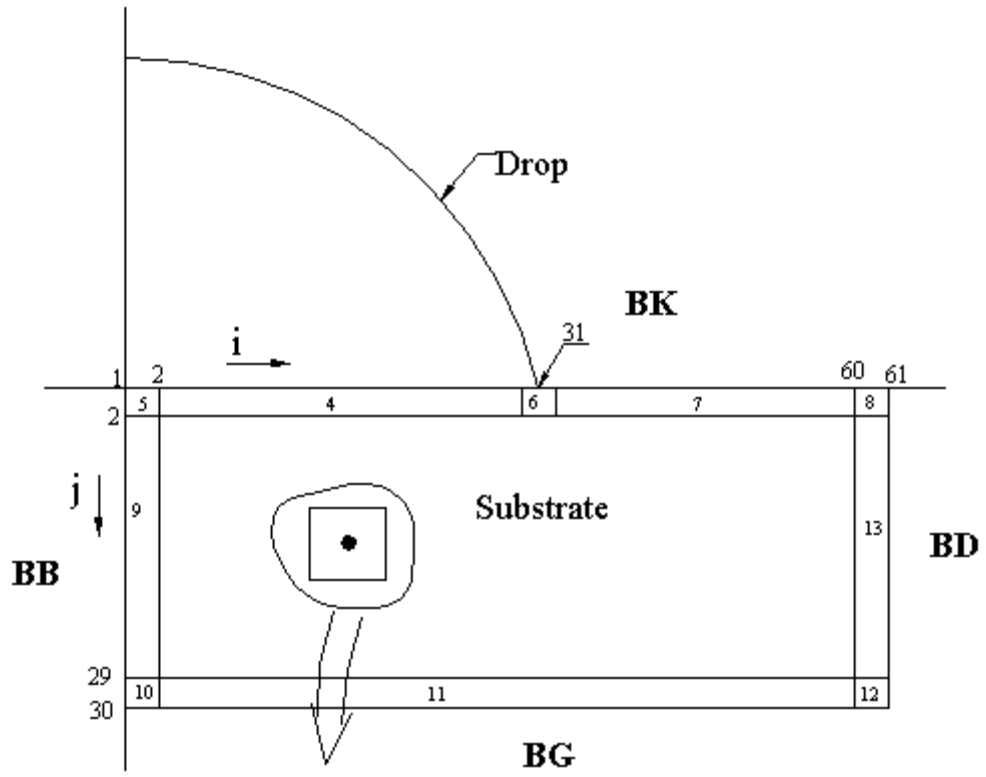


Figure 3.5 Temperature nodes under the drop and in the substrate

Nodal temperature equations for the interior nodes (i=2,60 and j=2,29):

$$A10 = -\frac{rCp}{k_s dt} r^2 \left[\left(\frac{rr_{i+1} + rr_i}{2} \right)^2 - \left(\frac{rr_i + rr_{i-1}}{2} \right)^2 \right] \left(\frac{\tilde{z}_{j+1} - \tilde{z}_{j-1}}{2} \right) \quad (3.52)$$

$$BG = (T_{i,j} - T_{i,j+1}) \frac{\left[\left(\frac{rr_{i+1} + rr_i}{2} \right)^2 - \left(\frac{rr_i + rr_{i-1}}{2} \right)^2 \right]}{(\tilde{z}_{j+1} - \tilde{z}_j)} \quad (3.53)$$

$$BB = (T_{i,j} - T_{i-1,j}) \frac{\left[\left(\frac{rr_i + rr_{i-1}}{2} \right) (\tilde{z}_{j+1} - \tilde{z}_{j-1}) \right]}{rr_i - rr_{i-1}} \quad (3.54)$$

$$BD = (T_{i,j} - T_{i+1,j}) \frac{\left[\left(\frac{rr_{i+1} + rr_i}{2} \right) (\tilde{z}_{j+1} - \tilde{z}_{j-1}) \right]}{rr_{i+1} - rr_i} \quad (3.55)$$

$$BK = (T_{i,j} - T_{i,j-1}) \frac{\left[\left(\frac{rr_{i+1} + rr_i}{2} \right)^2 - \left(\frac{rr_i + rr_{i-1}}{2} \right)^2 \right]}{(\tilde{z}_j - \tilde{z}_{j-1})} \quad (3.56)$$

$$TN_{i,j} = T_{i,j} + \frac{(BK + BG + BB + BD)}{A10} \quad (3.57)$$

$TN_{i,j}$ is new temperature of node i, j after time interval dt.

rr_i : Notation used in the computer program for nondimensional radial direction.

\tilde{z}_j : Notation used in the computer program for nondimensional axial direction.

BG, BB, BD, BK are defined as south, west, east and north directions, respectively. BB and BK are set to be 0 for the special nodes 5, 9, 10 and 7, 8. These points are considered as thermally insulated.

Nodal temperature equations for the node 4 (i=2,30 and j=1):

$$A10 = -\frac{rCp}{k_s dt} r^2 \left[\left(\frac{rr_{i+1} + rr_i}{2} \right)^2 - \left(\frac{rr_i + rr_{i-1}}{2} \right)^2 \right] \left(\frac{\tilde{z}_{j+1} - \tilde{z}_j}{2} \right) \quad (3.58)$$

$$BG = (T_{i,j} - T_{i,j+1}) \frac{\left[\left(\frac{rr_{i+1} + rr_i}{2} \right)^2 - \left(\frac{rr_i + rr_{i-1}}{2} \right)^2 \right]}{(\tilde{z}_{j+1} - \tilde{z}_j)} \quad (3.59)$$

$$BB = (T_{i,j} - T_{i-1,j}) \frac{\left[\left(\frac{rr_i + rr_{i-1}}{2} \right) (\tilde{z}_{j+1} - \tilde{z}_j) \right]}{rr_i - rr_{i-1}} \quad (3.60)$$

$$BD = (T_{i,j} - T_{i+1,j}) \frac{\left[\left(\frac{rr_{i+1} + rr_i}{2} \right) (\tilde{z}_{j+1} - \tilde{z}_j) \right]}{rr_{i+1} - rr_i} \quad (3.61)$$

$$BK = (T_{i,j} - 1) \left[\left(\frac{rr_{i+1} + rr_i}{2} \right)^2 - \left(\frac{rr_i + rr_{i-1}}{2} \right)^2 \right] F_r \quad (3.62)$$

Nodal temperature equations for the node 5 (i=1 and j=1):

$$A10 = -\frac{rCp}{k_s dt} r^2 \left(\frac{rr_{i+1} + rr_i}{2} \right)^2 \left(\frac{\tilde{z}_{j+1} - \tilde{z}_j}{2} \right) \quad (3.63)$$

$$BG = (T_{i,j} - T_{i,j+1}) \frac{\left(\frac{rr_{i+1} + rr_i}{2} \right)^2}{(\tilde{z}_{j+1} - \tilde{z}_j)} \quad (3.64)$$

$$BB = 0 \quad (3.65)$$

$$BD = (T_{i,j} - T_{i+1,j}) \frac{\left[\left(\frac{rr_{i+1} + rr_i}{2} \right) (\tilde{z}_{j+1} - \tilde{z}_j) \right]}{rr_{i+1} - rr_i} \quad (3.66)$$

$$BK = (T_{i,j} - 1) \left(\frac{rr_{i+1} + rr_i}{2} \right)^2 F_r \quad (3.67)$$

Nodal temperature equations for the node 6 (i=31 and j=1):

A10, BG, BB, BD points are same as Eq. (3.58), (3.59), (3.60), (3.61), respectively.

$$BK = (T_{i,j} - 1) \left[\left(\frac{rr_{i+1} + rr_i}{2} \right)^2 - \left(\frac{rr_i + rr_{i-1}}{2} \right)^2 \right] \frac{F_r}{2} \quad (3.67)$$

The most important phenomena in dropwise condensation is the heat conduction through the droplet. Temperature distribution in the surface under the droplet plays important role in the heat transfer through a droplet.

Thermal resistance of condensate is getting smaller as one approaches to the edge of the droplet. Temperature of the substrate under the droplet changes drastically as one gets near the edge of the droplet. Consequently, temperature nodes

close to the droplet edge should be chosen very close to each other in the radial and axial direction.

In order to avoid sudden temperature changes and to get more accurate results; an exponential variation of the distance between nodal points such as Eq. (3.68) is employed. With this equation the intervals of these nodes become smaller and getting very close from center of droplet to the edge in the radial direction. So, nondimensional radial distance between $i=1$ and $i=29$ is found by;

$$rr_i = 1 - (0.0001)e^{[0.3070113(30-i)]} \quad (3.68)$$

To large distances from the edge of the droplet a gradually increasing increments in the nondimensional radial direction is targeted. Between $i=32$ and $i=60$;

$$rr_i = 1 + (0.0001)e^{[0.3070113(i-30)]} \quad (3.69)$$

Just like in the radial direction, in the axial direction the intervals are taken closer. As one gets close to the edge of the droplet between $j=1$ and $j=30$ nondimensional axial \tilde{z}_j distances is obtained according to the equation below;

$$\tilde{z}_j = (0.0001)e^{[0.4111759(j-1)]} \quad (3.70)$$

The values of nondimensional radial distance rr_i in the radial direction and nondimensional axial distance \tilde{z}_j in the axial direction are given in Appendix B.

In the previous section drop resistance parameter is defined in terms of nondimensional parameters A and B as follows;

$$F_r = \frac{1}{B + (1 - \tilde{r}) \left[q - a \sin \left(\frac{(1 - \tilde{r})}{\left(\frac{2}{\sin q} \right)} \right) \right]} A \quad (3.71)$$

In the model nodes 4, 5, 6 which are the nodes at the interface between the drop and the substrate play important role in the heat transfer. In order to obtain the heat transfer through the droplet, conservation of energy principle is used. Equations are written as:

$$TN_{i,j} - T_{i,j} = \frac{(T_{i,j} - 1) \left[\left(\frac{rr_{i+1} + rr_i}{2} \right)^2 - \left(\frac{rr_i + rr_{i-1}}{2} \right)^2 \right] \left[\frac{1}{\frac{k_s}{h_i r} + (1 - rr_i) \left[q - a \sin \left(\frac{(1 - rr_i)}{\left(\frac{2}{\sin q} \right)} \right) \right]} \frac{k_s}{k_d} \right]}{-\frac{rCp}{k_s dt} r^2 \left[\left(\frac{rr_{i+1} + rr_i}{2} \right)^2 - \left(\frac{rr_i + rr_{i-1}}{2} \right)^2 \right] \left(\frac{\tilde{z}_{j+1} - \tilde{z}_j}{2} \right)} \quad (3.72)$$

Outer and inner nondimensional radius:

$$r_o^* = \left(\frac{rr_{i+1} + rr_i}{2} \right) \quad (3.73)$$

$$r_i^* = \left(\frac{rr_i + rr_{i-1}}{2} \right) \quad (3.74)$$

Substituting Eq. (3.74) and Eq. (3.73) into the Eq. (3.72):

$$TN_{i,j} - T_{i,j} = \frac{(1 - T_{i,j}) \left[r_o^{*2} - r_i^{*2} \right] \left[\frac{1}{\frac{k_s}{h_i r} + (1 - rr_i) \left[q - a \sin \left(\frac{(1 - rr_i)}{\left(\frac{2}{\sin q} \right)} \right) \right]} \frac{k_s}{k} \right]}{\frac{rCp}{k_s dt} r^2 \left(r_o^{*2} - r_i^{*2} \right) \left(\frac{\tilde{z}_{j+1} - \tilde{z}_j}{2} \right)} \quad (3.75)$$

The steps between the equations are presented in Appendix C.

Eq. (3.76), (3.77), (3.78) defines Q_{num} (heat transfer calculated by numerical methods which is nondimensional), Q_{nd} (nondimensional heat transfer), Q (dimensional heat transfer), respectively.

$$Q_{num} = F_r (1 - T_{i,1}) p (r_o^{*2} - r_i^{*2}) \quad (3.76)$$

$$Q_{nd} = Q_{num} \frac{k_s}{k} \quad (3.77)$$

$$Q = Q_{num} r k_s \Delta T \quad (3.78)$$

The heat flux at the base of the droplet is obtained dividing the heat transfer through the drop by drop base area.

$$Q'' = \frac{Q}{p r^2} \quad (3.79)$$

3.2.2 Average Temperature Under the Droplet

In order to find average nondimensional temperature under the droplet; nondimensional temperature of each node is multiplied with area of each segment and divided into the total droplet area. Consequently the average nondimensional temperature under the droplet can be expressed as:

$$T_{av} = \frac{T_{1,l} p r^2 \left(\frac{r r_2 + r r_1}{2} \right)^2 + T_{2,l} p r^2 \left[\left(\frac{r r_3 + r r_2}{2} \right)^2 - \left(\frac{r r_2 + r r_1}{2} \right)^2 \right] + \dots + T_{31,l} p r^2 (r r_{31}^2 - r r_{30}^2)}{p r^2 r_1^2 + p r^2 r_2^2 + \dots + p r^2 r_{31}^2} \quad (3.80)$$

$$T_{av} = \frac{\sum_{i=1}^{31} T_{i,1} A_i}{\sum_{i=1}^{31} A_i} \quad (3.81)$$

Eq. (3.81) gives the average nondimensional temperature of the single droplet. In order to find the dropwise condensation average nondimensional temperature (T_{ad}), average nondimensional temperature of drop to substrate interface integrated over the size distribution of the drops.

$$T_{ad} = df_{co} \left(\frac{r_1 + r_0}{2} \right) T_{av} \left(\frac{r_1 + r_0}{2} \right) + df_{co} \left(\frac{r_2 + r_1}{2} \right) T_{av} \left(\frac{r_2 + r_1}{2} \right) + \dots + df_{co} \left(\frac{r_{10000} + r_{9999}}{2} \right) T_{av} \left(\frac{r_{10000} + r_{9999}}{2} \right) \quad (3.82)$$

3.2.3 Total Heat Transfer and Heat Flux in Dropwise Condensation

Heat transfer through a single droplet is first calculated as explained in the previous section then total heat transfer is obtained by integrating the heat transfer through the entire drop population in dropwise condensation.

For the numerical calculation the complete radius interval of the dropsize distribution from r_{\min} to r_{\max} is divided in m separate intervals to obtain the incremental heat transfer values in df_{co} . The fraction of area occupied by droplets in the size range dr becomes, from Eq. (2.1):

$$d[f_{co}(r)] = d \left[1 - \left(\frac{r}{r_{\max}} \right)^n \right]$$

$$df_{co}(r) = n \left(\frac{r}{r_{\max}} \right)^{n-1} \frac{dr}{r_{\max}} \quad (3.83)$$

m : The number of divisions between r_{\min} to r_{\max} (taken as 10000):

$$r_{\max} = k^m r_{\min}$$

$$k = \sqrt[m]{\frac{r_{\max}}{r_{\min}}} \quad (3.84)$$

$$r_i = k^i r_{\min} \quad (3.85)$$

i : 1, 2, 3...10000

With such a scheme the discrete value of the drop radius would be as follows:

$$i = 0 \quad r_0 = r_{\min}$$

$$i = 1 \quad r_1 = k r_{\min}$$

$$i = 2 \quad r_2 = k^2 r_{\min}$$

.

.

$$i = 10000 \quad r_{10000} = k^{10000} r_{\min} = r_{\max}$$

From Eq. (3.83), area increments for droplets, df_{co} can be expressed as:

$$df_{co}\left(\frac{r_i + r_{i-1}}{2}\right) = n \left[\frac{\left[\frac{r_i + r_{i-1}}{2} \right]}{r_{\max}} \right]^{n-1} \frac{(r_i - r_{i-1})}{r_{\max}} \quad (3.86)$$

Employing Eq. (3.86), the fraction of area covered by droplets on the condenser surface area at each increment, $df_{co}(r_i)$:

$$df_{co}\left(\frac{r_1 + r_0}{2}\right) = n \left[\frac{\left[\frac{r_1 + r_0}{2} \right]}{r_{\max}} \right]^{n-1} \frac{(r_1 - r_0)}{r_{\max}}$$

$$df_{co}\left(\frac{r_2 + r_1}{2}\right) = n \left[\frac{\left[\frac{r_2 + r_1}{2} \right]}{r_{\max}} \right]^{n-1} \frac{(r_2 - r_1)}{r_{\max}}$$

·
·

$$df_{co}\left(\frac{r_{10000} + r_{9999}}{2}\right) = n \left[\frac{\left[\frac{r_{10000} + r_{9999}}{2} \right]}{r_{\max}} \right]^{n-1} \frac{(r_{10000} - r_{9999})}{r_{\max}}$$

Employing Eq. (3.86) and individual heat transfer through the droplets, the total dropwise condensation heat transfer (Q_{dc}) is written as:

$$Q_{dc} = df_{co}\left(\frac{r_1 + r_0}{2}\right) q\left(\frac{r_1 + r_0}{2}\right) + df_{co}\left(\frac{r_2 + r_1}{2}\right) q\left(\frac{r_2 + r_1}{2}\right) + \dots + df_{co}\left(\frac{r_{10000} + r_{9999}}{2}\right) q\left(\frac{r_{10000} + r_{9999}}{2}\right) \quad (3.87)$$

The total dropwise condensation heat flux (Q''_{dc}) then becomes:

$$Q''_{dc} = \frac{df_{co} \left(\frac{r_1 + r_0}{2} \right) q \left(\frac{r_1 + r_0}{2} \right)}{p \left(\frac{r_1 + r_0}{2} \right)^2} + \frac{df_{co} \left(\frac{r_2 + r_1}{2} \right) q \left(\frac{r_2 + r_1}{2} \right)}{p \left(\frac{r_2 + r_1}{2} \right)^2} + \dots + \frac{df_{co} \left(\frac{r_{10000} + r_{9999}}{2} \right) q \left(\frac{r_{10000} + r_{9999}}{2} \right)}{p \left(\frac{r_{10000} + r_{9999}}{2} \right)^2} \quad (3.88)$$

3.2.4 Dropwise Condensation Heat Transfer Coefficient

Since total dropwise condensation heat flux and average dropwise condensation temperature has been calculated, so dropwise condensation heat transfer coefficient can be calculated by using Eq. (3.89):

$$h_{dc} = \frac{Q''_{dc}}{(1 - T_{ad}) \times 100} \quad (3.89)$$

CHAPTER 4

RESULTS AND DISCUSSIONS

Dropwise condensation on different substrate materials has been investigated mathematically and numerically in the previous chapter. Temperature distributions, heat transfer, heat flux and heat transfer coefficient are studied by means of the computer program with respect to the effect of the substrate material and drop radius. These results are described and represented graphically.

Results are also compared with results in the literature.

4.1 Computation Results for the Temperature Distribution Under the Droplet and in the Substrate

In the previous chapter differential equations are obtained for temperature distribution but, analytical solution of these differential equations are quite complicated. Thus these equations are not solved. In order to obtain the temperature distribution under the droplet and substrate material, the FORTRAN program which is developed is used. Program code follows the following steps.

Although condensing droplet substance can be taken as any liquid in the computer program developed in this study, taking the majority of the condenser applications into account, water is taken as the droplet substance and in calculating

the interfacial heat transfer coefficient h_i and in evaluating other thermal properties water thermal properties at average medium temperature are taken as the basis. Water thermal conductivity (k_d) is taken as $0.645 \text{ W/m}^2\text{K}$. In the study parameter 'A', which determine substrate thermal conductivity (k_s), is taken as 0.01, 0.1, 1, 10, 20, 50, 70, 100. By using Eq. (3.28) substrate thermal conductivity is calculated. In the second step, radius of droplet is determined according to the other dimensionless parameter 'B' with Eq. (3.29). In the study parameter 'B' is taken as 0.001, 0.0013, 0.0016, 0.002, 0.004, 0.006, 0.008, 0.01, 0.1, 1, 10, 100. Total temperature difference is taken as the largest possible for the condensation of water on a surface. Thus, temperature of the vapor and droplet is taken as $100 \text{ }^\circ\text{C}$ (373 K) and the temperature of the substrate is taken as $0 \text{ }^\circ\text{C}$ (273 K) at infinitely large distances from the surface of condensation. In the FORTRAN program developed for the temperature of substrate and for the temperature of vapor, nondimensional values 0 and 1, are used respectively. So the temperature values are represented as nondimensional in the tables and graphs in the study.

4.1.1 Temperature Distribution Under a Single Droplet and Substrate Material

Temperature distribution is dependent to substrate thermal conductivity (A) and drop radius (B). Variation of temperature distribution at the $\tilde{z} = 0$ and $\tilde{z} = 9.99 \times 10^{-5}$ for the B=0.001 and A=0.01, 0.1, 1, 10, 100; is shown in Figure 4.1, Figure 4.2 and Figure 4.3, Figure 4.4, respectively.

The data used in Figure 4.1 and Figure 4.3 is given in Appendix E.1 and E.2, respectively.

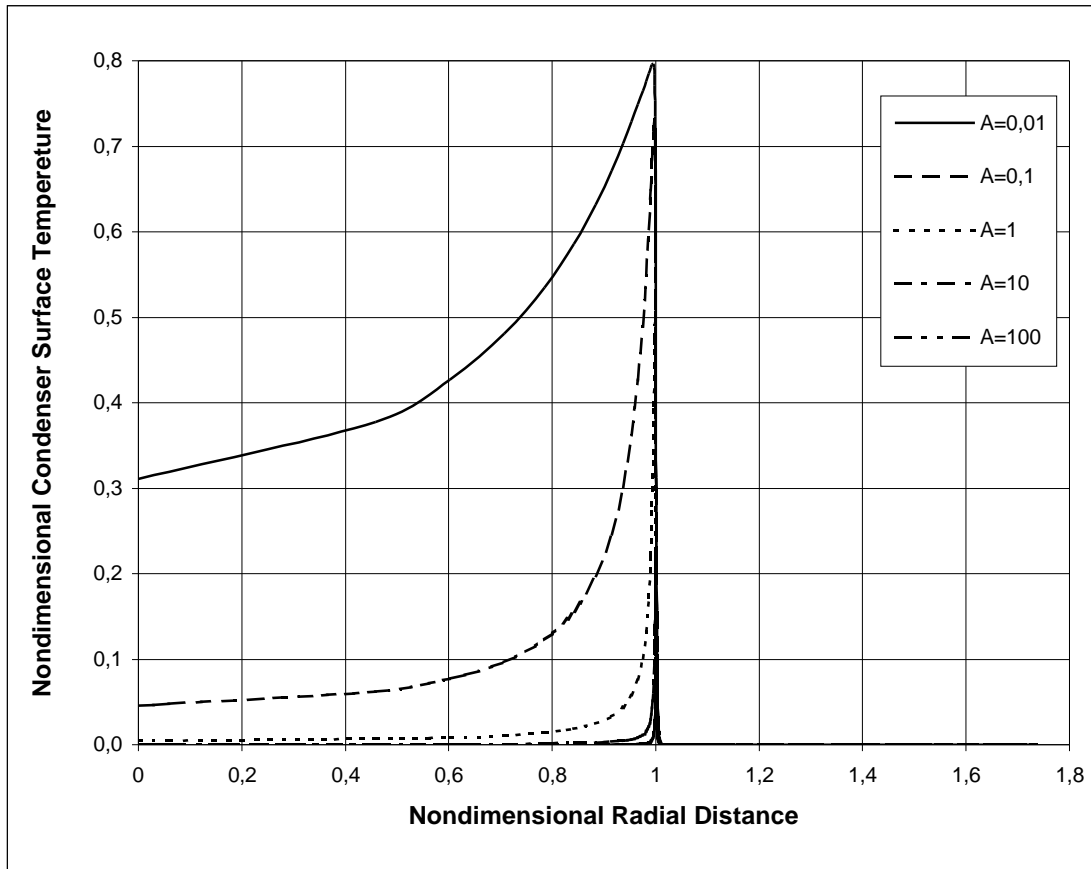


Figure 4.1 Variation of nondimensional temperature as a function of nondimensional radial distance at nondimensional axial distance $\tilde{z} = 0$ for $B=0.001$

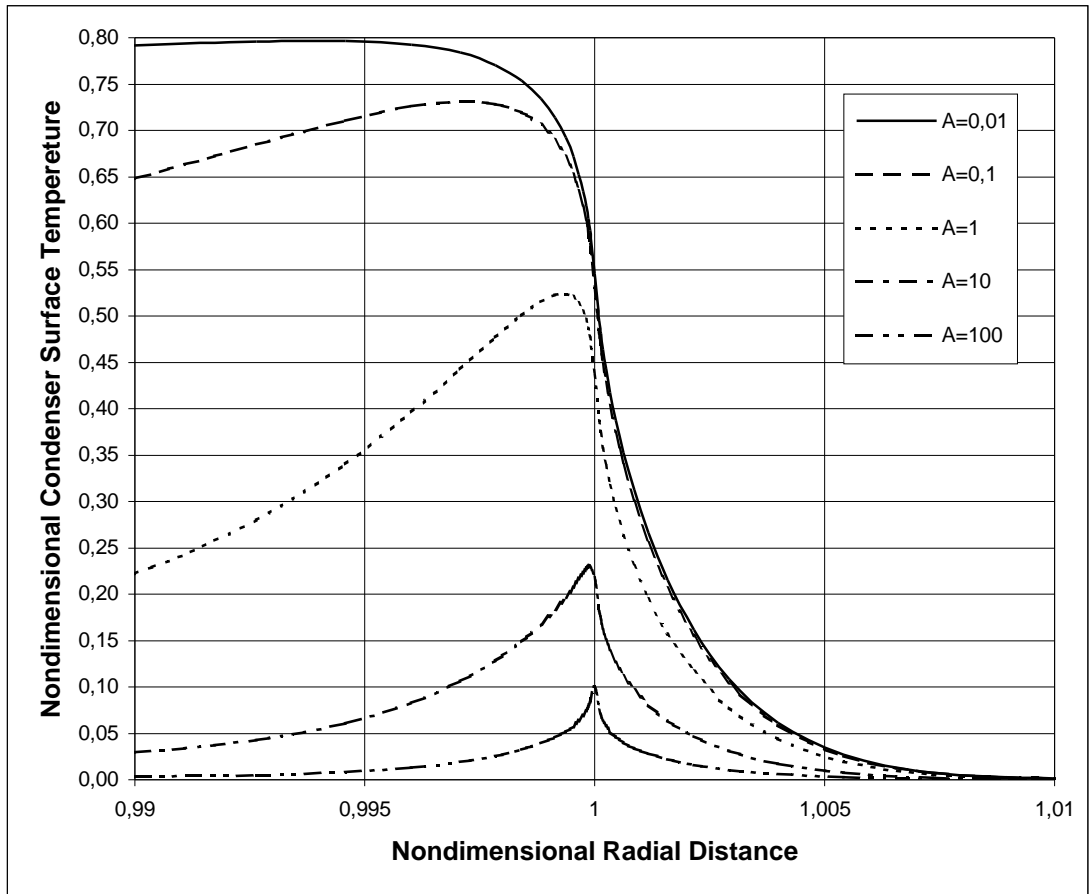


Figure 4.2 Variation of nondimensional temperature as a function of nondimensional radial distance at nondimensional axial distance $\tilde{z} = 0$ for $B=0.001$

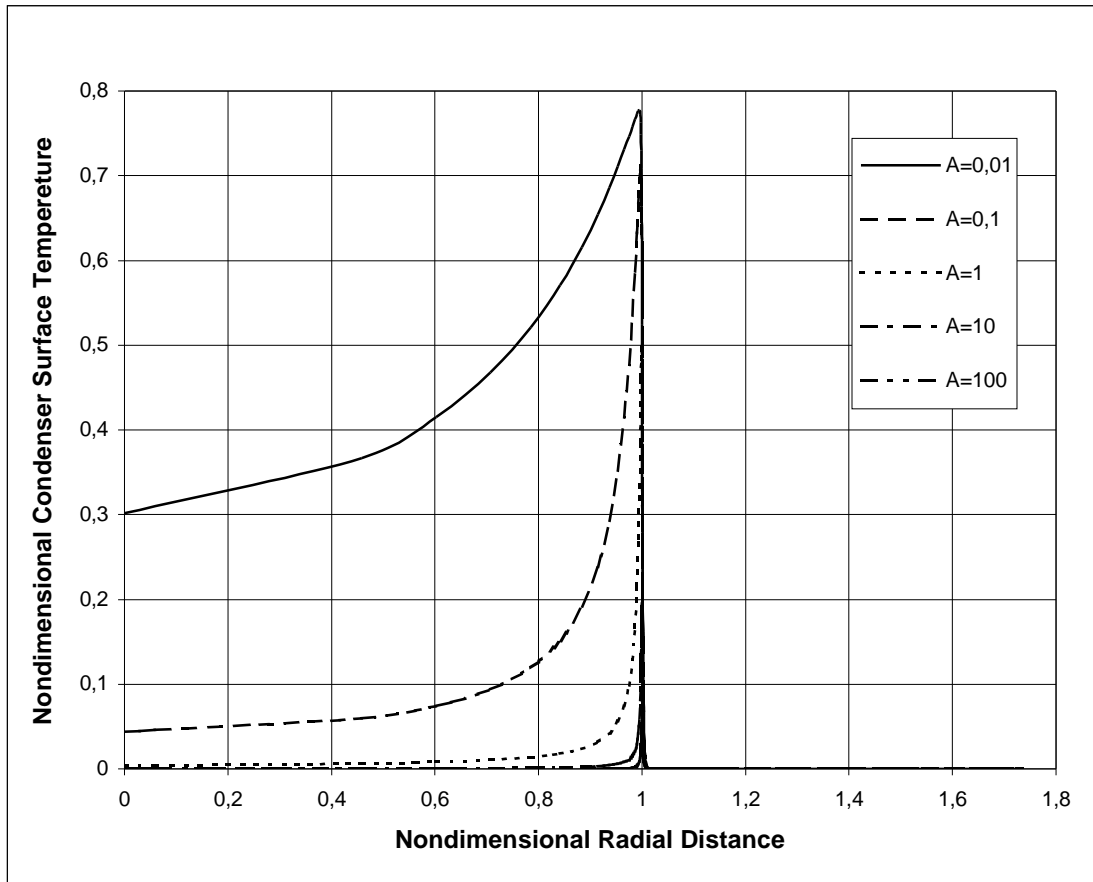


Figure 4.3 Variation of nondimensional temperature as a function of nondimensional radial distance at nondimensional axial distance $\tilde{z} = 9.99 \times 10^{-5}$ for $B=0.001$

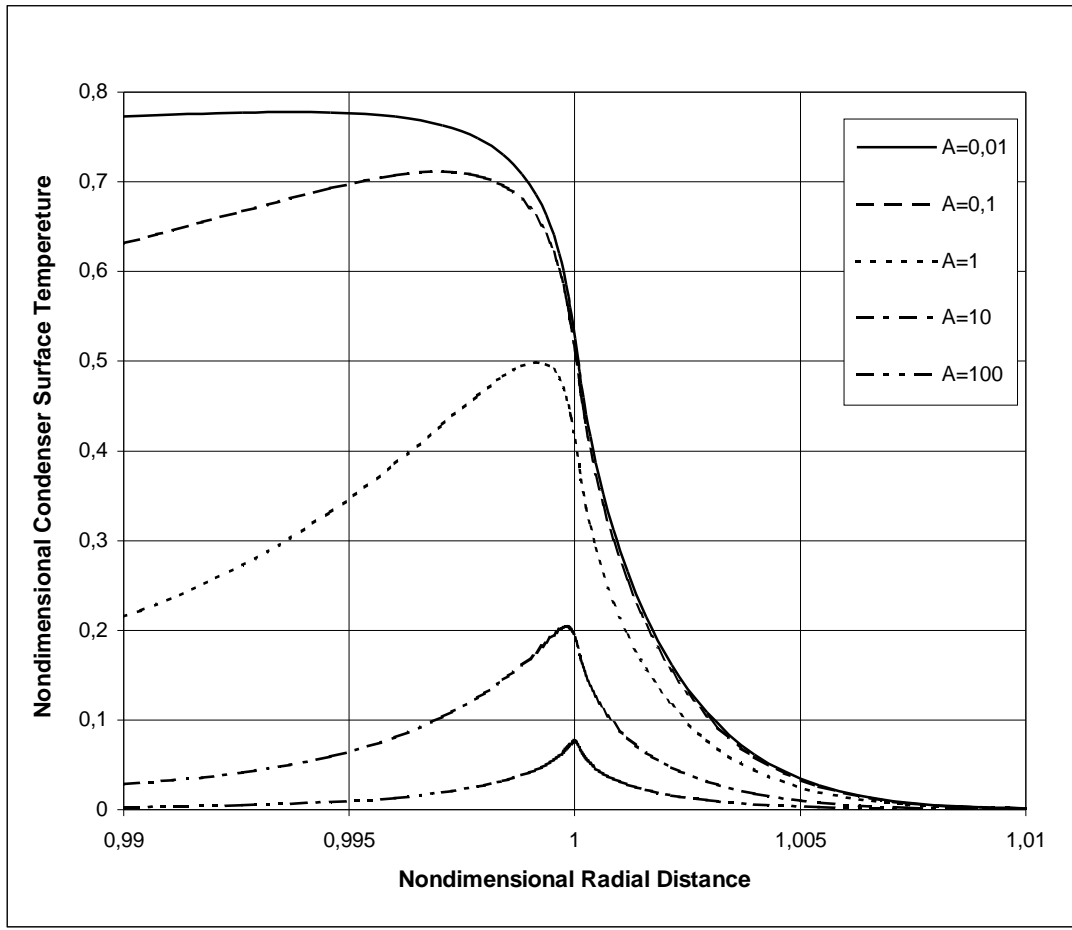


Figure 4.4 Variation of nondimensional temperature as a function of nondimensional radial distance at nondimensional axial distance $\tilde{z} = 9.99 \times 10^{-5}$ for $B=0.001$

It is seen in Figure 4.1 and Figure 4.3 that drop to substrate interface as temperatures increase from center to the edge of the droplet. Hurst and Olson [27] also obtained similar results in their experimental study. It is seen also that drop to surface interface temperatures decrease as the substrate thermal conductivity (A) increase.

As it is seen in Figure 4.1 substrate thermal conductivity increases as A increases and consequently substrate thermal resistance decreases. As a consequence of the decrease of the thermal resistance of the substrate, drop to substrate interface

temperature decreases. For smaller values of A ($A=0.01$), nondimensional drop to substrate interface temperature increases up to 0.8 which results in a considerable decrease in the temperature potential between the vapor and the condenser surface and as a result heat flux decreases considerably. In other words, as the thermal conductivity of the substrate material decreases, since the heat transfer through the droplet decreases heat transfer and the heat transfer coefficient in dropwise condensation should decrease.

On the other hand (as it is seen in Fig E.1 and Fig. E.3) as the droplet size decrease with an increase in B , drop to substrate interface temperature decrease considerably and for $B=0.01$, the maximum nondimensional drop to substrate interface temperature becomes 0.26.

In Figure 4.2 and Figure 4.4 the detailed variation of temperature at the edge of droplet is shown. Another important observation that can be inferred from the examination of the Figure 4.2 and Figure 4.4 is that the maximum drop to substrate interface temperature does not occur just at the edge of the droplet but rather inside the base area of the droplet and that as the substrate thermal conductivity decreases the maximum substrate surface temperature moves toward the center of the droplet.

An interesting observation that can also be extract from Figure 4.1 is that just at the edge of the droplet a sharp change in the substrate surface temperature takes place. In addition to that on the insulated surface of the substrate beyond the edge of the droplet away from the droplet a considerable increase in the temperature is observed. As one goes away from the edge of the droplet nondimensional substrate surface temperature gradually drops to zero.

From the examination of the Figure E.1 and Figure E.3 it can be seen that as the value of the parameter B changes (as the drop size changes) no significant change at the nondimensional location of the maximum drop to substrate interface temperature is discerned.

Variation of temperature distribution at the drop to surface interface for $B=0.01, 0.1, 1, 10, 100$ is given in Appendix E.3, E.4, E.5, E.6, E.7, respectively.

4.1.2 Average Temperature

After surface temperature under a single droplet is obtained, these temperatures are multiplied with area of each segment and divided by total droplet base area to obtain the weighted average surface temperature with respect to the area. This gives the surface average temperature under the droplet as given by Eq. (3.81). Variation of average temperature with droplet radius for $A=100$ is shown in Figure 4.5 and Figure 4.6.

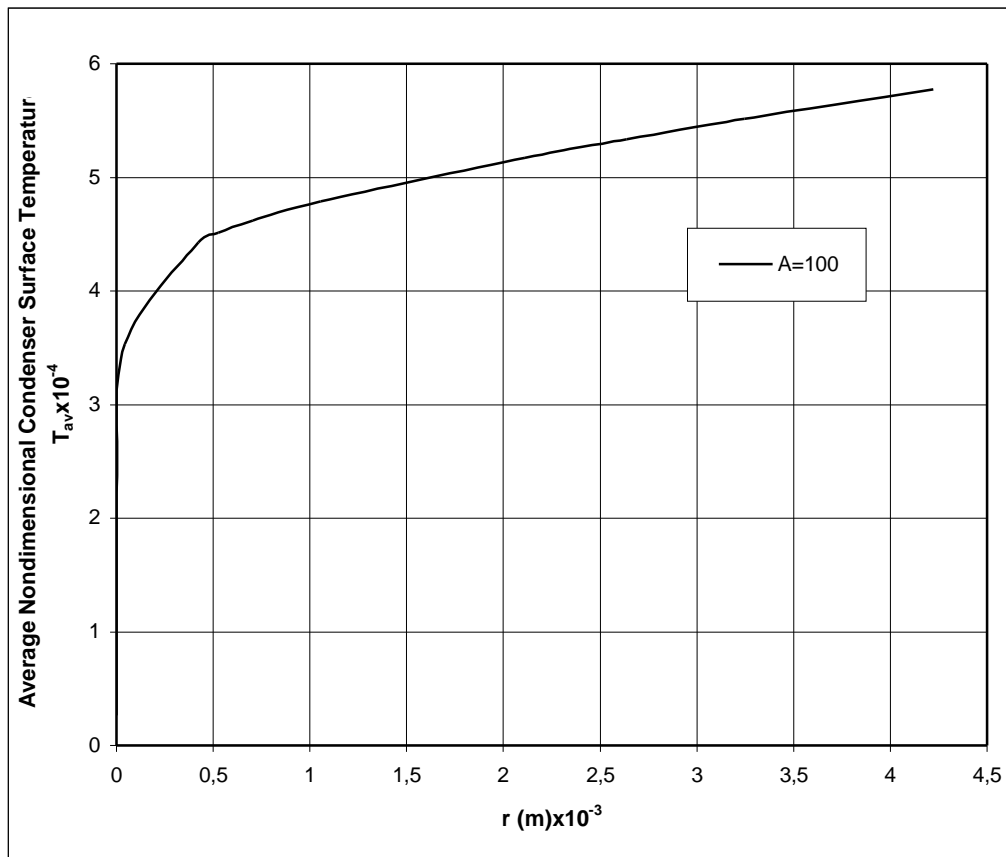


Figure 4.5 Variation of average nondimensional condenser surface temperature at the drop base area as a function of drop radius for $A=100$

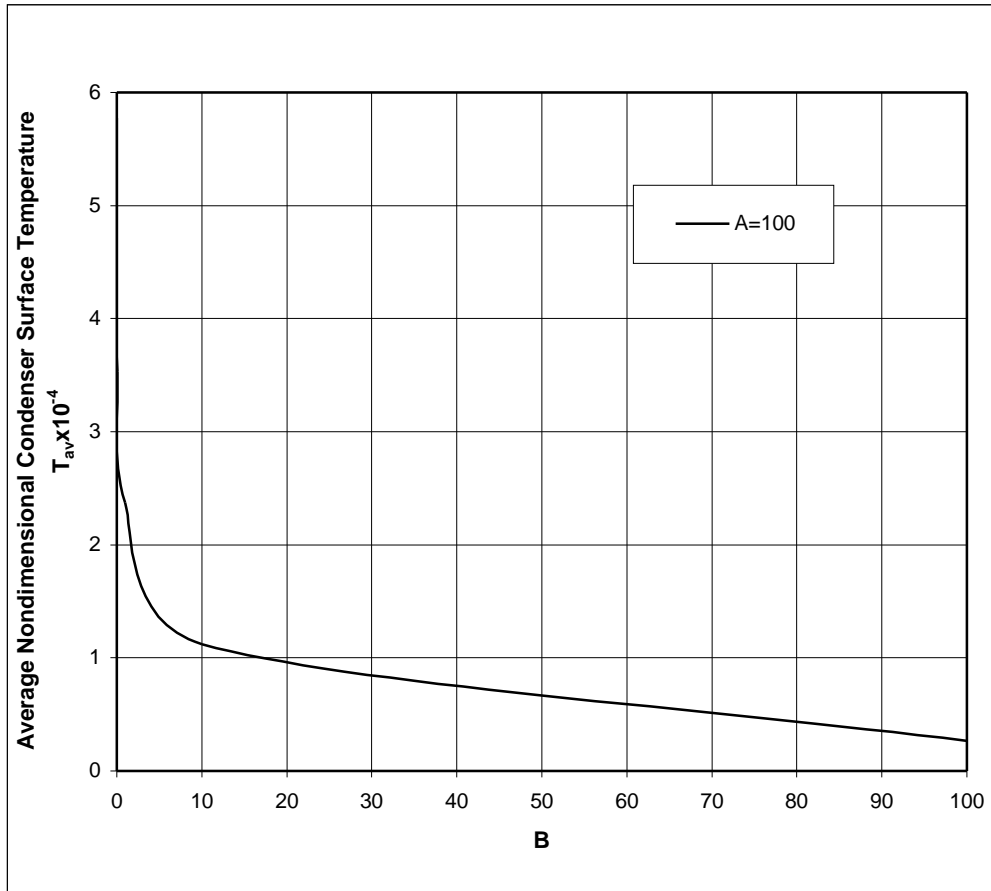


Figure 4.6 Variation of average nondimensional condenser surface temperature with B

It can be seen from Figure 4.5 and Figure 4.6 that average temperature under large droplets is higher than smaller ones. That is, as the radius of droplet gets smaller, surface average temperature decreases.

The data of average temperature at $A=100$ is given in Appendix E.8. Also variation of average temperature for $A=1$ and $A=0.01$ is given in Appendix E.9, E.10, respectively.

Variation of average nondimensional condenser surface temperature with respect to A is shown in Figure 4.7. It is deduced from the Figure 4.7 that surface

average temperature under the droplet decreases as substrate thermal conductivity (A) increases.

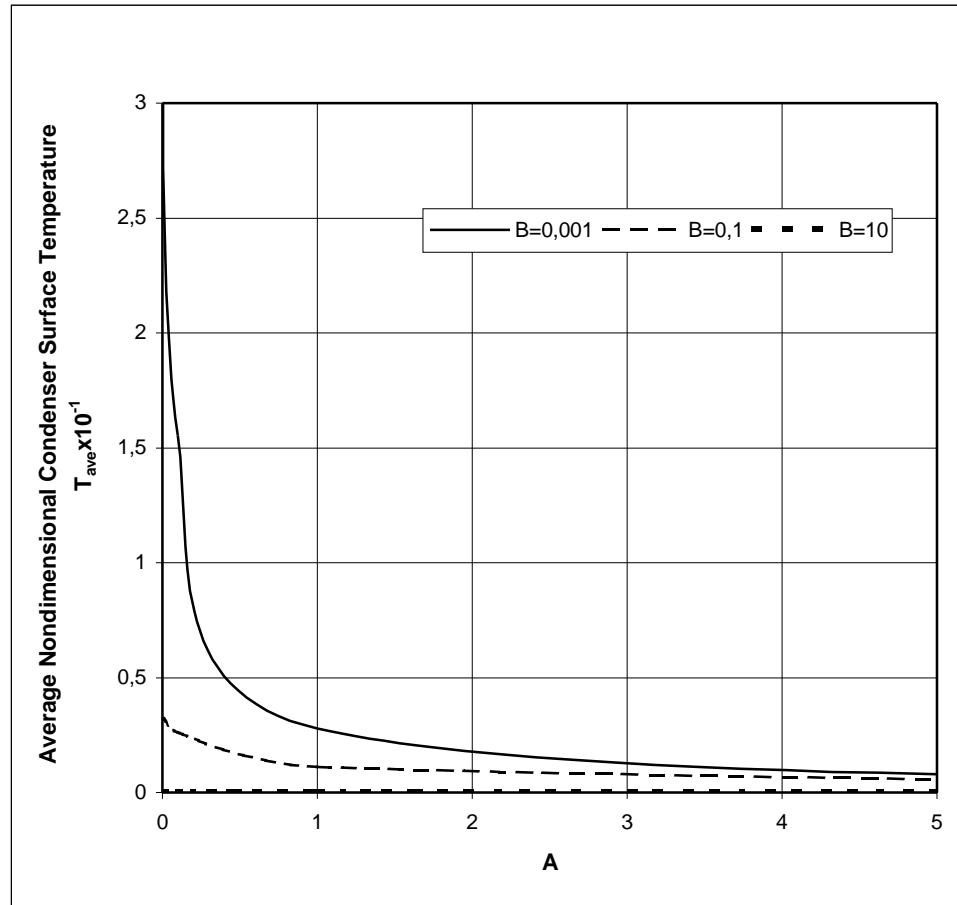


Figure 4.7 Variation of average nondimensional condenser surface temperature with A

Average temperature at the surface at the substrate as a function of substrate thermal conductance for the entire drop population is obtained by using Eq. (3.82). Variation of this average temperature is shown in Table 4.1 and Figure 4.8, respectively.

Table 4.1 Dropwise condensation average nondimensional temperature data

A	T_{ad}
0.01	2.03588E-01
0.1	7.72344E-02
1	1.95700E-02
10	3.27861E-03
20	1.74879E-03
50	7.38096E-04
70	5.32888E-04
100	3.76354E-04

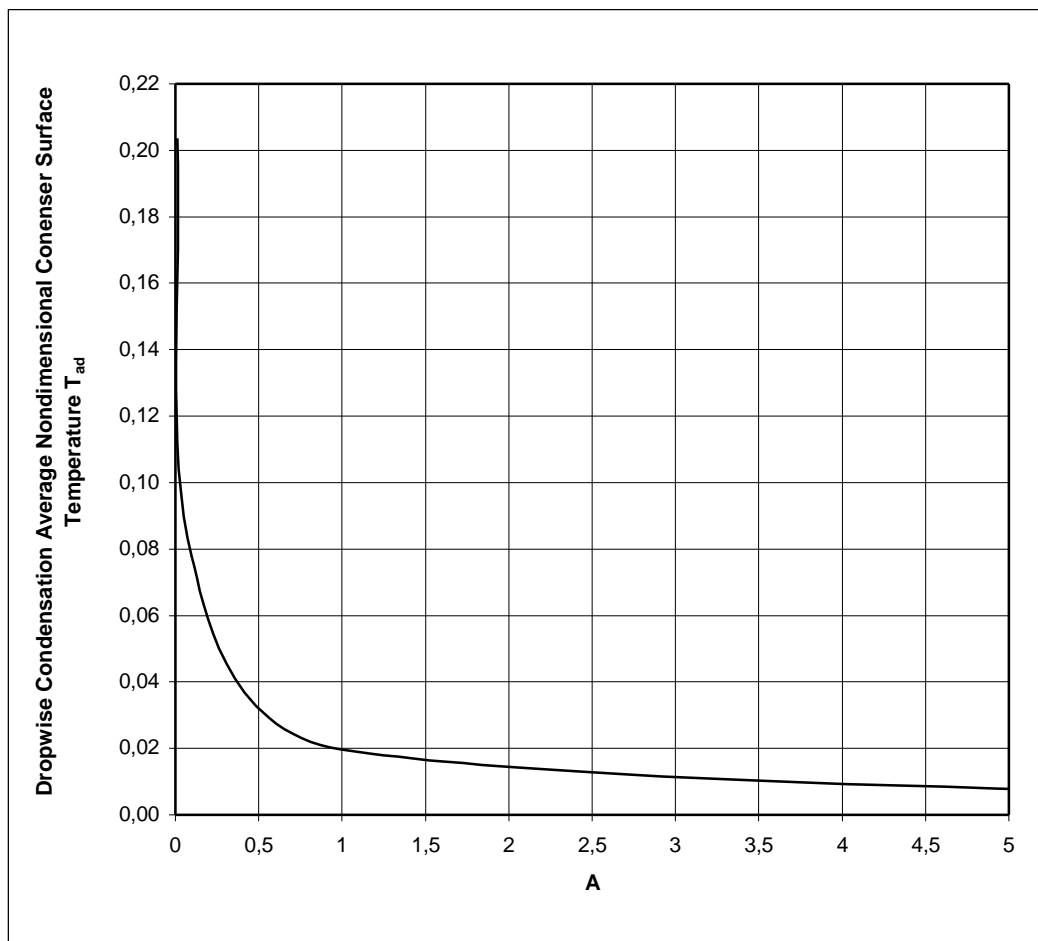


Figure 4.8 Variation of dropwise condensation average nondimensional temperature with A

It can be seen from Figure 4.8 that substrate surface average temperature for entire drop population decreases, as A (substrate thermal conductivity) increases.

4.2 Computation Results for the Heat Transfer in Dropwise Condensation Including the Substrate Effect

In the previous section temperatures under the droplet and in the substrate are obtained. In this section heat transfer and heat flux results for a single droplet and for entire drop population on the surface using the dropsize distribution are given. By using Eq. (3.76), Eq. (3.77), Eq. (3.78); Q_{num} , Q_{nd} (nondimensional heat transfer), Q (dimensional heat transfer) is obtained for a single droplet, respectively. The bare spaces between the drops are considered completely inactive. This model assumes that the influence on a droplet of a neighboring droplets is negligible.

The maximum drop size that should be taken in the calculations should obviously be the departure size of the droplets. Nevertheless, the departure size of the droplets in dropwise condensation depends on various factors like pressure and temperature of the surrounding as well as body forces and surface roughness. Measurements show that on metal surfaces, the departure radius of water droplet is slightly larger than 2 mm. Therefore, in this study the maximum drop radius is taken as 2 mm and minimum drop radius is taken as 2.6×10^{-6} m for the dropsize distribution. The contact angle is taken as 65° .

4.2.1 Effect of Droplet Radius on Heat Transfer and Heat Flux for a Single Droplet

Variation of heat transfer and heat flux with radius for $A=1$ is shown in Figure 4.9 and Figure 4.10, respectively.

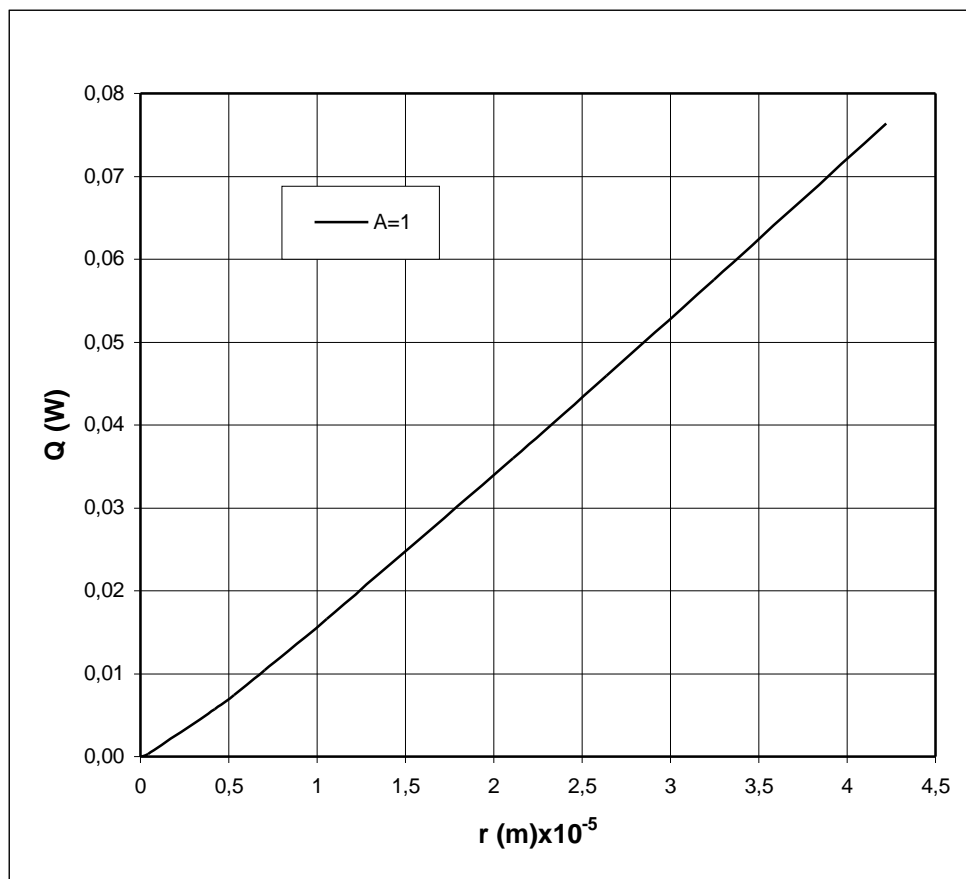


Figure 4.9 Variation of heat transfer with drop radius for $A=1$

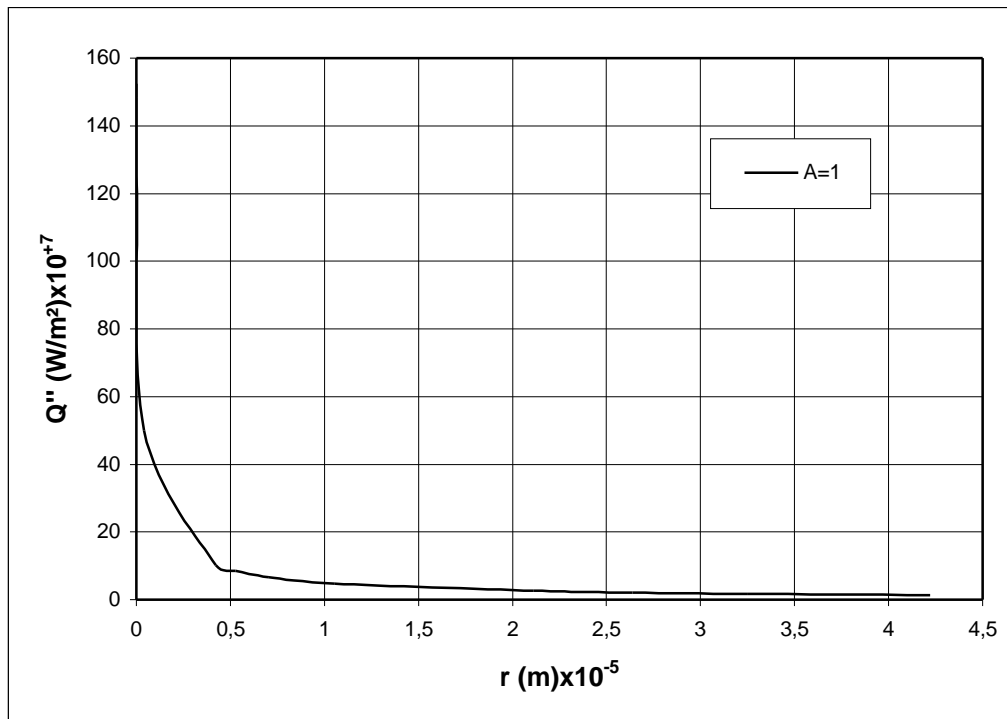


Figure 4.10 Variation of heat flux with drop radius for A=1

It is seen from Figure 4.9 that while drop radius becomes smaller, heat transfer decreases. On the other hand, it is seen from Figure 4.10 that as drop radius becomes smaller, heat flux increases.

The data and results of heat transfer and heat flux is given in Appendix F.1. Variation of heat transfer and heat flux with radius for A=0.01 and A=100 is shown in Appendix F.2 and Appendix F.3, respectively.

4.2.2 Effect of Substrate Material on Heat Transfer and Heat Flux

In dropwise condensation thermal conductivity of the substrate has an important effect on the rate of heat transfer. Large number of theoretical, analytical and experimental study were made to clarify this effect by researches. The results of these studies indicate that both heat transfer and heat transfer coefficient increase with the surface thermal conductivity. By using Eq. (3.77) and Eq. (3.78)

nondimensional heat transfer (Q_{nd}) and dimensional heat transfer (Q) is obtained for single droplets. The data and results of nondimensional heat transfer (Q_{nd}) is given in Appendix F.4.

Variation of nondimensional heat transfer (Q_{nd}) and dimensional heat transfer (Q) for $B=0.001$ is shown in Figure 4.11 and Figure 4.12, respectively.

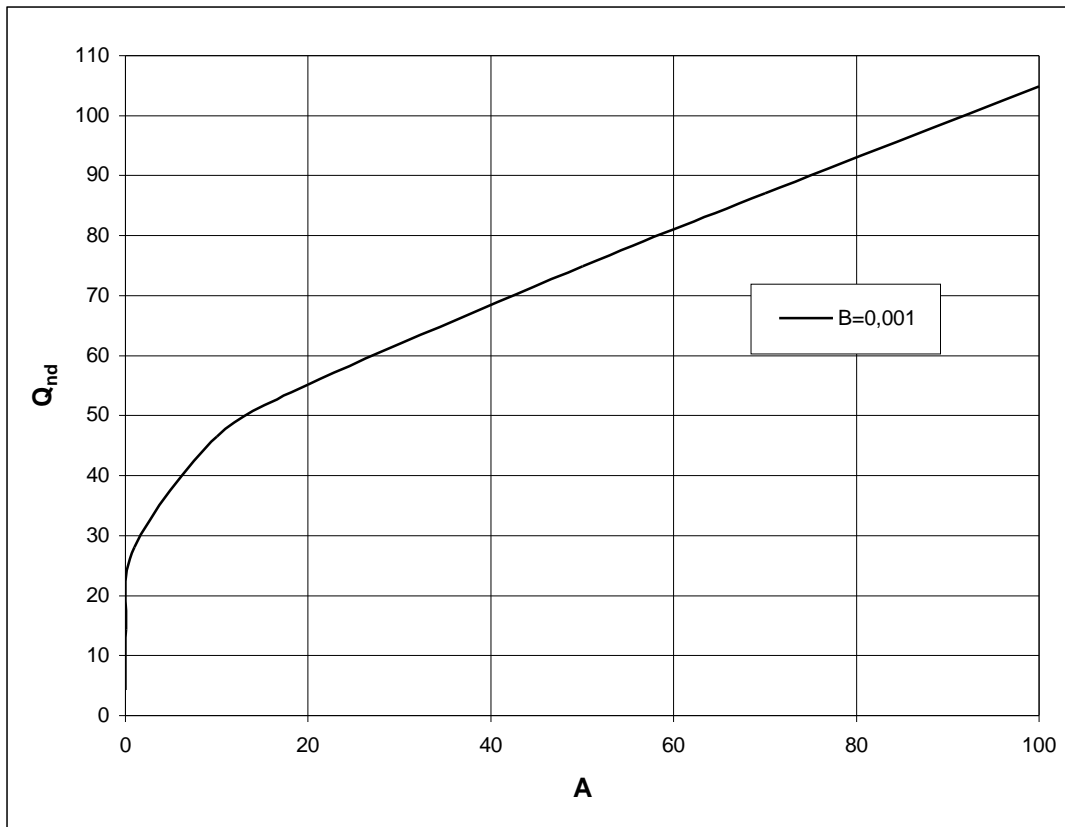


Figure 4.11 Variation of Q_{nd} with A for $B=0.001$

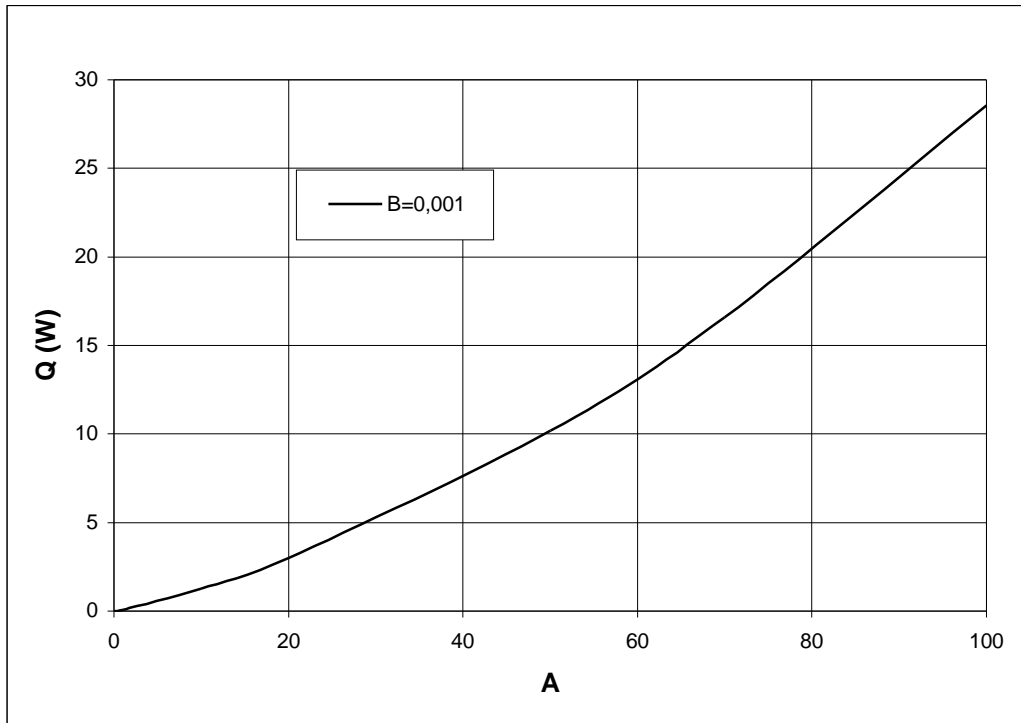


Figure 4.12 Variation of Q with A for B=0.001

It is deduced from Figure 4.11 that nondimensional heat transfer (Q_{nd}) increases with A (substrate thermal conductivity). It is also seen from Figure 4.12 that heat transfer (Q) increases with A (thermal conductivity) of substrate material.

Variation of nondimensional heat transfer (Q_{nd}) and dimensional heat transfer (Q) for B=0.01, 0.1, 1, 10, 100 is given in Appendix F.5.

One important factor that effects heat transfer through a single droplet is the drop conductance resistance. The other factor is interfacial resistance R_i . Although R_c decreases towards the edge of the droplet, R_i remains constant along the surface of the droplet. Thus, the major portion of heat transfer in dropwise condensation takes place near the edge of the droplet. Sum of these two resistances, gives total resistance over the substrate. In this study total resistance is denoted by nondimensional resistance parameter (F_r).

Variation of nondimensional drop resistance with nondimensional drop radius for a single droplet at $B=0.001$ and $A=1$ is given in Figure 4.13. The data used in Figure 4.13 is given in Appendix F.6.

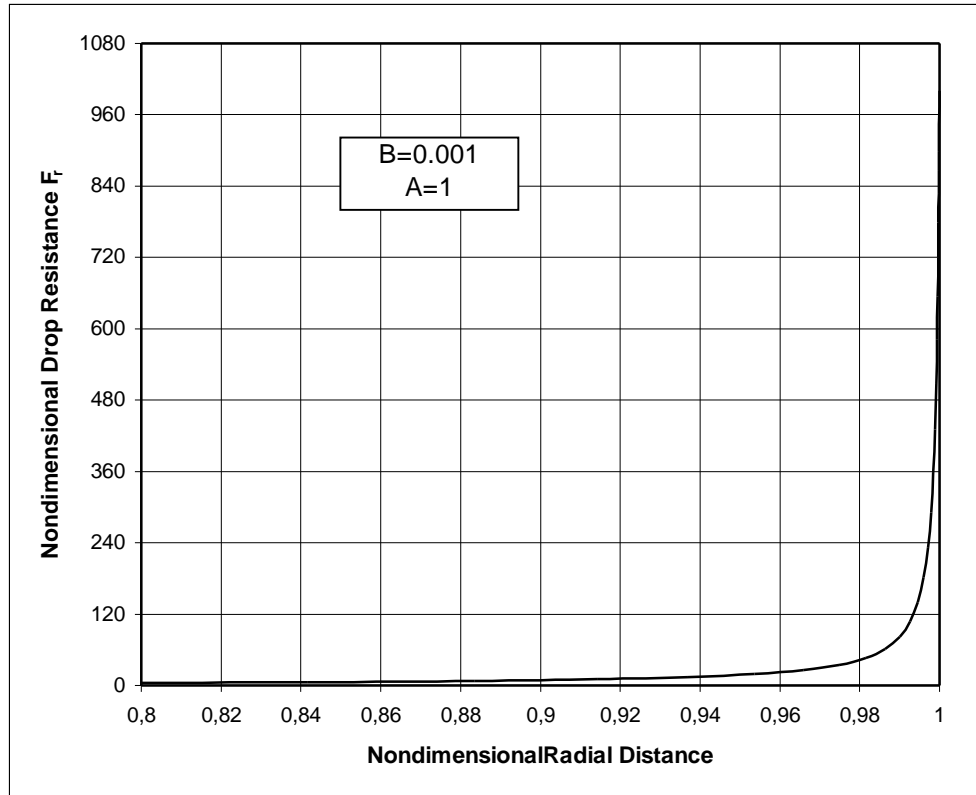


Figure 4.13 Variation of nondimensional resistance parameter with nondimensional drop radius for $B=0.001$ and $A=1$

It is seen from Figure 4.13 that nondimensional resistance parameter increases from center to edge of the droplet. Increase of nondimensional drop resistance means that total resistance of drop decreases towards the edge of droplet.

Variation of heat transfer and heat flux with A for a droplet radius which is $r=2.11 \times 10^{-4}$ m is shown in Figure 4.14 and Figure 4.15, respectively.

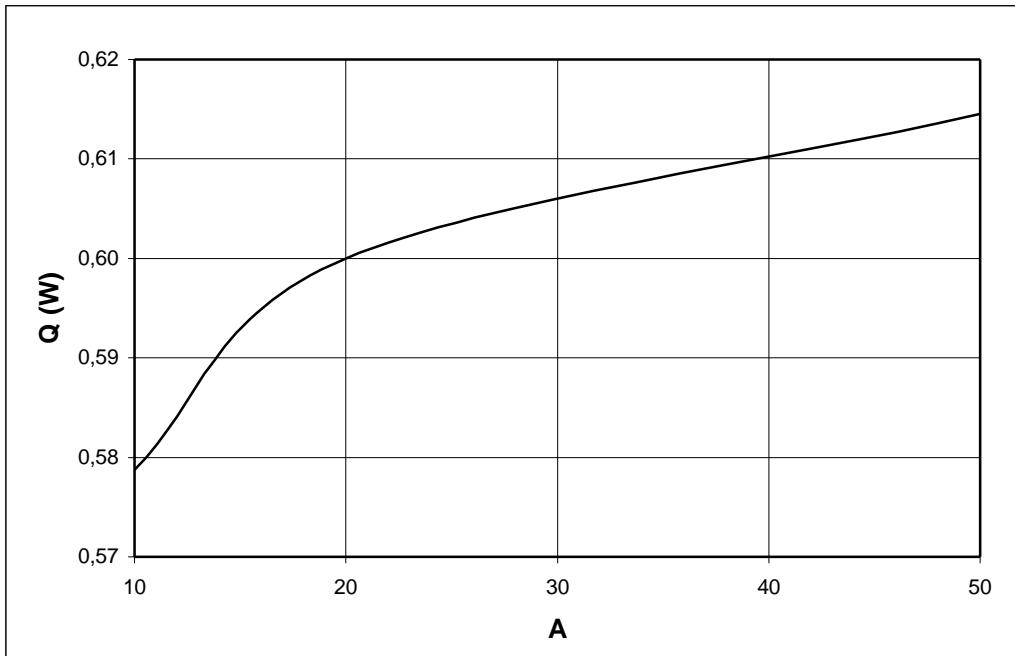


Figure 4.14 Variation of heat transfer with A for $r=2.11 \times 10^{-4}$ m

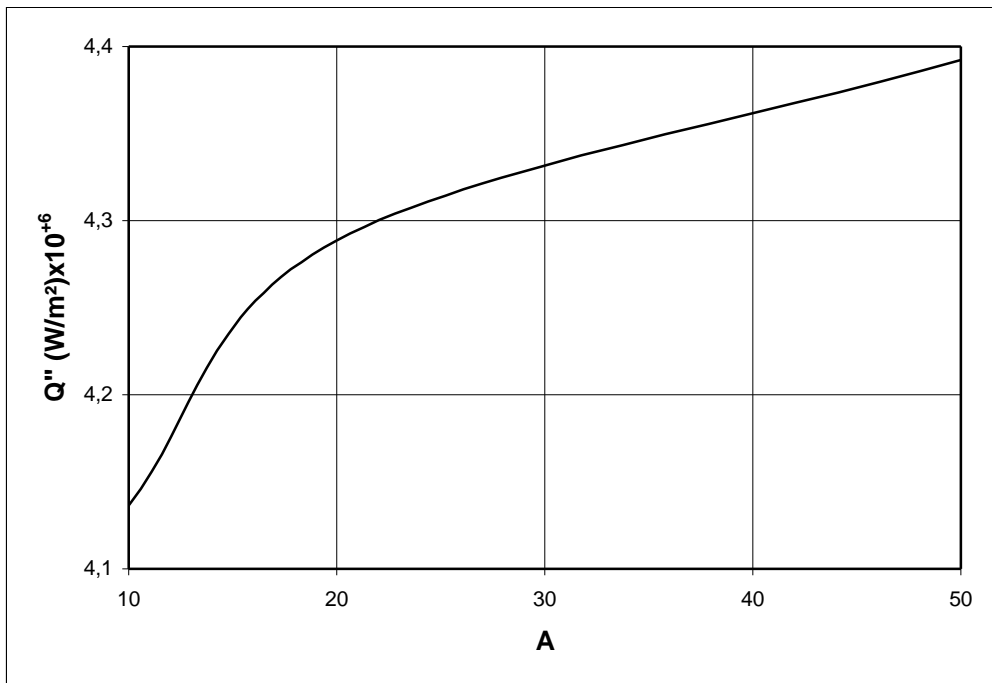


Figure 4.15 Variation of heat flux with A for $r=2.11 \times 10^{-4}$ m

It is seen from Figure 4.14 and Figure 4.15 that heat transfer and heat flux increases with substrate thermal conductivity for a given drop diameter on various surfaces. Variation of heat transfer and heat flux with A for $r=4.22 \times 10^{-6}$ m is given in Appendix F.7.

By using Eq. (3.77) nondimensional heat transfer (Q_{nd}) is obtained for droplets with respect to substrate thermal conductivity (A) and drop radius (B). Variation of nondimensional heat transfer (Q_{nd}) with B and A is shown in Figure 4.16.

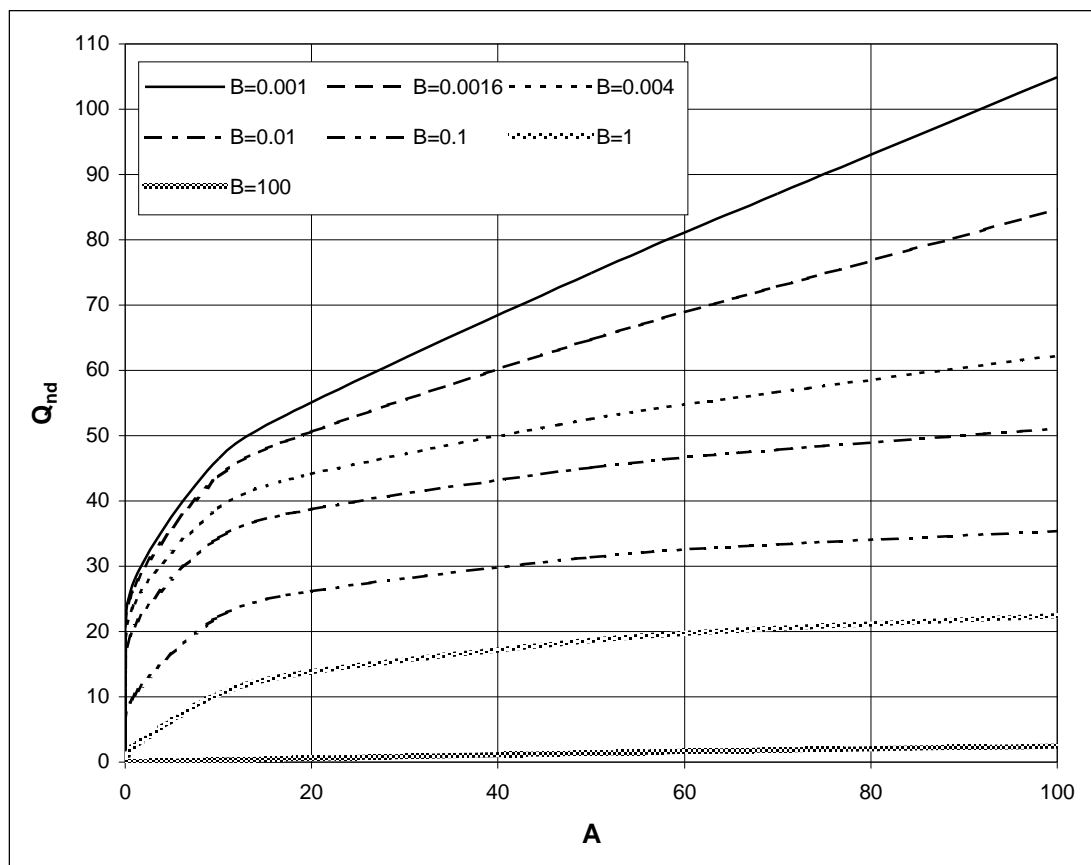


Figure 4.16 Variation of nondimensional heat transfer (Q_{nd}) with B and A

It is seen from Figure 4.16 that Q_{nd} increases with substrate thermal conductivity (A).

By using Eq. (3.78) heat transfer is obtained for single droplet with respect to substrate thermal conductivity (A) and drop radius (B). Variation of dimensional heat transfer (Q) with B and A is shown in Figure 4.17.

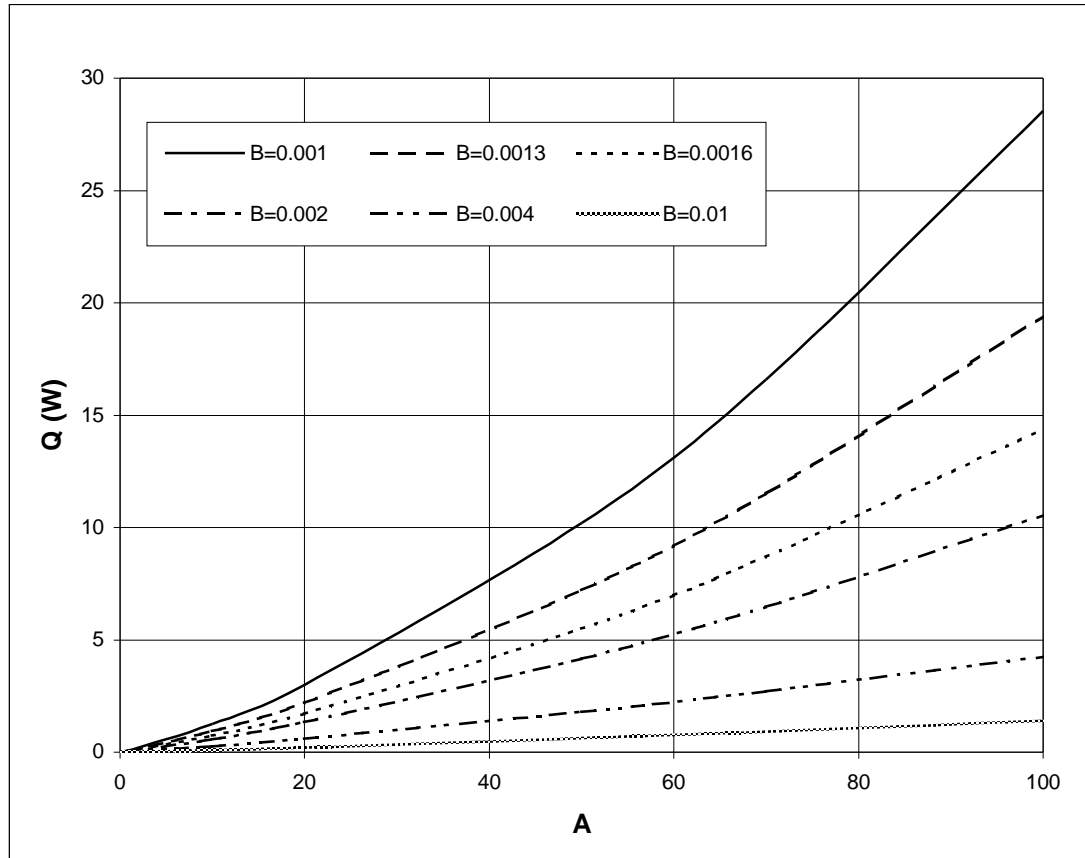


Figure 4.17 Variation of dimensional heat transfer (Q) with B and A

It is seen from Figure 4.17 that heat transfer (Q) increases with substrate thermal conductivity (A).

By employing Eq. (3.79) heat flux of droplets is obtained. Variation of heat flux (Q'') for B and A is shown in Figure 4.18.

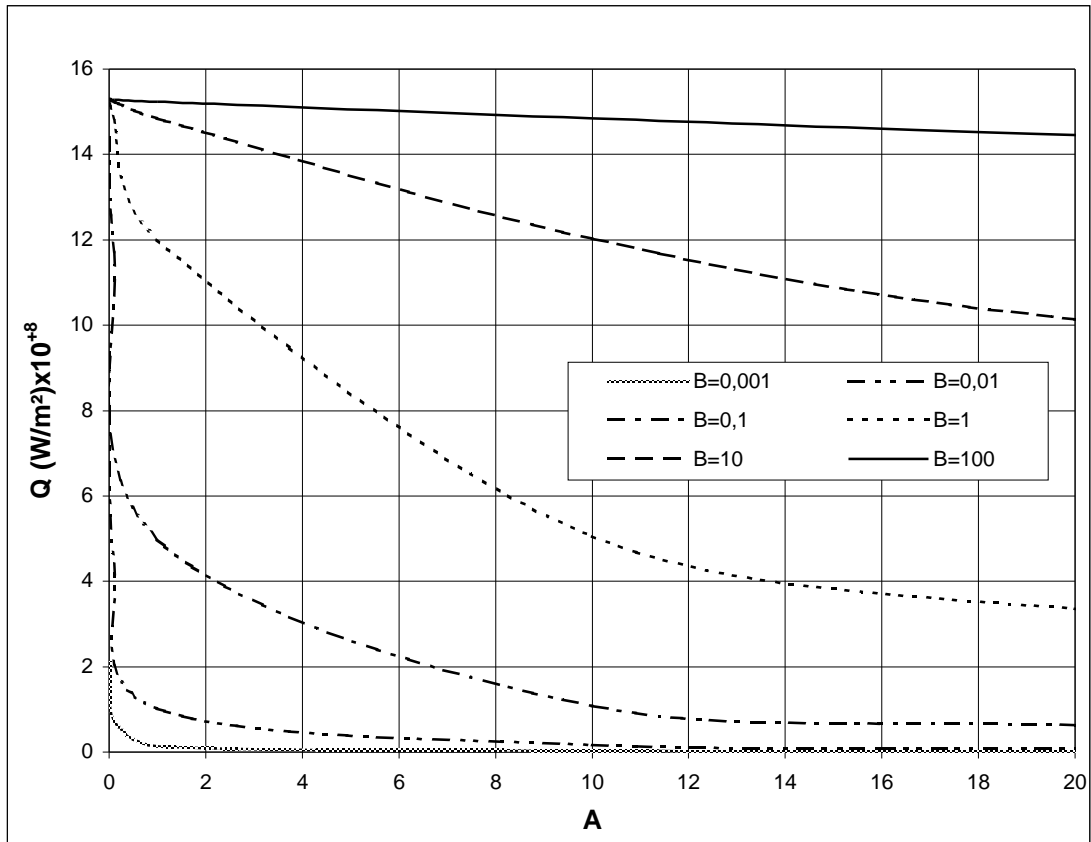


Figure 4.17 Variation of heat flux (Q'') with B and A

It is deduced from Figure 4.18 that heat flux (Q'') decreases as substrate thermal conductivity (A) increases.

Total dropwise condensation heat transfer (Q_{dc}) and total dropwise condensation heat flux (Q''_{dc}) is obtained by integrating the heat transfer through single droplets according to the size distribution of the drops. By using Eq. (3.87) and Eq. (3.88) total dropwise condensation heat transfer (Q_{dc}) and total dropwise condensation heat flux (Q''_{dc}) is obtained, respectively. The data of total dropwise condensation heat transfer (Q_{dc}) and total dropwise condensation heat flux (Q''_{dc}) is shown in Table 4.2.

Table 4.2 Variation of total dropwise condensation heat transfer (Q_{dc}) and total dropwise condensation heat flux (Q''_{dc}) data

A	Q_{dc} (W)	Q''_{dc} (W/m ²)
0.01	0.58959	5.316E+06
0.1	0.80160	1.154E+07
1	1.14167	1.596E+07
10	1.74664	1.763E+07
20	1.91517	1.785E+07
50	2.00914	1.796E+07
70	2.03352	1.798E+07
100	2.07118	1.800E+07

Variation of total dropwise condensation heat transfer (Q_{dc}) with A is shown in Figure 4.19.

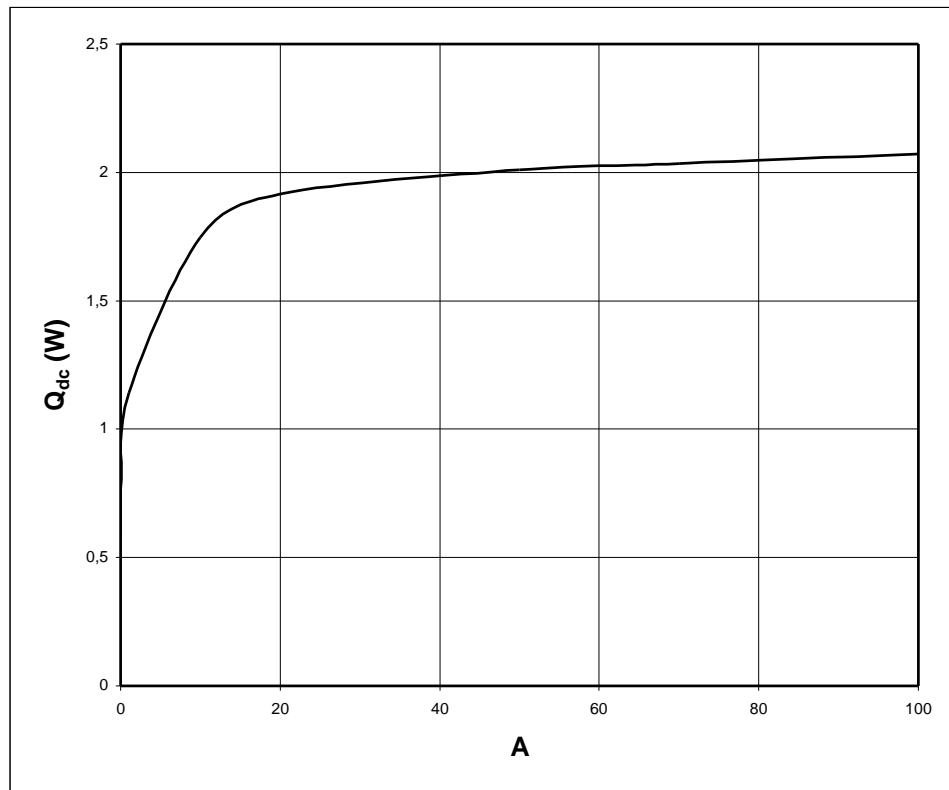


Figure 4.19 Variation of total dropwise condensation heat transfer (Q_{dc}) with A

Variation of total dropwise condensation heat flux (Q''_{dc}) with A is shown in Figure 4.20 and Figure 4.21.

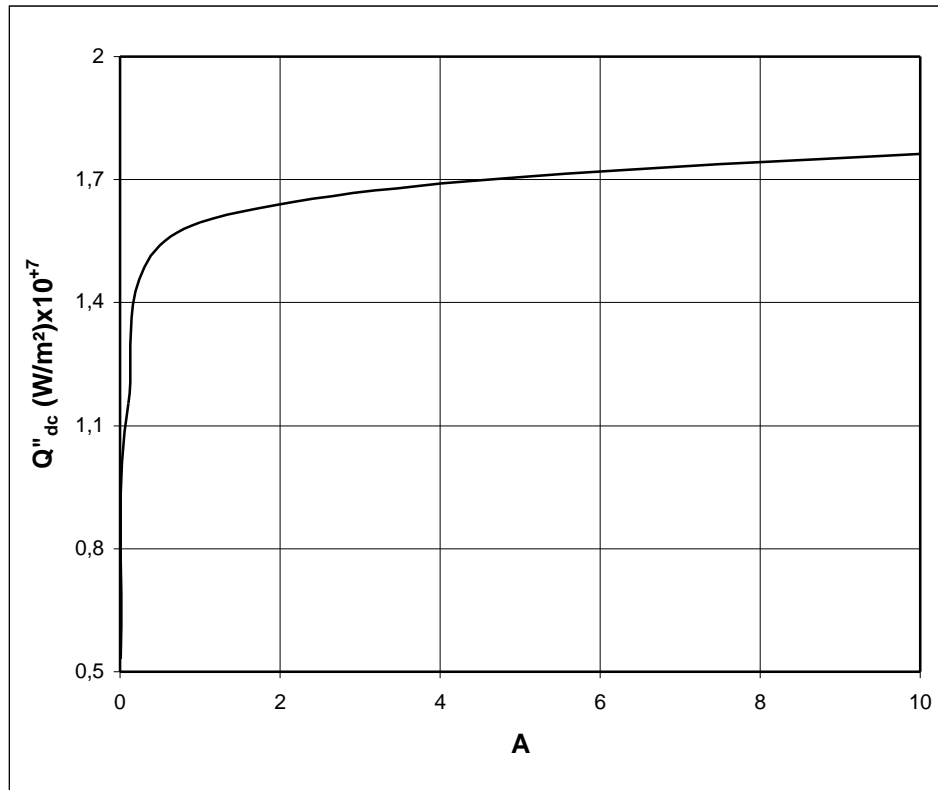


Figure 4.20 Variation of total dropwise condensation heat flux (Q''_{dc}) with A

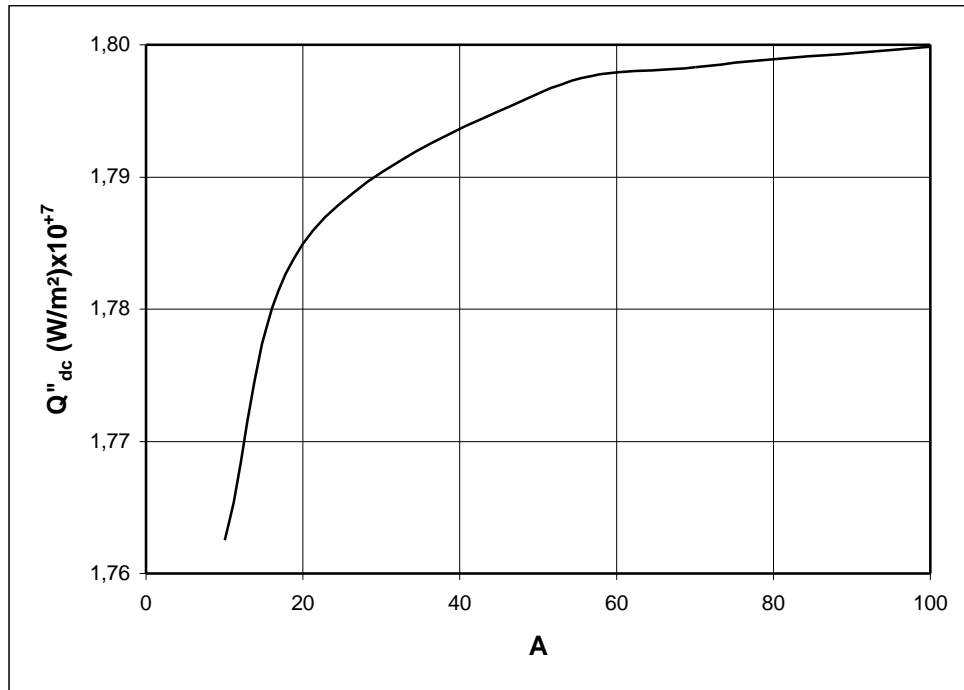


Figure 4.21 Variation of total dropwise condensation heat flux (Q''_{dc}) with A

It is seen from Figure 4.18 that total dropwise condensation heat transfer (Q_{dc}) increases with substrate thermal conductivity (A). Also in Figure 4.20 and Figure 4.21 total dropwise condensation heat flux (Q''_{dc}) increases with substrate thermal conductivity (A). It is deduced from figures that increase rate of Q_{dc} and Q''_{dc} is completely higher between $A=0.1$ and $A=10$. Between $A=10$ and $A=100$ Q_{dc} and Q''_{dc} increases gradually.

4.3 Dropwise Condensation Heat Transfer Coefficient

Dropwise condensation heat transfer coefficient is obtained by using Eq. (3.69). The data and variation of dropwise condensation heat transfer coefficient is shown in Table 4.3 and Figure 4.22, respectively.

Table 4.3 Dropwise condensation heat transfer coefficient data

A	h_{dc} (W/m ² K)
0.01	66746
0.1	125100
1	162781
10	176834
20	178807
50	179727
70	179899
100	180120

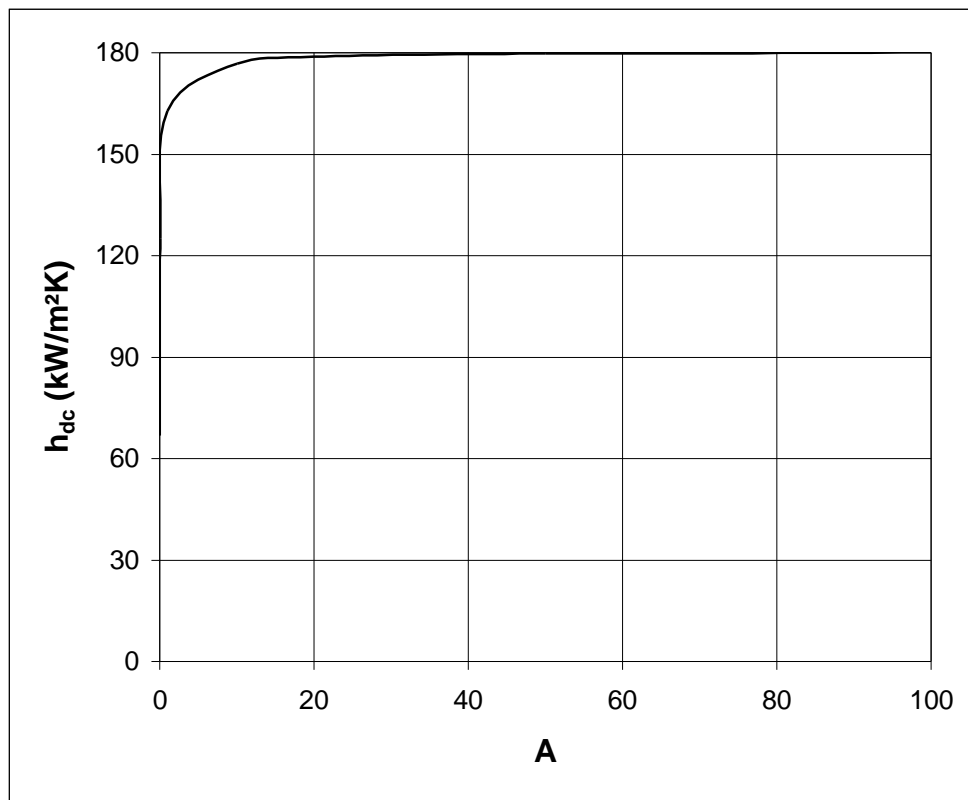


Figure 4.22 Variation of dropwise condensation heat transfer coefficient with A

It can be seen from the Figure 4.22 that the higher the thermal conductivity of the substrate material, higher the heat transfer coefficient is.

The results of this study shows that the surface thermal conductivity is an important parameter in dropwise condensation. And the dropwise condensation heat transfer coefficient is a function of the thermal conductivity of the substrate material.

4.4 Comparison of Numerical Results with the Results in the Literature

4.4.1 Comparison of Heat Transfer Coefficient

Heat transfer coefficient is one of the most important parameter in dropwise condensation. There are considerable amount of experimental, numerical and analytical study for the determination of heat transfer coefficient in the literature.

Tsuruta, Tanaka and Togashi [33] made an experimental verification of constriction resistance theory in dropwise condensation heat transfer. They studied the effect of thermal properties of the condenser material on dropwise condensation heat transfer experimentally.

Quart glass, stainless steel and carbon steel are employed as the condenser materials in the experiment.

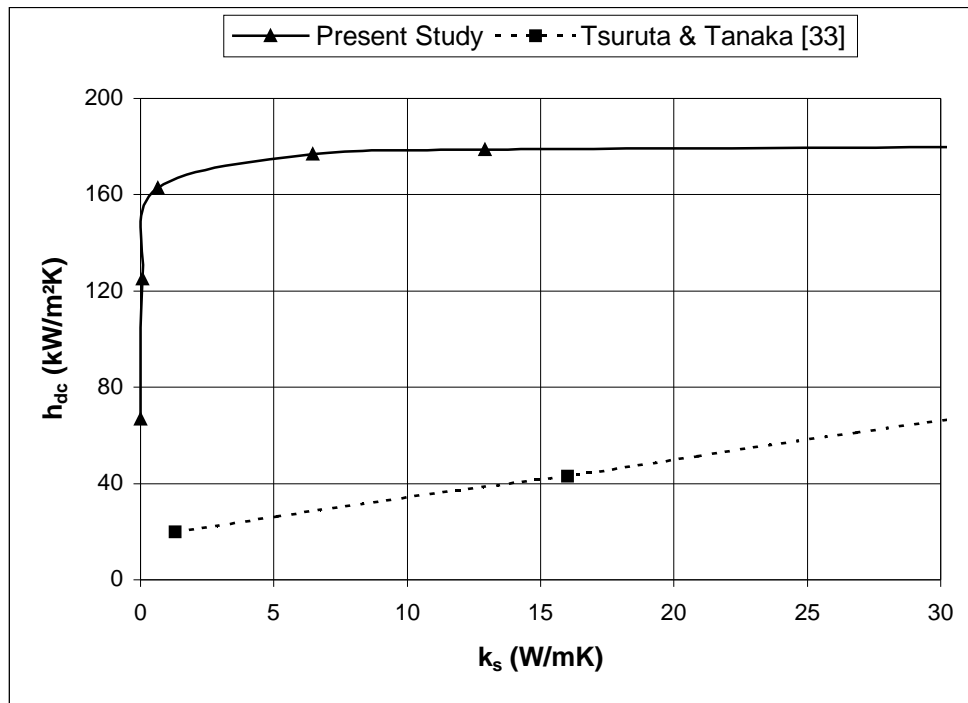


Figure 4.23 Comparison of heat transfer coefficients between the present study and Tanaka et. al [33]

In the present study and in the Tanaka's experimental study the pressure is taken as 100 kPa. It is seen from Figure 4.23 that heat transfer coefficients obtained by the present study are higher than those found by Tanaka et. al [33]. The reasons can be constriction resistance, environmental factors like noncondensibles gases.

Tsuruta and Tanaka [61] made an theoretical study on the constriction resistance in dropwise condensation. In their research, the effect of the thermal conductivity of the condenser material on dropwise condensation heat transfer coefficient decreases with the decrease in substrate thermal conductivity. That is, heat transfer coefficient increases with substrate thermal conductivity in the present study as Tsuruta and Tanaka's study. However values obtained in the present study is higher than those found by Tsuruta and Tanaka. The results of heat transfer coefficients are presented in Figure 4.24 from Tsuruta and Tanaka study and present study.

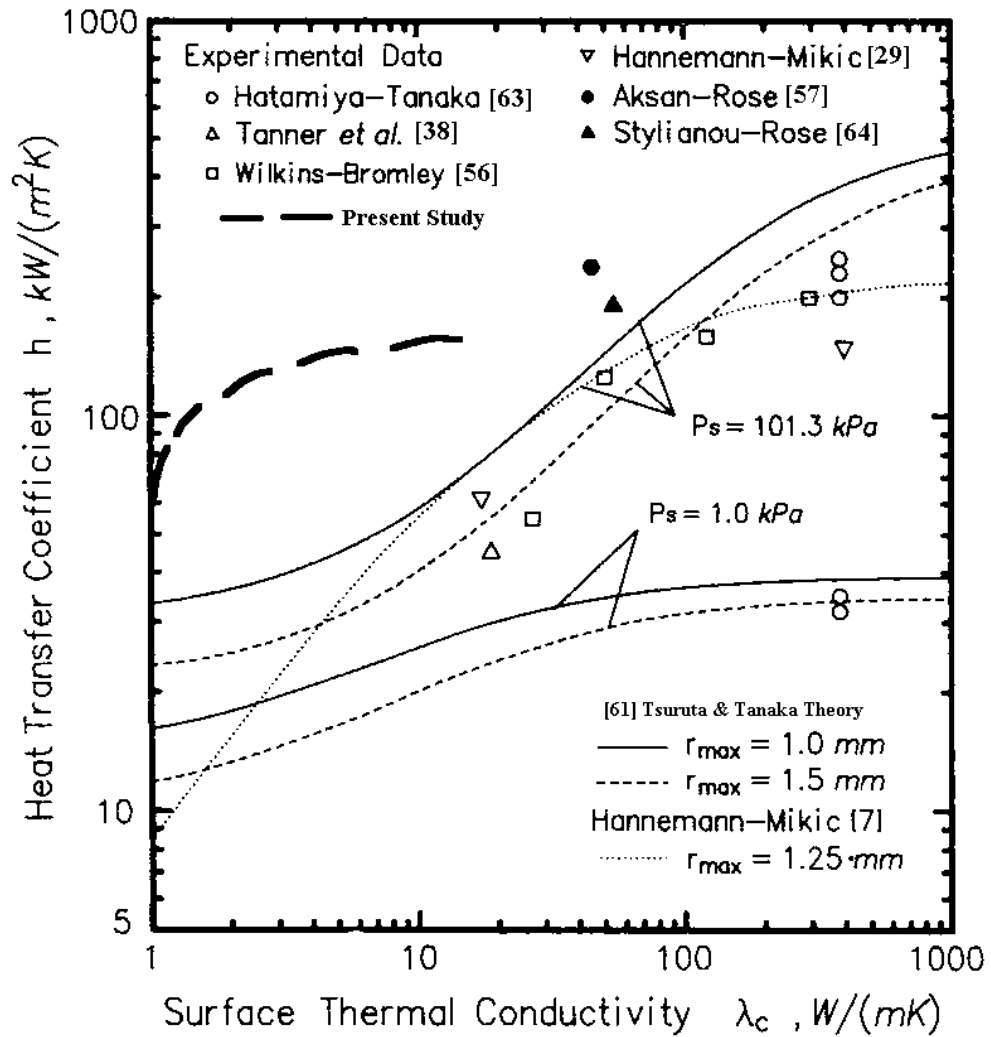


Figure 4.24 Comparison of heat transfer coefficients between the present study and Tsuruta and Tanaka study [61]

Hannemann and Mikic [59] made an analysis of the effect of surface thermal conductivity on the rate of heat transfer in dropwise condensation. They reported an analysis and correlation of the thermal constriction resistance in dropwise condensation. They concluded that heat transfer coefficient increases with substrate thermal conductivity. Comparison of heat transfer coefficients between the present study and literature is shown Figure 4.25.

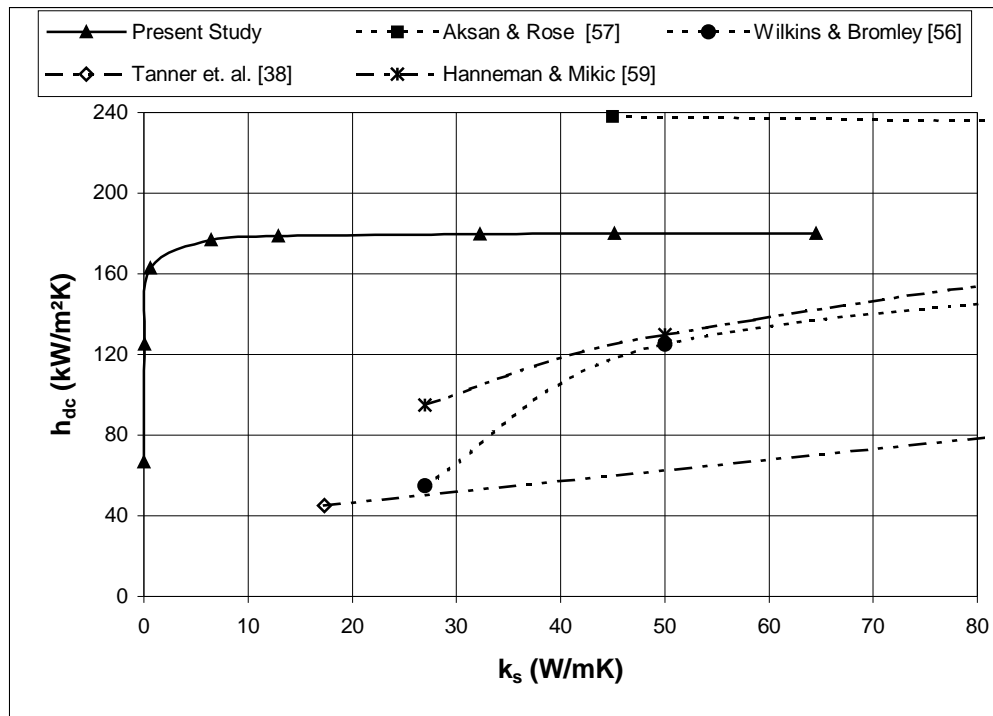


Figure 4.25 Comparison of heat transfer coefficients between the present study and literature

It is seen that the values in Figure 4.25 is not the same as the present study. In these experiments since noncondensable gases, surface finish, pressure, promoter and other factors effects dropwise condensation heat transfer, the results obtained in their experiments are considerably different then the calculated results of this study.

It is seen from Figure 4.26 that heat transfer coefficients found by present study are higher than those found by Hanneman & Mikic [59] and the other experimental analysis. On the other hand the experimental results of Aksan and Rose [57] are higher than the values obtained in the present study.

Yu-Ting Wu, Chun-Xin Yang and Xiu-Gan Yuan [17] made theoretical study for the dropwise condensation heat transfer on the four kinds of surfaces; copper, zinc, carbon steel and stainless steel. The results indicate that the heat transfer coefficients are dependent on the surface thermal conductivity. In the present study

and in the Yu Ting Wu et. al. [17] experimental study the pressure is taken as 100 kPa.

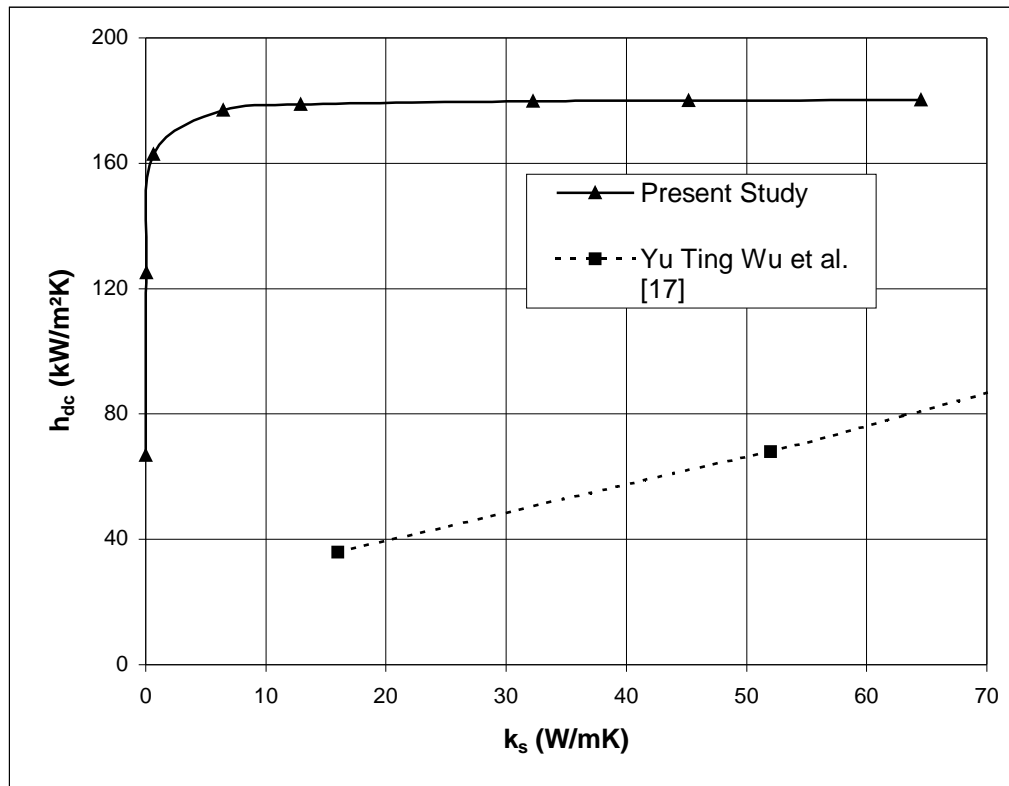


Figure 4.26 Comparison of heat transfer coefficients between the present study and Yu Ting Wu et. al. study [17]

It is seen from Figure 4.26 that heat transfer coefficients found by present study are higher than those found by Yu Ting Wu et. al. [17].

The most important result obtained in this study and in the studies of the literature is that the substrate thermal conductivity effects the dropwise condensation phenomena. Both the results of this study and the results of the studies of literature shows that heat transfer and heat transfer coefficient increases with substrate thermal conductivity.

CHAPTER 5

CONCLUSIONS

A numerical method to calculate the substrate effect in dropwise condensation is proposed in this study. FORTRAN program is used to calculate the temperature distribution in the substrate where the substrate thermal conductivity and drop radius are taken as variables. By using these temperatures, heat transfer and heat flux are obtained for a given droplet.

This theoretical study of dropwise condensation shows that heat transfer and heat flux are effected by surface thermal conductivity and drop radius.

It is concluded from the results that as the droplet size decrease drop to substrate interface temperature decrease considerably. Another important observation that can be inferred from the results that as the substrate material thermal conductivity decreases the maximum substrate surface temperature moves toward the center of the droplet. It is also concluded that for low conductivity substrate materials vapor-to-surface temperature differences are small.

The results indicate that the heat transfer and heat flux are dependent on the surface thermal conductivity and increase with the increasing substrate material thermal conductivity. Dropwise condensation heat transfer coefficient increases as the substrate material thermal conductivity increases.

Comparison of the numerical results with the results in the literature show that the heat transfer coefficients found by the present study are higher than those found in the literature.

REFERENCES

1. Çengel, Y. A., Heat Transfer – A Practical Approach, International Edition, 1998, McGraw-Hill.
2. E. Schmidt, W. Schurig, W. Sellschop, “Versuche über die Kondensation von Wasserdampf in Film — und Tropfenform, Tech. Mech. Thermodyn. (Forsch. Ing. Wes.), 1, 53–63, 1930.
3. Jakob, M., “Heat Transfer in Evaporation and Condensation – II”, Mechanical Engineering, 58, p. 729–739, 1936.
4. E. Baer and J. M. McKelvey, “Heat Transfer in Dropwise Condensation”, Delaware Science Symposium, University of Delaware, 1958.
5. Welch, J.F. and Westwater, J.W. “Microscopic Study of Dropwise Condensation”, International Heat Transfer Conference, Colorado, USA, p. 302, 1961.
6. G. Tammann and W. Boehme, “Die Zahl der Wassertropfen bei der Kondensation auf verschiedenen festen Stoffen”, Annalen der Physik, vol. 5, 1935, pp. 77-80.
7. McCormick, J.L. and Baer, E., “Dropwise Condensation on Horizontal Surfaces”, Developments in Mechanics, Pergamon Press, N.Y., pp. 749-75, 1965.

8. McCormick , J.L. and Baer , E. , “ On the Mechanism of Heat Transfer in Dropwise Condensation”, *Journal of Colloid Science*, vol.18, 1963, pp.208-216.
9. Umur , A. and Griffith , P. , “Mechanism of Dropwise Condensation ,” *Trans. ASME ,Journal of Heat Transfer* , 87C , pp. 275-282, 1965.
10. Graham, C. and Griffith , P. , “Dropsize Distribution and Heat Transfer in Dropwise Condensation , ” *Int. J. Heat Mass Transfer* ,16 , p. 337-346, 1973.
11. Rose, J. W. and Glicksman, L. R., “ Dropwise Condensation-The Distribution of Drop Sizes”, *Int. J. Heat and Mass Transfer*, vol.11, pp.411-425, 1973.
12. Fatica N. and Katz , D.L , “Dropwise Condensation”, *Chem. Eng. Progress*, 45, No.11, pp.661–674, 1949.
13. Sugawara, S. and Michiyoshi, I., “Dropwise Condensation”, *Mem. Fac. Engng, Kyoto Univ.*, 18, No.2, 1956.
14. Wenzel, H., “Der Wärmeübergang bei der Tropfenkondensation”, *Linde-Ber. Tech. Wiss.* 18, 44, 1964.
15. Gose, E. E., Mucciardi, A. N. and Baer, E., “Model for Dropwise Condensation on Randomly Distributed Sites”, *Int. J. Heat Mass Transfer*, 10, 15, 1967.
16. Tanasawa, I. and Tachibana, F., “A synthesis of the total process of dropwise condensation using the method of computer simulation”, *Proc. Fourth Int. Heat Transfer Conference* 6, 1970.
17. Yu-Ting Wu, Chen-Xin Yang and Xiu-Gan Yuan, “A Theoretical Study of the Effect of Surface Thermal Conductivity on Heat Transfer coefficient in Dropwise Condensation”, *Numerical Heat Transfer, part A*, 40, p. 169-179, 2001.

18. Le Fevre , E.J. and Rose , J.W. , ‘‘A Theory of Heat Transfer by Dropwise Condensation ,’’ Proc. of 3rd. Inter. Heat Transfer Conf. , 2 , pp.362 – 375, 1966.
19. Tanaka , H. , ‘‘Measurements of Dropsize Distributions during Transient Dropwise Condensation ‘’ , Trans. A.S.M.E. , Journal of Heat Transfer , 97 , pp.341-346, 1975.
20. Wu, H. W. and Maa, J. R., ‘‘On the heat transfer in dropwise condensation’’, The Chemical Engineering Journal, vol.12, pp.225-231, 1976.
21. Maa J. R., ‘‘Drop size distribution and heat flux of dropwise condensation’’, Chemical Engineers J., vol.16, pp.171-176, 1978.
22. Tanaka H., ‘‘A theoretical study of dropwise condensation’’, Transactions of the ASME Journal of Heat Transfer, 97, pp.72-78, 1975.
23. Tanaka H., ‘‘Measurement of drop size distribution during transient dropwise condensation’’, Transactions of the ASME Journal of Heat Transfer, 97, pp.341-346, 1975.
24. Tanaka H., ‘‘Further developments of dropwise condensation theory’’, Transactions of the ASME Journal of Heat Transfer, 101, pp.603-611, 1979.
25. Tanner , D.W. , Pope , D. , Potter , C.J. and West , D. , ‘‘Heat Transfer in Dropwise Condensation-Part I, The Effects of Heat Flux, Steam Velocity and Non-Condensable gas Concentration’’, Int. J. Heat Mass Transfer , 8 , pp.419 – 426, 1965.
26. Tanner , D.W. , Pope , D. , Potter , C.J. and West , D. , ‘‘Heat transfer in dropwise condensation at low steam pressures in the absence and presence of noncondensable gas’’, Int. J. Heat Mass Transfer, 11, pp.181 – 190, 1968.

27. Hurst , C.J. and Olson , D.R. ,’’Conduction through Droplets during Dropwise Condensation , ’’ J. Heat Transfer ,95 ,pp 12-20, 1973.
28. Peter Griffith and Man Suk Lee, “The Effect of Surface Thermal Properties and Finish on Dropwise Condensation”, Int. J. Heat Mass Transfer, 10, p. 697-707, 1967.
29. Mikic B. B. and R. J. Hannemann, “An Experimental Investigation Into the Effect of Surface Thermal Conductivity on the Rate of Heat Transfer in Dropwise Condensation”, Int. J. Heat and Mass Transfer, 19, p. 1309-1317, 1976.
30. Mikic B. B. “On Mechanism of Dropwise Condensation”, Int. J. Heat and Mass Transfer, 12, p. 1311-1323, 1969.
31. Sadhal, S. S. and Plesset, M. S., “Effect of solid properties and contact angle in dropwise condensation theory”, Transactions of the ASME Journal of Heat Transfer, 101, pp.48-54, 1979.
32. Rose J. W., “Effect of condenser tube material on heat transfer during dropwise condensation of steam”, Int. J. Heat and Mass Transfer, 21, p.835-840, 1978.
33. Tsuruta T., Tanaka H. and Togashi S., “Experimental verification of constriction resistance theory in dropwise condensation heat transfer”, Int. J. Heat and Mass Transfer, vol.34, p.2787-2796, 1991.
34. Rose J. W., “The effect of surface thermal conductivity on dropwise condensation heat transfer”, Int. J. Heat and Mass Transfer, 21, p.80-81, 1978.
35. Othmer , D.F. , “ The Condensation of Steam ” Industrial and Engineering Chemistry , 21 , p.576, 1929.

36. E. J. Le Fevre and J. W. Rose, "An Experimental Study of Heat Transfer by Dropwise Condensation", *Int. J. Heat and Mass Transfer*, 8, p. 1117-1133, 1965.
37. E. Citakoğlu and J. W. Rose, "Dropwise Condensation-Some Factors Influencing the Validity of Heat Transfer Measurements", *Int. J. Heat and Mass Transfer*, 11, p. 523-537, 1968.
38. Tanner , D.W. , Pope , D. , Potter , C.J. and West , D. , "Heat Transfer in Dropwise Condensation-Part II, Surface Chemistry", *Int. J. Heat Mass Transfer*, 8 , pp.427 – 436, 1965.
39. Rose, J. W., Boone, D. H., Marto, P. J., Wanniarachchi, A. S. and Holden, K. M., "The Use of Organic Coatings to Promote Dropwise Condensation of Steam", *Journal of Heat Transfer*, 109, p. 768-774, 1987.
40. D.C. Zhang, Z.Q. Lin, J.F. Lin, New surface materials for dropwise condensation, in: *Proceedings of the 8th International Heat Transfer Conference '86*, Vol. 4, San Francisco, p. 1677–1682, 1986.
41. D.C. Zhang, Z.Q. Lin, J.F. Lin, New method for achieving dropwise condensation. III. Determination of dropwise-condensation-heat transfer coefficient and life-time tests of heat transfer surfaces, *J. Chem. Ind. Eng. (China)*, 38, 274–280, 1987.
42. Q. Zhao, D.C. Zhang, J.F. Lin, Surface materials with dropwise condensation made by ion implantation technology, *Int. J. Heat Mass Transfer*, 34, p. 2833–2835 , 1991.
43. Y.J. Song, X.H. Ma, D.Q. Xu, J.F. Lin, Condensation of steam on chromium, in: *Proceedings of China–Japan Chemical Engineering Conference*, Tianjin University Press, Tianjin, p. 688–695, 1991.

44. S.S. Finnicum, J.W. Westwater, Dropwise condensation of steam on chromium, *Int. J. Heat Mass Transfer*, 32, p. 1541–1549, 1989.
45. Q. Zhao, D. C. Zhang, X. B. Zhu, D. Q. Xu, Z. Q. Lin, J. F. Lin, Industrial Application of Dropwise Condensation, *Heat Transfer* 1990, 4, p. 391-394, 1990.
46. Q. Zhao, B. M. Burnside, Dropwise Condensation of Steam on Iron Implanted Condenser Surfaces, *Heat Recovery Syst. CHP*, 14, p. 525-534, 1994.
47. Q. Zhao, J. F. Lin, Research Progress on Industrial Application of Dropwise Condensation, *Chem. Ind. Eng. Progress (China)*, 53, p. 17-20, 1991.
48. Q. Zhao, D. Q. Xu, Dropwise Condensation Surface With Corrosion Resistant Properties, *Corrosion Rev.*, 11, p. 97-103, 1993.
49. Q. Zhao, D. C. Zhang, X. B. Zhu, D. Q. Xu, J. F. Lin, The Dropwise Condensation Condenser Design, *Nat. J.*, 14 (3), p. 232-233, 1991.
50. Q. Zhao, G. Q. Wang, Vertical Dropwise Condensation Shell and Tube Heat Exchanger for Steam With Water Cooling, Patent No.91100529.3, China Patent Bureau, Patent Authority, Dalian University of Technology/Dalian Power Station.
51. G. Q. Wang, Q. Zhao, G. Li, F. Fu, S. Li, Vertical Dropwise Condensation Shell and Tube Heat Exchanger for Steam With Water Cooling, Patent No.91100592.6, China Patent Bureau, Patent Authority, Dalian University of Technology/Dalian Power Station.
52. X.H. Ma, B.X. Wang, D.Q. Xu, J.F. Lin, Experimental investigation of dropwise condensation lifetime for polymer surfaces, *J. Eng. Thermophys.*, 18, p. 196–200, 1997.

53. X.H. Ma, Dropwise condensation on PTFE coated surfaces and the catastrophe transition mechanisms between dropwise and film condensation, Ph.D. Thesis, Dalian University of Technology, 1994.
54. A.W. Adamson, Physical Chemistry of Surfaces, 5th Edition, Wiley, New York, 1990.
55. D.K. Owens, R.C. Wendt, Estimation of the surface free energy of polymers, J. Appl. Polym. Sci., 13, p. 1741–1747, 1967.
56. D. G. Wilkins, L. A. Bromley, “Dropwise condensation phenomena”, A. I. Ch. E. Journal, vol.19, pp.839-845, 1973.
57. S. N. Aksan and J. W. Rose, “Dropwise condensation-the effect of thermal properties of the condenser material”, Int. J. Heat and Mass Transfer, vol.16, pp. 461-467, 1973.
58. Mikic B. B. “Thermal constriction resistance due to non-uniform surface conditions, contact resistance at non-uniform interface pressure”, Int. J. Heat and Mass Transfer, vol.15, pp. 1497-1500, 1970.
59. Mikic B. B. and R. J. Hannemann, “An analysis of the effect of surface thermal conductivity on the rate of heat transfer in dropwise condensation”, Int. J. Heat and Mass Transfer, vol.19, p. 1299-1307, 1976.
60. R. J. Hannemann, “ Condensing surface thickness effects in dropwise condensation”, Int. J. Heat and Mass Transfer, vol.21, pp. 65-66, 1978.
61. Tsuruta T., Tanaka H., “A theoretical study on the constriction resistance in dropwise condensation”, Int. J. Heat and Mass Transfer, vol.34, p.2779-2786, 1991.

62. C. Graham, "The limiting heat transfer mechanism of dropwise condensation", Ph.D. Thesis, Massachusetts Institute of Technology, 1969
63. S. Hatamiya and H. Tanaka, "Dropwise condensation of steam at low pressures", *Int. J. Heat and Mass Transfer*, vol.30, p.497-507, 1987.
64. S. A. Stylianou and J. W. Rose, "Dropwise condensation on surfaces having different thermal conductivities", *Trans. Am. Soc. Mech. Engrs., Series C, J. Heat Transfer* 102, pp. 477-482, 1980

APPENDIX A

FORTRAN SOURCE PROGRAM

```
IMPLICIT REAL(A-H,O-Z)
```

```
DIMENSION T(61,30),TN(61,30),rr(62) ,zz(31)
open(9, file='r6k3.dat')
open(8, file='r6k3b.dat')
```

```
! rrr rdamla olacak
! rksub rk thermal conductivity
```

```
h_fg=2257000.
T_v=(100.+273.)
gam=1.
P_v=100000.
G=461.
h_i=(2.*gam/(2.-gam))*(1./(2.*3.1416))**(1./2.)*P_v*h_fg**2./
1(T_v**(5./2.)*G**(3./2.))
rk=0.6450
```

```
rksub=0.645*100 ! A=rksub/rk, A=100
rrr=rksub/h_i/0.0001/10. ! rdamla, B=rksub/(hi*rrr), B=0.001
c rrr = damlan □ n yar □ cap □ ! c
rdamla=rrr
conang=65./180.*3.1416 ! radyan olmas □ n □ tek et
```

```
c open(50, file='Result50.dat')
c write(50,*)h_i ,h_fg ,T_v ,gam ,P_v ,G ,rk ,rksub ,rrr ,rdamla ,conang
```

```
open(97, file='Result97.dat')
write(97,*) rrr
```

```
cp=444.
ro=8900.
```

```

tme=0.0
uc=0.0001      !
kedge=30      !
mr=30         !
drl=(alog(1.)-alog(uc))/kedge
alfa=rksub/(ro*cp)
delx=uc*exp(drl)*rdamla
biot=h_i*delx/rksub
dt=0.1/(1.+biot)*(delx)**2/alfa*.1

do 100 i=1,kedge
100 rr(i)=1.-uc*exp(drl*(kedge-i))

do 110 i=kedge+2,mr+kedge+1
110 rr(i)=1.+uc*exp(drl*(i-kedge-2))
c   rr(kedge+1)=1+uc
c   rr(kedge)=1.

rr(30)=0.9999
rr(31)=1.0

ucz=.0001     !           !
nz=30        !           !
dzl=((alog(10.))-alog(ucz))/(nz-2)

do 120 i=1,nz
120 zz(i+1)=ucz*exp(dzl*(i-1))      !

kenar=kedge+1      ! <<-----
nnz=nz
nnr=kedge+1+mr

do 125 i=1,nnr      !BUNLARI initialization
                        !icin muhafaza et
do 125 j=1,nnz      !
125 T(i,j)=0.      !

c   open(56, file='Result56.dat')
c   write(56,*)i ,j ,T

```

```

c 125 write(*,*)T(i,j),i,j  !
c   xx=F(.1)                !
c   write(*,*)xx
      !-----
      nyaz=0
127 tme=tme+dt

      nyaz=nyaz+1

      open(57, file='Result57.doc')
      write(57,*)tme

      if(nyaz.eq.0)go to 716
      write(9,*)tme

```

716 continue

```

do 131 i=2,nnr-1
do 130 j=2,nnz-1

```

```

      A10=-ro*cp/(rksub*dt)*rdamla**2*(((rr (i+1)+rr (i))/2)**2-
      1((rr (i)+rr (i-1))/2)**2)*((zz (j+1)-zz (j-1))/2)
      BG=(T (i,j)-T (i,j+1))*(((rr (i+1)+rr (i))/2)**2-((rr (i)+
      1rr (i-1))/2)**2)/(zz (j+1)-zz (j))
      BB=(T (i,j)-T (i-1,j))*(((rr (i)+rr (i-1))/2)*(zz (j+1)-
      1zz (j-1)))/(rr (i)-rr (i-1))
      BD=(T (i,j)-T (i+1,j))*(((rr (i+1)+rr (i))/2)*(zz (j+1)-
      1zz (j-1)))/(rr (i+1)-rr (i))
      BK=(T (i,j)-T (i,j-1))*(((rr (i+1)+rr (i))/2)**2-((rr (i)+
      1rr (i-1))/2)**2)/(zz (j)-zz (j-1))

```

```

      anum=abs(BK+BG+BB+BD)
      den=abs(a10)

```

```

      TN (i,j)=T (i,j)+(BK+BG+BB+BD)/A10

```

```

c   GO TO 130
c 132 TN (i,j)=T (i,j)

```

```

c   open(61, file='Result61.dat')
c   write(61,*)i ,j ,TN(i,j)

```

130 continue ! write(*,*)i,j,a10,bg,bb,bd,bk,tn(i,j)

131 continue

c damla altı kuzey kenar orta kısım 4

j=1

do 140 i=2,kenar-1

Fr=1/(rksub/(h_i*rrr)+(1-rr(i))*((conang)-asin((1-rr(i))/
1(2/sin(conang))))*rksub/(rk))

c open(63, file='Result63.dat')

c write(63,*) i, Fr

A10=-ro*cp/(rksub*dt)*rdamla**2*((rr (i+1)+rr (i))/2)**2-
1((rr (i)+rr (i-1))/2)**2)*((zz (j+1)-zz (j))/2)
BG= (T (i,j)-T (i,j+1))*((rr (i+1)+rr (i))/2)**2-
1((rr (i)+rr (i-1))/2)**2)/(zz (j+1)-zz (j))
BB= (T (i,j)-T (i-1,j))*((rr (i)+rr (i-1))/2)*
1(zz (j+1)-zz (1))/(rr (i)-rr (i-1))
BD= (T (i,j)-T (i+1,j))*((rr (i+1)+rr (i))/2)*
1(zz (j+1)-zz (1))/(rr (i+1)-rr (i))
BK= (T (i,j)-1)*((rr (i+1)+rr (i))/2)**2-
1((rr (i)+rr (i-1))/2)**2)*(Fr)

TN (i,j)=T (i,j)+(BK+BG+BB+BD)/A10

140 continue

c damla altı kuzey kenar damla merkezi 5

j=1

i=1

Fr=1/(rksub/(h_i*rrr)+(1-rr(i))*((conang)-asin((1-rr(i))/
1(2/sin(conang))))*rksub/(rk))

A10= -ro*cp/(rksub*dt)*rdamla**2*((rr (i+1)+rr (i))/2)**2*
1((zz (j+1)-zz (j))/2)
BG= (T (i,j)-T (i,j+1))*((rr (i+1)+rr (i))/2)**2/
1(zz (j+1)-zz (j))
BB= 0.0
BD= (T (i,j)-T (i+1,j))*((rr (i+1)+rr (i))/2)*

$$1(zz(j+1)-zz(1))/((rr(i+1)-rr(i)))$$

$$BK = (T(i,j)-1) * ((rr(i+1)+rr(i))/2)^2 * (Fr)$$

$$TN(i,j) = T(i,j) + (BK + BG + BB + BD) / A10$$

c damla altı damla ucu **6**

$$j=1$$

$$i = \text{kenar} \quad ! \text{ kenar ?}$$

$$Fr = 1 / (rksub / (h_i * rrr) + (1 - rr(i)) * ((\text{conang}) - \text{asin}((1 - rr(i)) / 1(2 / \sin(\text{conang})))) * rksub / (rk))$$

$$A10 = -ro * cp / (rksub * dt) * rdamla^2 * (((rr(i+1) + 1rr(i))/2)^2 - ((rr(i) + rr(i-1))/2)^2) * ((zz(j+1) - zz(j))/2)$$

$$BG = (T(i,j) - T(i,j+1)) * (((rr(i+1) + rr(i))/2)^2 - ((rr(i) + 1rr(i-1))/2)^2) / (zz(j+1) - zz(j))$$

$$BB = (T(i,j) - T(i-1,j)) * (((rr(i) + rr(i-1))/2) * 1(zz(j+1) - zz(1)) / (rr(i) - rr(i-1)))$$

$$BD = (T(i,j) - T(i+1,j)) * (((rr(i+1) + rr(i))/2) * 1(zz(j+1) - zz(1)) / (rr(i+1) - rr(i)))$$

$$BK = (T(i,j) - 1) * (((rr(i+1) + rr(i))/2)^2 - 1((rr(i) + rr(i-1))/2)^2) * (Fr / 2.)$$

$$TN(i,j) = T(i,j) + (BK + BG + BB + BD) / A10$$

c izole yuzey kuzey kenar orta kısım **7**

$$j=1$$

$$\text{do } 150 \quad i = \text{kenar} + 1, \text{ nnr} - 1$$

$$A10 = -ro * cp / (rksub * dt) * rdamla^2 * (((rr(i+1) + rr(i))/2)^2 - 1((rr(i) + rr(i-1))/2)^2) * ((zz(j+1) - zz(j))/2)$$

$$BG = (T(i,j) - T(i,j+1)) * (((rr(i+1) + rr(i))/2)^2 - 1((rr(i) + rr(i-1))/2)^2) / (zz(j+1) - zz(j))$$

$$BB = (T(i,j) - T(i-1,j)) * (((rr(i) + rr(i-1))/2) * (zz(j+1) - 1zz(1)) / (rr(i) - rr(i-1)))$$

$$BD = (T(i,j) - T(i+1,j)) * (((rr(i+1) + rr(i))/2) * (zz(j+1) - 1zz(1)) / (rr(i+1) - rr(i)))$$

$$BK = 0.0$$

$$TN(i,j) = T(i,j) + (BK + BG + BB + BD) / A10$$

150 continue

c izole yuzey kuzey kenar kose **8**

$$j=1$$

i=nnr

```
A10= -ro*cp/(rksub*dt)*rdamla**2*((rr (i+1)+
1rr (i))/2)**2-((rr (i)+rr (i-1))/2)**2*((zz (j+1)-zz (j))/2)
BG= (T (i,j)-T (i,j+1))*(((rr (i+1)+rr (i))/2)**2-
1((rr (i)+rr (i-1))/2)**2)/(zz (j+1)-zz (j))
BB= (T (i,j)-T (i-1,j))*(((rr (i)+rr (i-1))/2)*
1(zz (j+1)-zz (1)))/(rr (i)-rr (i-1))
BD= (T (i,j))*(((rr (i+1)+rr (i))/2)*(zz (j+1)-zz (1)))/
1(rr (i+1)-rr (i))
BK= 0.0
TN (i,j)=T (i,j)+(BK+BG+BB+BD)/A10
```

c batı orta **9**

i=1

do 160 j=2,nnz-1

```
A10= -ro*cp/(rksub*dt)*rdamla**2*((rr (i+1)+rr (i))/2)**2*
1((zz (j+1)-zz (j-1))/2)
BG= (T (i,j)-T (i,j+1))*(((rr (i+1)+rr (i))/2)**2)/
1(zz (j+1)-zz (j))
BB= 0.0

BD= (T (i,j)-T (i+1,j))*(((rr (i+1)+rr (i))/2)*
1(zz (j+1)-zz (j-1)))/(rr (i+1)-rr (i))
BK= (T (i,j)-T (i,j-1))*(((rr (i+1)+rr (i))/2)**2)/
1(zz (j)-zz (j-1))

TN (i,j)=T (i,j)+(BK+BG+BB+BD)/A10
```

160 continue

c doğu orta **13**

i=nnr

do 165 j=2,nnz-1

```
A10=-ro*cp/(rksub*dt)*rdamla**2*((rr (i+1)+rr (i))/2)**2-
1((rr (i)+rr (i-1))/2)**2*((zz (j+1)-zz (j-1))/2)
BG= (T (i,j)-T (i,j+1))*(((rr (i+1)+rr (i))/2)**2-
1((rr (i)+rr (i-1))/2)**2)/(zz (j+1)-zz (j))
BB= (T (i,j)-T (i-1,j))*(((rr (i)+rr (i-1))/2)*(zz (j+1)-
1zz (j-1)))/(rr (i)-rr (i-1))
BD= (T (i,j)-0.0)*(((rr (i+1)+rr (i))/2)*(zz (j+1)-
1zz (j-1)))/(rr (i+1)-rr (i))
BK= (T (i,j)-T (i,j-1))*(((rr (i+1)+rr (i))/2)**2-
```

$$1((rr(i)+rr(i-1))/2)**2)/(zz(j)-zz(j-1))$$

$$TN(i,j)=T(i,j)+(BK+BG+BB+BD)/A10$$

165 continue

c batı alt uc **10**

i=1

j=nnz

$$A10=-ro*cp/(rksub*dt)*rdamla**2*((rr(i+1)+rr(i))/2)**2*1((zz(j+1)-zz(j-1))/2)$$

$$BG=(T(i,j)-0)*(((rr(i+1)+rr(i))/2)**2)/(zz(j+1)-zz(j))$$

$$BB=0.0$$

$$BD=(T(i,j)-T(i+1,j))*(((rr(i+1)+rr(i))/2)*1(zz(j+1)-zz(j-1)))/(rr(i+1)-rr(i))$$

$$BK=(T(i,j)-T(i,j-1))*(((rr(i+1)+rr(i))/2)**2)/1(zz(j)-zz(j-1))$$

$$TN(i,j)=T(i,j)+(BK+BG+BB+BD)/A10$$

c güney orta **11**

j=nnz

do 170 i=2,nnr-1

$$A10=-ro*cp/(rksub*dt)*rdamla**2*((rr(i+1)+1rr(i))/2)**2-((rr(i)+rr(i-1))/2)**2)*((zz(j+1)-zz(j-1))/2)$$

$$BG=(T(i,j)-0.0)*(((rr(i+1)+rr(i))/2)**2-1((rr(i)+rr(i-1))/2)**2)/(zz(j+1)-zz(j))$$

$$BB=(T(i,j)-T(i-1,j))*(((rr(i)+rr(i-1))/2)*1(zz(j+1)-zz(j-1)))/(rr(i)-rr(i-1))$$

$$BD=(T(i,j)-T(i+1,j))*(((rr(i+1)+rr(i))/2)*1(zz(j+1)-zz(j-1)))/(rr(i+1)-rr(i))$$

$$BK=(T(i,j)-T(i,j-1))*(((rr(i+1)+rr(i))/2)**2-1((rr(i)+rr(i-1))/2)**2)/(zz(j)-zz(j-1))$$

$$TN(i,j)=T(i,j)+(BK+BG+BB+BD)/A10$$

170 continue

c güney sağ köşe **12**

```

i=nnr
j=nnz

A10=-ro*cp/(rksub*dt)*rdamla**2*(((rr (i+1)+rr (i))/2)**2-
1((rr (i)+rr (i-1))/2)**2)*((zz (j+1)-zz (j-1))/2)
BG=(T (i,j)-0.0)*(((rr (i+1)+rr (i))/2)**2-((rr (i)+
1rr (i-1))/2)**2)/(zz (j+1)-zz (j))
BB=(T (i,j)-T (i-1,j))*(((rr (i)+rr (i-1))/2)*
1(zz (j+1)-zz (j-1)))/(rr (i)-rr (i-1))
BD=(T (i,j)-0.0)*(((rr (i+1)+rr (i))/2)*(zz (j+1)-
1zz (j-1)))/(rr (i+1)-rr (i))
BK=(T (i,j)-T (i,j-1))*(((rr (i+1)+rr (i))/2)**2-
1((rr (i)+rr (i-1))/2)**2)/(zz (j)-zz (j-1))
TN (i,j)=T (i,j)+(BK+BG+BB+BD)/A10

do 129 j=1,nnz
do 129 i=1,nnr

129 T(i,j)=TN(i,j)
c write(*,*)TN(kedge,1),kedge,1 !

open(86, file='Result86.doc')
write(86,*) TN(kedge,1),kedge,1

qtot=0

write(*,*) i , j , (T(i,1),i=1,nnr)

open(87, file='Result87.doc')
write(87,*) i , j ,(T(i,1),i=1,nnr)

if(nyaz.eq.50000)go to 777
go to 888
777 open(88, file='Result88.doc')
do 810 j=1,30
do 810 i=1,61

write(88,*) i , j ,T(i,j)
810 continue

j=1
do 778 i=1,31

```

```
Fr=1/(rksub/(h_i*rrr)+(1-rr(i))*((conang)-asin((1-rr(i))/
1(2/sin(conang)))))*rksub/(rk))
```

```
open(66, file='Result66.dat')
write(66,*) i, Fr
```

778 continue

888 continue

```
tq=0
taver=0
qa=0.0
bbr0=0.0
tcm=0.0
```

```
do 133 i=1,kedge-1
Fr=1/(rksub/(h_i*rrr)+(1-rr(i))*((conang)-asin((1-rr(i))/
1(2/sin(conang)))))*rksub/(rk))
Frp=1/(rksub/(h_i*rrr)+(1-rr(i+1))*((conang)-asin((1-rr(i+1))/
1(2/sin(conang)))))*rksub/(rk))
```

```
c open(89, file='Result89.dat')
c write(89,*) i ,Fr ,Frp
```

```
qtot=qtot+(Fr+Frp)/2*(3.1416)*(rr(i+1)**2-rr(i)**2)*
1(1.-(T(i,1)+T(i+1,1))/2)
tq=tq+(Fr+Frp)/2*(3.1416)*(rr(i+1)**2-rr(i)**2)*
1(1.-(T(i,1)+T(i+1,1))/2)*(T(i,1)+T(i+1,1))/2
```

```
taver=taver+(3.1416)*(rr(i+1)**2-rr(i)**2)*
1(T(i,1)+T(i+1,1))/2
```

```
qa=qa+(Fr+Frp)/2*(rr(i+1)**2-rr(i)**2)*(1.-(T(i,1)+T(i+1,1))/2)
```

```
bbr0=bbr0+(Fr+Frp)/2*(rr(i+1)**2-rr(i)**2)
```

```
tcm=tcm+(Fr+Frp)/2*(rr(i+1)**2-rr(i)**2)*((T(i,1)+T(i+1,1))/2)
```

```
c write(*,*)qtot,tq,taver,qa,bbr0,tcm
```

133 continue

```
r0=1/bbr0
tcm=tcm*r0
```

```
      rcon=(tcm-taver)/qa  
c    write(*,*)qa,taver,tcm,r0,rcon
```

```
      if(nyaz.eq.50000)go to 156  
      go to 127  
156 continue  
      do 126 j=1,nnz  
      do 126 i=1,nnr
```

```
      if(nyaz.eq.0)go to 126  
      write(9,*)rr(i),zz(j),tn(i,j)  
126 continue
```

```
      do 141 i=1,nnr  
      if(nyaz.eq.0)go to 141  
      write(8,*) i,rr(i),T(i,1)
```

```
141 continue
```

```
      END
```

APPENDIX B

Table B.1 Variation of nondimensional radial distance rr_i

i	rr_i	i	rr_i
1	0	32	1.0001
2	0.4588306	33	1.000136
3	0.6018929	34	1.000185
4	0.7071356	35	1.000251
5	0.7845566	36	1.000341
6	0.8415107	37	1.000464
7	0.8834086	38	1.000631
8	0.9142304	39	1.000858
9	0.9369043	40	1.001166
10	0.9535841	41	1.001585
11	0.9658545	42	1.002154
12	0.9748811	43	1.002929
13	0.9815215	44	1.003981
14	0.9864064	45	1.005412
15	0.9900	46	1.007356
16	0.9926436	47	1.01
17	0.9945883	48	1.013594
18	0.9960189	49	1.018479
19	0.9970714	50	1.025119
20	0.9978456	51	1.034145
21	0.9984151	52	1.046416
22	0.9988341	53	1.063096
23	0.9991423	54	1.08577
24	0.999369	55	1.116591
25	0.9995359	56	1.158489
26	0.9996585	57	1.215443
27	0.9997488	58	1.292864
28	0.9998152	59	1.398107
29	0.999864	60	1.541169
30	0.9999	61	1.735642
31	1.0000		

Table B.2 Variation of nondimensional axial distance z_j

j	Z_j
1	0
2	9.9999997E-05
3	1.5085906E-04
4	2.2758459E-04
5	3.4333198E-04
6	5.1794742E-04
7	7.8137073E-04
8	1.1787686E-03
9	1.7782793E-03
10	2.6826956E-03
11	4.0470897E-03
12	6.1054020E-03
13	9.2105530E-03
14	1.3894954E-02
15	2.0961799E-02
16	3.1622775E-02
17	4.7705825E-02
18	7.1968563E-02
19	0.1085711
20	0.1637894
21	0.2470911
22	0.3727593
23	0.5623413
24	0.8483428
25	1.279802
26	1.930698
27	2.912632
28	4.39397
29	6.628703
30	9.999999
31	15.08591

APPENDIX C

$$\frac{rCp(TN_{i,j} - T_{i,j})}{dt} = \frac{(1 - T_{i,j})[r_o^{*2} - r_i^{*2}] \left[\frac{1}{\frac{k_s}{h_i r} + (1 - rr_i) \left[q - a \sin \left(\frac{(1 - rr_i)}{\left(\frac{2}{\sin q} \right)} \right) \right] \frac{k_s}{k}} \right] k_s}{r^2 (r_o^{*2} - r_i^{*2}) \Delta z}$$

$$\frac{\Delta TrCp(TN_{i,j} - T_{i,j})}{dt} = \frac{\Delta T (1 - T_{i,j}) [r_o^{*2} - r_i^{*2}] \Pi \left[\frac{1}{\frac{k_s}{h_i r} + (1 - rr_i) \left[q - a \sin \left(\frac{(1 - rr_i)}{\left(\frac{2}{\sin q} \right)} \right) \right] \frac{1}{k}} \right] k_s}{\Pi r^2 (r_o^{*2} - r_i^{*2}) \Delta z}$$

$$\frac{\Delta TrCp(TN_{i,j} - T_{i,j})}{dt} = \frac{\Delta T (1 - T_{i,j}) [r_o^{*2} - r_i^{*2}] \Pi \left[\frac{1}{\frac{1}{h_i r} + (1 - rr_i) \left[q - a \sin \left(\frac{(1 - rr_i)}{\left(\frac{2}{\sin q} \right)} \right) \right] \frac{1}{k}} \right] \frac{1}{k}}{\Pi r^2 (r_o^{*2} - r_i^{*2}) \Delta z \frac{r}{r}}$$

$$V = \Pi r^2 (r_o^{*2} - r_i^{*2}) \Delta z$$

$$\frac{\Delta TrVCp(TN_{i,j} - T_{i,j})}{dt} = \Delta T (1 - T_{i,j}) [r_o^{*2} - r_i^{*2}] \Pi \left[\frac{1}{\frac{1}{h_i r} + (1 - rr_i) \left[q - a \sin \left(\frac{(1 - rr_i)}{\left(\frac{2}{\sin q} \right)} \right) \right] \frac{1}{k}} \right] \frac{1}{k}$$

$$\frac{\Delta U}{\Delta t} = \frac{r}{r} \Delta T (1 - T_{i,j}) [r_o^{*2} - r_i^{*2}] \Pi \left[\frac{1}{\left[\frac{1}{h_i r} + (1 - rr_i) \left[q - a \sin \left(\frac{(1 - rr_i)}{(2/\sin q)} \right) \right] \right] \frac{1}{k}} \right] r$$

$$\frac{\Delta U}{\Delta t} = r^2 \Delta T (1 - T_{i,j}) [r_o^{*2} - r_i^{*2}] \Pi \left[\frac{1}{\left[\frac{1}{h_i} + (1 - rr_i) \left[q - a \sin \left(\frac{(1 - rr_i)}{(2/\sin q)} \right) \right] \right] \frac{r}{k}} \right]$$

$$\frac{\Delta U}{\Delta t} = r^2 \Delta T \Pi (1 - T_{i,j}) [r_o^{*2} - r_i^{*2}] \left[\frac{1}{\left[\frac{1}{h_i} + (1 - rr_i) \left[q - a \sin \left(\frac{(1 - rr_i)}{(2/\sin q)} \right) \right] \right] \frac{r}{k}} \right] \frac{r}{r}$$

$$\frac{\Delta U}{\Delta t} = r^2 \Delta T \Pi \frac{1}{r} (1 - T_{i,j}) [r_o^{*2} - r_i^{*2}] \left[\frac{1}{\left[\frac{1}{h_i r} + (1 - rr_i) \left[q - a \sin \left(\frac{(1 - rr_i)}{(2/\sin q)} \right) \right] \right] \frac{1}{k}} \right]$$

$$\frac{\Delta U}{\Delta t} = r^2 \Delta T \Pi \frac{1}{r} (1 - T_{i,j}) [r_o^{*2} - r_i^{*2}] \left[\frac{1}{\left[\frac{1}{h_i r} + (1 - rr_i) \left[q - a \sin \left(\frac{(1 - rr_i)}{(2/\sin q)} \right) \right] \right] \frac{1}{k}} \right] \frac{k_s}{k_s}$$

$$\frac{\Delta U}{\Delta t} = r \Delta T_s (1 - T_{i,j}) [r_o^{*2} - r_i^{*2}] \left[\frac{1}{\left[\frac{k_s}{h_i r} + (1 - rr_i) \left[q - a \sin \left(\frac{(1 - rr_i)}{(2/\sin q)} \right) \right] \right] \frac{k_s}{k}} \right] \Pi$$

APPENDIX D

MATHCAD PROGRAM SOURCE

$$B = k_s / (h_i \cdot r) \quad A = k_s / k$$

$$h_i := 1.5281966 \cdot 10^7 \cdot \frac{\text{W}}{\text{m}^2 \cdot \text{K}} \quad A := 0.01 \quad k := 0.645 \cdot \frac{\text{W}}{\text{m} \cdot \text{K}} \quad \text{water thermal conductivity}$$

$$k_s := A \cdot k$$

$$k_s = 6.45 \times 10^{-3} \text{ m}^{-1} \text{ K}^{-1} \text{ W} \quad \text{substrate thermal cond.}$$

$$B := 0.001$$

$$r := \frac{k_s}{h_i \cdot B} \quad r = 4.220661 \times 10^{-7} \text{ m}$$

$$i := 1..32 \quad r_i := 1 - 0.0001 \cdot e^{[0.307011346 \cdot (30-i)]}$$

i =

1
2
3
4
5
6
7
8
9
10
11
12
13
14
15
16
17
18
19
20
21
22
23
24
25
26
27
28
29
30
31
32

$r_i =$

0.2643577
0.4588305
0.6018928
0.7071355
0.7845565
0.8415107
0.8834086
0.9142304
0.9369043
0.9535841
0.9658545
0.9748811
0.9815215
0.9864064
0.99
0.9926436
0.9945883
0.9960189
0.9970714
0.9978456
0.9984151
0.9988341
0.9991423
0.999369
0.9995358
0.9996585
0.9997488
0.9998152
0.9998641
0.9999
0.9999264
0.9999459

$r_1 := 0$

$r_1 = 0$

$r_{31} := 1$

$r_{32} := 1.0001$

$r_{31} = 1$

$r_{32} = 1.0001$

$c_{i+1} := r_i$

$d_{i-1} := r_i$

$c_2 = 0$

$d_2 = 0.60189$

$r_2 = 0.45883$

$c_3 = 0.45883$

$d_3 = 0.70714$

$r_3 = 0.60189$

$$\begin{pmatrix} Fr_{1,1} \\ Fr_{2,1} \\ Fr_{3,1} \\ Fr_{4,1} \\ Fr_{5,1} \\ Fr_{6,1} \\ Fr_{7,1} \\ Fr_{8,1} \\ Fr_{9,1} \\ Fr_{10,1} \\ Fr_{11,1} \\ Fr_{12,1} \\ Fr_{13,1} \\ Fr_{14,1} \\ Fr_{15,1} \\ Fr_{16,1} \\ Fr_{17,1} \\ Fr_{18,1} \\ Fr_{19,1} \\ Fr_{20,1} \\ Fr_{21,1} \\ Fr_{22,1} \\ Fr_{23,1} \\ Fr_{24,1} \\ Fr_{25,1} \\ Fr_{26,1} \\ Fr_{27,1} \\ Fr_{28,1} \\ Fr_{29,1} \\ Fr_{30,1} \\ Fr_{31,1} \end{pmatrix} := \begin{pmatrix} 130.862 \\ 172.456 \\ 208.584 \\ 254.283 \\ 309.266 \\ 372.567 \\ 442.27 \\ 515.548 \\ 589.013 \\ 659.279 \\ 723.544 \\ 779.967 \\ 827.756 \\ 867.019 \\ 898.478 \\ 923.182 \\ 942.275 \\ 956.853 \\ 967.881 \\ 976.162 \\ 982.349 \\ 986.952 \\ 990.367 \\ 992.894 \\ 994.764 \\ 996.142 \\ 997.159 \\ 997.908 \\ 998.46 \\ 998.867 \\ 1 \times 10^3 \end{pmatrix} \quad Fr_{1,1} = 130.862$$

$$\begin{pmatrix} T_{1,1} \\ T_{2,1} \\ T_{3,1} \\ T_{4,1} \\ T_{5,1} \\ T_{6,1} \\ T_{7,1} \\ T_{8,1} \\ T_{9,1} \\ T_{10,1} \\ T_{11,1} \\ T_{12,1} \\ T_{13,1} \\ T_{14,1} \\ T_{15,1} \\ T_{16,1} \\ T_{17,1} \\ T_{18,1} \\ T_{19,1} \\ T_{20,1} \\ T_{21,1} \\ T_{22,1} \\ T_{23,1} \\ T_{24,1} \\ T_{25,1} \\ T_{26,1} \\ T_{27,1} \\ T_{28,1} \\ T_{29,1} \\ T_{30,1} \\ T_{31,1} \end{pmatrix} := \begin{pmatrix} 0.311 \\ 0.377 \\ 0.427 \\ 0.481 \\ 0.535 \\ 0.586 \\ 0.632 \\ 0.671 \\ 0.703 \\ 0.729 \\ 0.749 \\ 0.765 \\ 0.776 \\ 0.785 \\ 0.792 \\ 0.796 \\ 0.796 \\ 0.792 \\ 0.784 \\ 0.771 \\ 0.754 \\ 0.735 \\ 0.714 \\ 0.693 \\ 0.672 \\ 0.653 \\ 0.635 \\ 0.619 \\ 0.605 \\ 0.592 \\ 0.546 \end{pmatrix}$$

$$Q_1 := Fr_{1,1} \cdot \left(\frac{rr_2 + rr_1}{2} \right)^2 \cdot (1 - T_{1,1}) \cdot \pi \quad Q_{31} := Fr_{31,1} \cdot \left[(rr_{31})^2 - (rr_{30})^2 \right] \cdot (1 - T_{31,1}) \cdot \pi$$

$$Q_1 = 14.9082668$$

$$Q_{31} = 0.2852424$$

$$Q_{\text{num}} := Q_1 + Q_{31} + \sum_{i=2}^{30} Fr_{i,1} \cdot (1 - T_{i,1}) \cdot \pi \cdot \left[\left(\frac{d_i + rr_i}{2} \right)^2 - \left(\frac{rr_i + c_i}{2} \right)^2 \right]$$

$$Q_{\text{num}} = 4.2988591 \times 10^2$$

$$q_{\text{num}} := |Q_{\text{num}}|$$

$$Q_{\text{num}} = 4.298859 \times 10^2$$

$$Q_{\text{nondim}} := Q_{\text{num}} \cdot \frac{k_s}{k}$$

$$Q_{\text{nondim}} = 4.29886$$

$$\Delta T := 100 \cdot K$$

$$Q := Q_{\text{num}} \cdot \Delta T \cdot r \cdot k_s$$

$$Q = 1.17029 \times 10^{-4} W$$

$$i := 1..31$$

$$A_i := \left[\left(\frac{d_i + r_i}{2} \right)^2 - \left(\frac{r_i + c_i}{2} \right)^2 \right]$$

$$A_1 = 0.0526313$$

$$A_2 = 0.22865$$

$$A_{31} := \left[(r_{31})^2 - (r_{30})^2 \right]$$

$$A_{31} = 1.9999000 \times 10^{-4}$$

$$A_{\text{total}} := \sum_{i=1}^{31} A_i$$

$$A_{\text{total}} = 1.0001$$

$$T_{\text{ave}} := \frac{\sum_{i=1}^{31} T_{i,1} \cdot A_i}{\sum_{i=1}^{31} A_i}$$

$$T_{\text{ave}} = 0.5113038$$

APPENDIX E

RESULTS FOR TEMPERATURE DISTRIBUTIONS

E.1 Variation of temperature at $\tilde{z} = 0$ for $B=0.001$

The variation of temperature at surface of the substrate for $B=0.001$ is given in Table E.1.

Table E.1 Variation of temperature at $\tilde{z} = 0$ for $B=0.001$

	A=0.01	A=0.1	A=1	A=10	A=100
i	T_(i,1)	T_(i,1)	T_(i,1)	T_(i,1)	T_(i,1)
1	0.3106135	0.045532327	0.004769023	0.000479172	4.79387E-05
2	0.3773975	0.061821498	0.00658744	0.000663074	6.63516E-05
3	0.4270595	0.076788969	0.008315541	0.000838436	8.39138E-05
4	0.4808818	0.096911058	0.010729923	0.00108453	0.000108568
5	0.5349712	0.1230729	0.014037632	0.001423542	0.000142556
6	0.5860518	0.1561735	0.01852545	0.001887195	0.000189068
7	0.6317708	0.1968873	0.024575265	0.002518939	0.000252527
8	0.6708666	0.2454018	0.03268791	0.003378353	0.000338972
9	0.7030749	0.3010484	0.043499671	0.004546815	0.000456733
10	0.7288389	0.3621536	0.057812735	0.006135007	0.000617269
11	0.7489945	0.4260538	0.076601349	0.008296785	0.000836562
12	0.7645004	0.4895033	0.1010156	0.011247218	0.001137553
13	0.7762852	0.5492517	0.1323845	0.015308141	0.001555282
14	0.7851455	0.6027421	0.172189	0.021028802	0.002159408
15	0.7916369	0.6483152	0.2217385	0.02952856	0.00315679
16	0.7956765	0.6847119	0.2799933	0.042563334	0.005067232
17	0.7963092	0.7106807	0.3409383	0.060886819	0.008468523
18	0.7924716	0.7258815	0.3967182	0.082890183	0.013373389
19	0.7837956	0.731277	0.4425085	0.1060846	0.019319503
20	0.7706501	0.7285375	0.476979	0.128551	0.025797645
21	0.7538646	0.7194945	0.5008005	0.1492081	0.032441419
22	0.7345064	0.7059135	0.5154217	0.1675633	0.039031234

Table E.1 Continued

23	0.7137122	0.6894032	0.5224884	0.1834537	0.045449365
24	0.692559	0.6713825	0.5236323	0.196877	0.051638413
25	0.6719363	0.6530092	0.5203689	0.2079109	0.057582419
26	0.6525478	0.6351943	0.5140572	0.2166172	0.063276142
27	0.6347483	0.6184675	0.5058011	0.2230693	0.06874641
28	0.6187428	0.603165	0.4964925	0.2272762	0.073968105
29	0.6045951	0.5894565	0.4868447	0.2293213	0.078850679
30	0.5922233	0.577344	0.4773751	0.2294721	0.083282277
31	0.5457392	0.5311556	0.4359659	0.2182481	0.100253
32	0.4952526	0.4806055	0.3866988	0.1813098	0.074846126
33	0.4807645	0.4661795	0.3731548	0.1721687	0.069206908
34	0.463277	0.4488239	0.3572161	0.1620884	0.063442037
35	0.4424717	0.4282475	0.3387543	0.1511778	0.057707202
36	0.4175362	0.4036739	0.3172139	0.1392523	0.051946461
37	0.3877646	0.3744407	0.2921671	0.1261885	0.046103764
38	0.3527331	0.3401676	0.2634492	0.1119909	0.040163793
39	0.312106	0.3005674	0.2309847	0.096698813	0.034120888
40	0.266027	0.2558205	0.1950693	0.080502935	0.028024027
41	0.2151868	0.2066305	0.1563757	0.063714415	0.021951541
42	0.1615861	0.1549499	0.1164661	0.046955761	0.016074512
43	0.1086013	0.1040216	0.07775528	0.031118196	0.010636308
44	0.061712097	0.059064649	0.043999501	0.017553767	0.006026259
45	0.026921984	0.025762085	0.019181389	0.007669768	0.002662554
46	0.007815152	0.007481705	0.005585331	0.00225084	0.000794969
47	0.00128525	0.001231507	0.000923816	0.000376548	0.000135697
48	0.000107046	0.000102678	7.74617E-05	3.19658E-05	1.17488E-05
49	4.29506E-06	4.12414E-06	3.12881E-06	1.30662E-06	4.88895E-07
50	8.20178E-08	7.88316E-08	6.01205E-08	2.53844E-08	9.64985E-09
51	7.48317E-10	7.19895E-10	5.51677E-10	2.35286E-10	9.07126E-11
52	3.29175E-12	3.16933E-12	2.43951E-12	1.05005E-12	4.09987E-13
53	7.05076E-15	6.79365E-15	5.25051E-15	2.27926E-15	9.00168E-16
54	7.41809E-18	7.15254E-18	5.54867E-18	2.42769E-18	9.68882E-19
55	3.86191E-21	3.72604E-21	2.90062E-21	1.27843E-21	5.1517E-22
56	1.0008E-24	9.66163E-25	7.54585E-25	3.3487E-25	1.3616E-25
57	1.29729E-28	1.25309E-28	9.81671E-29	4.38475E-29	1.79788E-29
58	8.44362E-33	8.16016E-33	6.41107E-33	2.88116E-33	1.19072E-33
59	2.76791E-37	2.67629E-37	2.10836E-37	9.53025E-38	3.96806E-38
60	3.49904E-42	3.37433E-42	2.47609E-42	0	0
61	0	0	0	0	0

E.2 Variation of temperature at $\tilde{z} = 9.99 \times 10^{-5}$ for $B=0.001$

The variation of temperature at surface of the substrate for $B=0.001$ is given in Table E.2.

Table E.2 Variation of temperature at $\tilde{z} = 9.99 \times 10^{-5}$ for $B=0.001$

	A=0.01	A=0.1	A=1	A=10	A=100
i	T_(i,2)	T_(i,2)	T_(i,2)	T_(i,2)	T_(i,2)
1	0.3016622	0.044130005	0.004620865	0.000464272	4.64479E-05
2	0.3667386	0.059924327	0.006382866	0.000642457	6.42883E-05
3	0.415191	0.074440353	0.008057406	0.000812368	8.13044E-05
4	0.4677662	0.093960606	0.010397005	0.001050814	0.000105192
5	0.5206746	0.1193488	0.01360241	0.00137929	0.000138124
6	0.5707127	0.1514856	0.01795168	0.001828542	0.00018319
7	0.6155651	0.1910372	0.023815252	0.002440677	0.000244678
8	0.6539742	0.2382039	0.031679098	0.003273442	0.000328439
9	0.685658	0.2923557	0.042160999	0.004405741	0.00044255
10	0.7110304	0.3518886	0.056041025	0.005944932	0.000598122
11	0.7308981	0.4142299	0.074268013	0.008040401	0.000810671
12	0.7461953	0.4762267	0.097965702	0.010901271	0.001102495
13	0.7578266	0.5347045	0.1284405	0.014841522	0.001507768
14	0.766575	0.5871449	0.1671633	0.020400193	0.002094964
15	0.7729723	0.6318812	0.2154573	0.028683715	0.00306928
16	0.7768704	0.6675761	0.2723181	0.041432761	0.00494819
17	0.777177	0.6928127	0.3317393	0.059382454	0.008306253
18	0.7726845	0.7070687	0.3858187	0.08089865	0.013151838
19	0.7629623	0.7112001	0.4296567	0.1034578	0.01901661
20	0.7483981	0.7068596	0.4618609	0.1250951	0.02538288
21	0.7298979	0.6959297	0.4830741	0.1446722	0.031872135
22	0.7086392	0.6802748	0.4947665	0.1616284	0.038247105
23	0.6858854	0.6616265	0.4986634	0.175723	0.044364315
24	0.6628479	0.6415385	0.496536	0.1868786	0.050127357
25	0.6405432	0.6213089	0.490094	0.1951193	0.055458769

Table E.2 Continued

26	0.6198167	0.6019989	0.4809499	0.2005442	0.060261499
27	0.6011819	0.5843071	0.470496	0.2034238	0.064442948
28	0.5850146	0.5687507	0.4599213	0.2041991	0.067890927
29	0.5714785	0.5556026	0.450122	0.2034922	0.070542581
30	0.5604525	0.5448232	0.4415858	0.2019562	0.072438762
31	0.5250885	0.5099537	0.4117421	0.1920367	0.07645455
32	0.4877947	0.4729722	0.3781968	0.1728496	0.0676945
33	0.4754777	0.4607776	0.3672205	0.1665259	0.064629033
34	0.4597041	0.4451822	0.3532931	0.158589	0.060770083
35	0.4401086	0.4258466	0.3362327	0.1491061	0.056251682
36	0.415973	0.4020922	0.3156011	0.1380456	0.051180523
37	0.3867191	0.373387	0.2911262	0.1254785	0.045698244
38	0.3520289	0.3394611	0.2627732	0.1115673	0.039944131
39	0.3116346	0.300097	0.2305487	0.096446	0.034000456
40	0.2657169	0.2555127	0.1947935	0.080354027	0.02795816
41	0.2149896	0.2064359	0.156207	0.063629046	0.021916132
42	0.1614671	0.1548331	0.1163682	0.046908982	0.016056119
43	0.1085354	0.1039574	0.077702917	0.031094419	0.010627333
44	0.06168038	0.059033893	0.043975085	0.017543074	0.006022337
45	0.026909873	0.025750369	0.019172281	0.00766589	0.002661147
46	0.007811972	0.00747864	0.005582972	0.00224985	0.000794609
47	0.001284762	0.001231037	0.000923456	0.000376397	0.000135642
48	0.000107007	0.000102641	7.7433E-05	3.19537E-05	1.17443E-05
49	4.29354E-06	4.12269E-06	3.12769E-06	1.30614E-06	4.88716E-07
50	8.19895E-08	7.88043E-08	6.00996E-08	2.53754E-08	9.64642E-09
51	7.48063E-10	7.1965E-10	5.51488E-10	2.35204E-10	9.0681E-11
52	3.29065E-12	3.16827E-12	2.43868E-12	1.0497E-12	4.09847E-13
53	7.04842E-15	6.79139E-15	5.24875E-15	2.27849E-15	8.99863E-16
54	7.41564E-18	7.15017E-18	5.54683E-18	2.42688E-18	9.68557E-19
55	3.86064E-21	3.72482E-21	2.89966E-21	1.27801E-21	5.14999E-22
56	1.00047E-24	9.65848E-25	7.54338E-25	3.34759E-25	1.36115E-25
57	1.29687E-28	1.25268E-28	9.81351E-29	4.38331E-29	1.79729E-29
58	8.44088E-33	8.15752E-33	6.40899E-33	2.88022E-33	1.19033E-33
59	2.76701E-37	2.67543E-37	2.10768E-37	9.52715E-38	3.96677E-38
60	3.49904E-42	3.37433E-42	2.47609E-42	0	0
61	0	0	0	0	0

E.3 Variation of temperature at $\tilde{z} = 0$ for $B=0.01$

The variation of temperature at surface of the substrate for $B=0.01$ is shown in Figure E.1 and Figure E.2 .

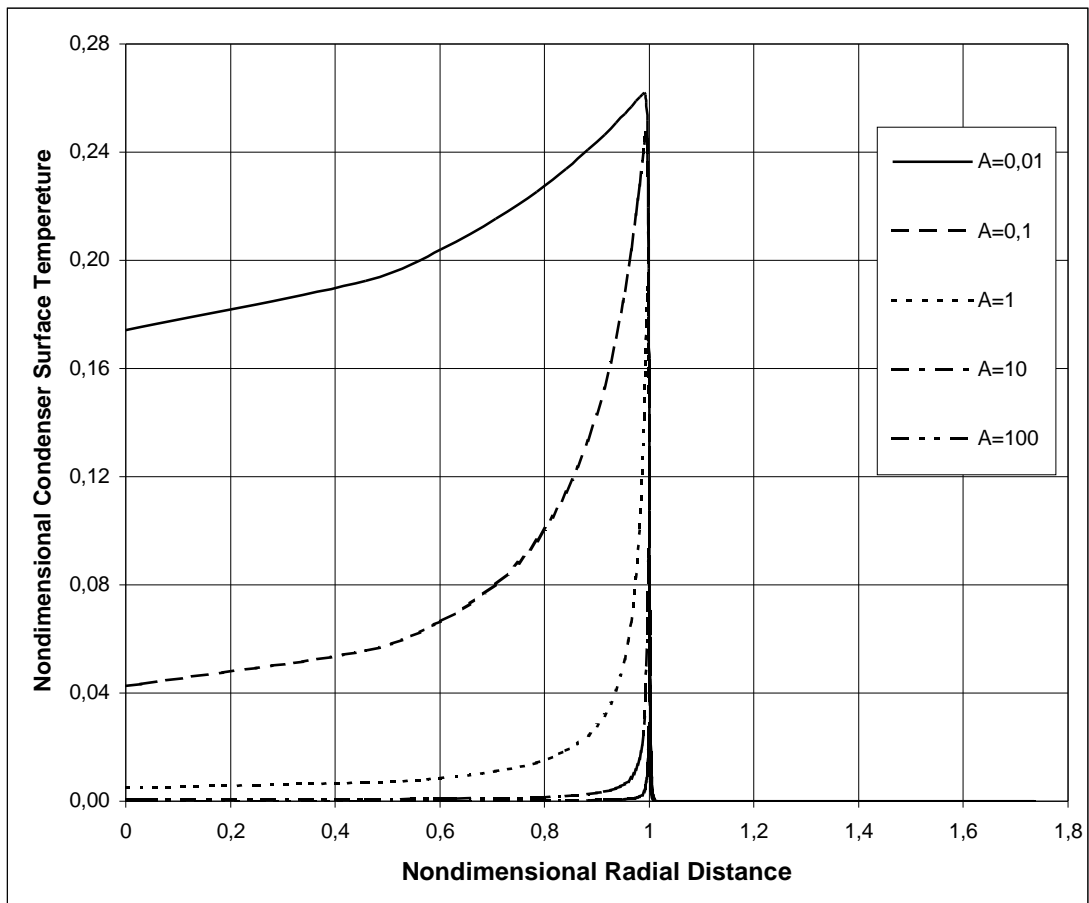


Figure E.1 Variation of nondimensional temperature as a function of nondimensional radial distance at nondimensional axial distance $\tilde{z} = 0$ for $B=0.01$

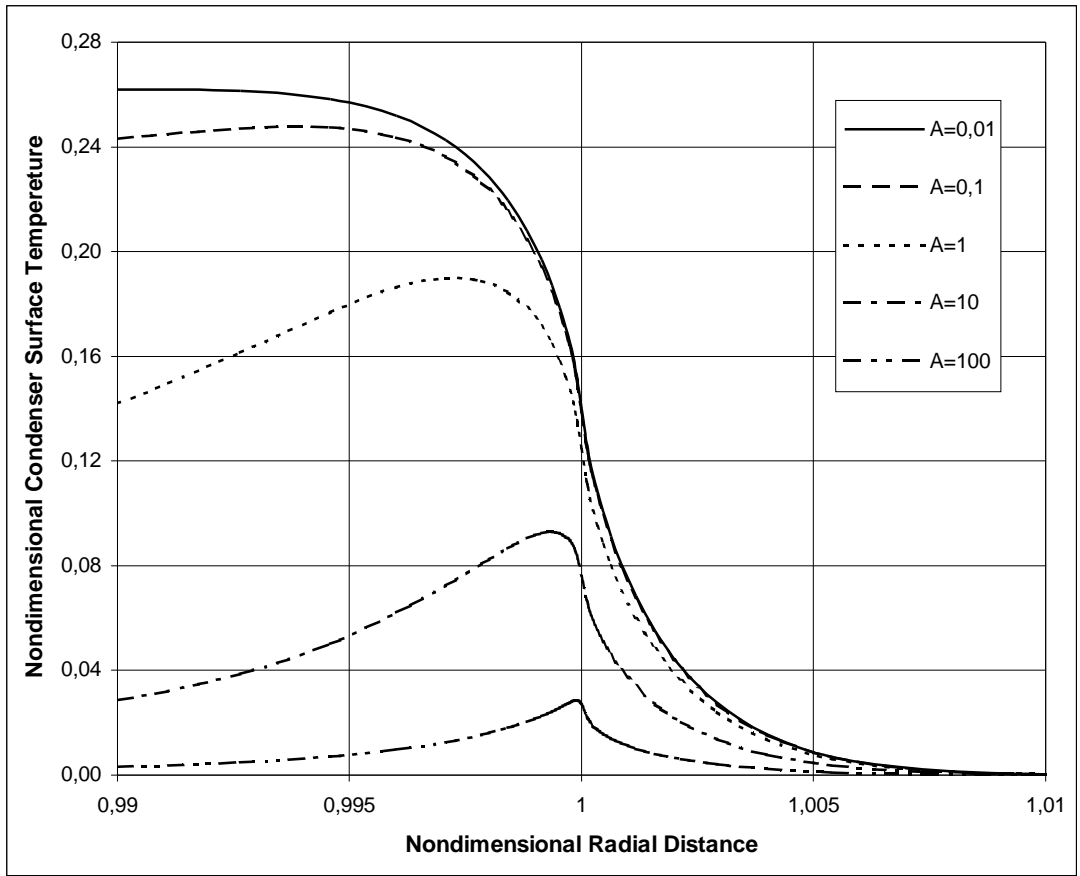


Figure E.2 Variation of nondimensional temperature as a function of nondimensional radial distance at nondimensional axial distance $\tilde{z} = 0$ for $B=0.01$

E.4 Variation of temperature at $\tilde{z} = 0$ for $B=0.1$

The variation of temperature at surface of the substrate for $B=0.1$ is shown in Figure E.3 and Figure E.4.

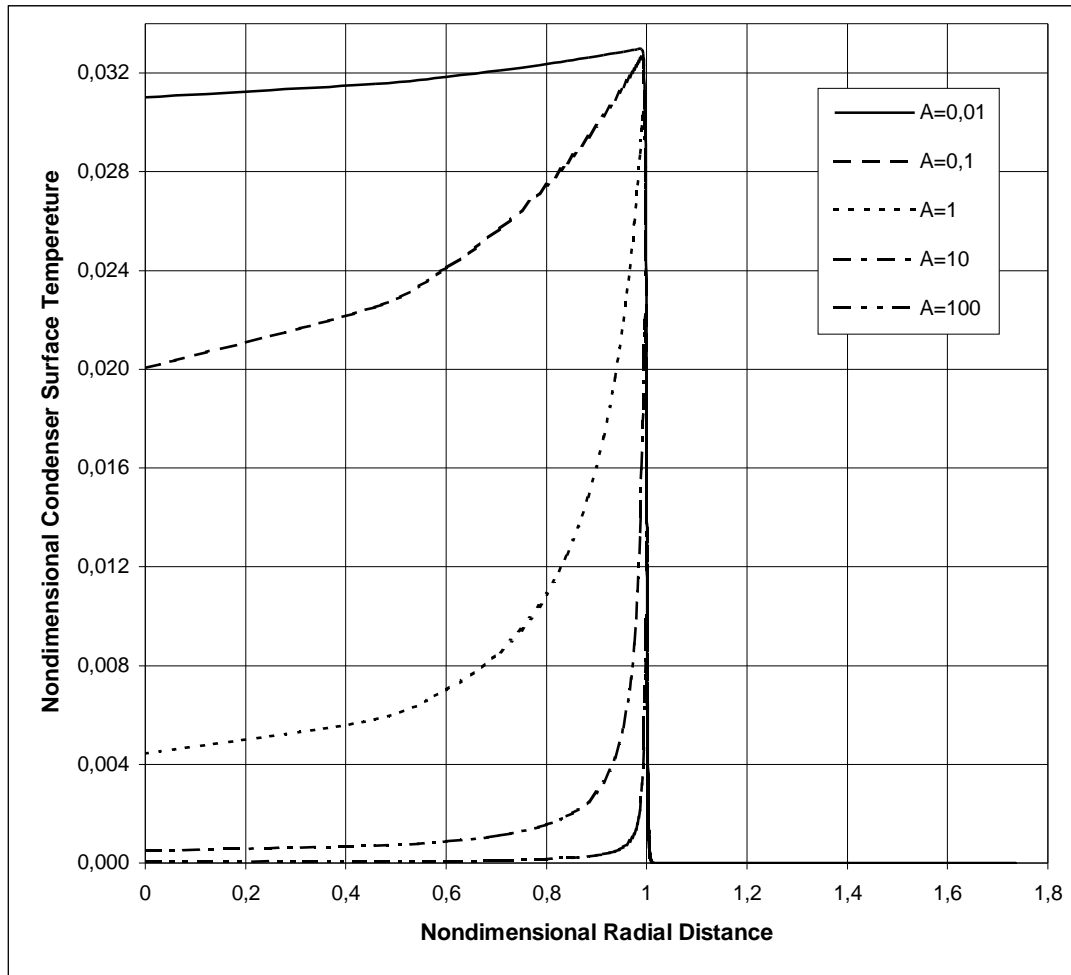


Figure E.3 Variation of nondimensional temperature as a function of nondimensional radial distance at nondimensional axial distance $\tilde{z} = 0$ for $B=0.1$

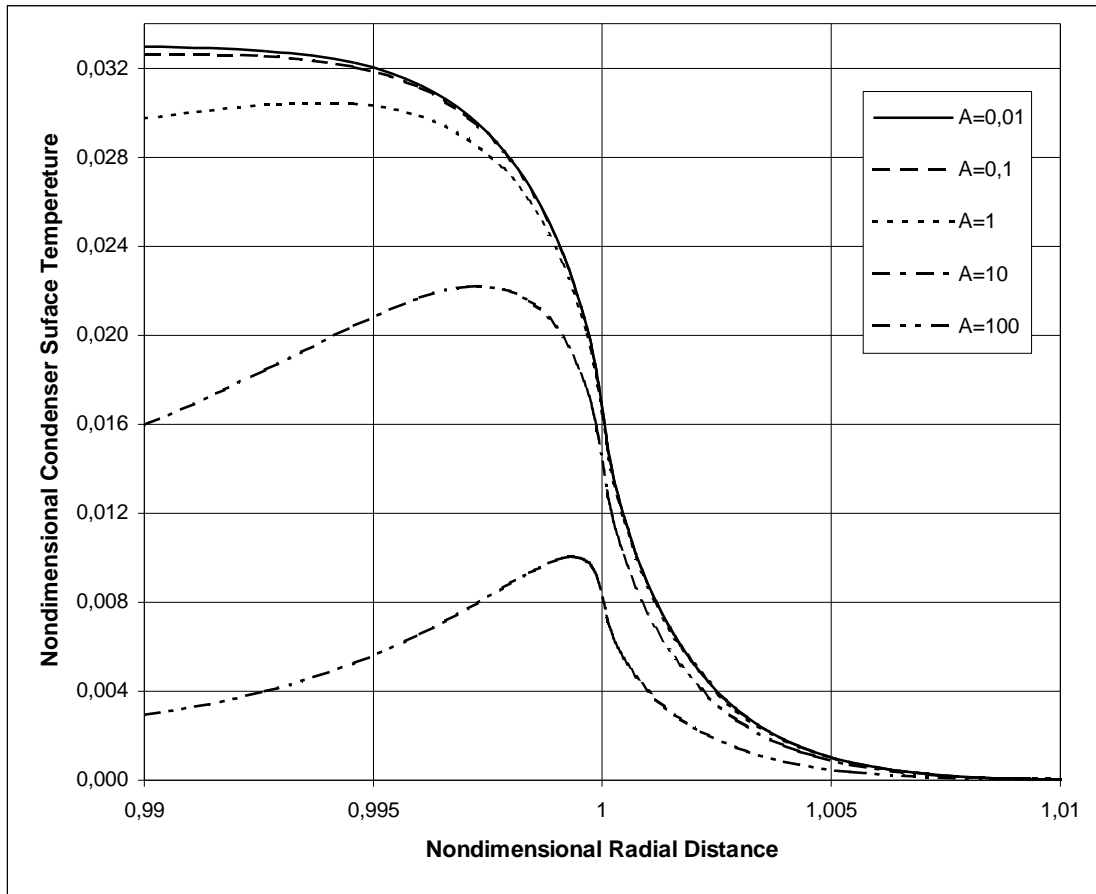


Figure E.4 Variation of nondimensional temperature as a function of nondimensional radial distance at nondimensional axial distance $\tilde{z} = 0$ for $B=0.1$

E.5 Variation of temperature at $\tilde{z} = 0$ for $B=1$

The variation of temperature at surface of the substrate for $B=1$ is shown in Figure E.5 and Figure E.6.

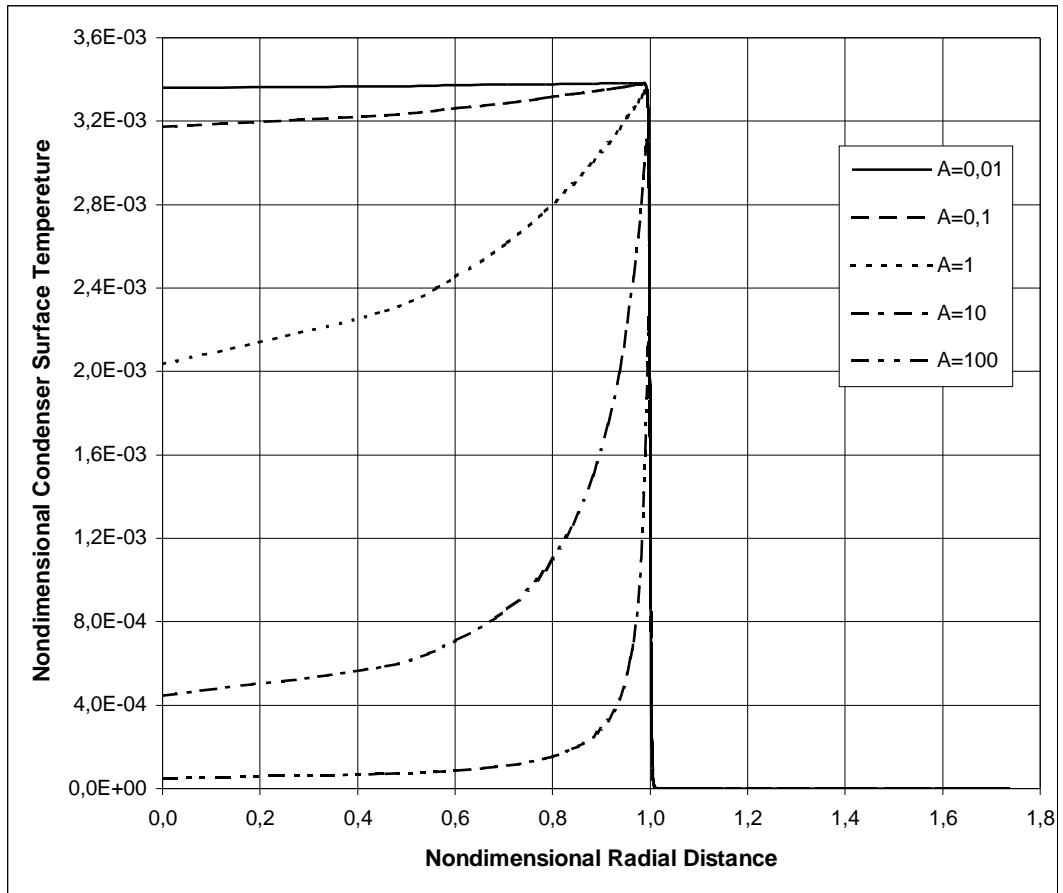


Figure E.5 Variation of nondimensional temperature as a function of nondimensional radial distance at nondimensional axial distance $\tilde{z} = 0$ for $B=1$

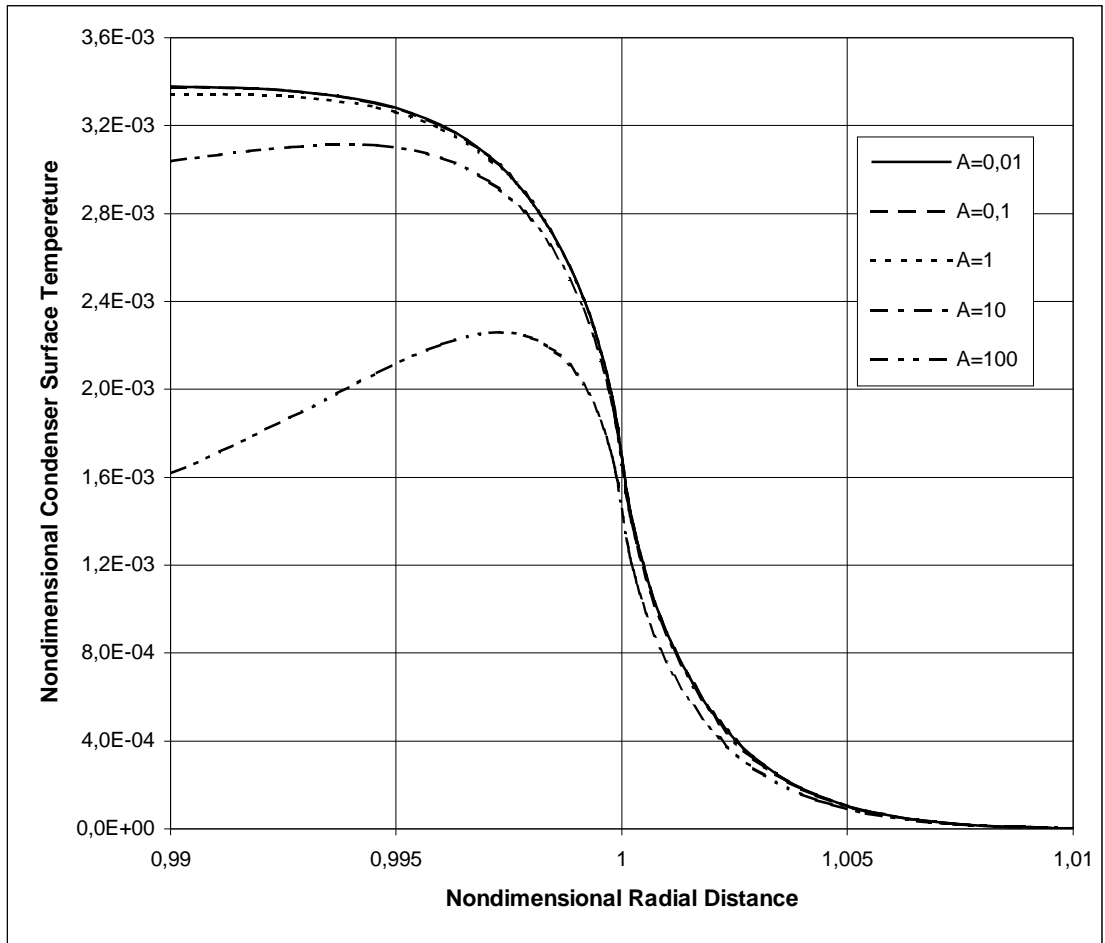


Figure E.6 Variation of nondimensional temperature as a function of nondimensional radial distance at nondimensional axial distance $\tilde{z} = 0$ for B=1

E.6 Variation of temperature at $\tilde{z} = 0$ for $B=10$

The variation of temperature at surface of the substrate for $B=10$ is shown in Figure E.7 and Figure E.8.

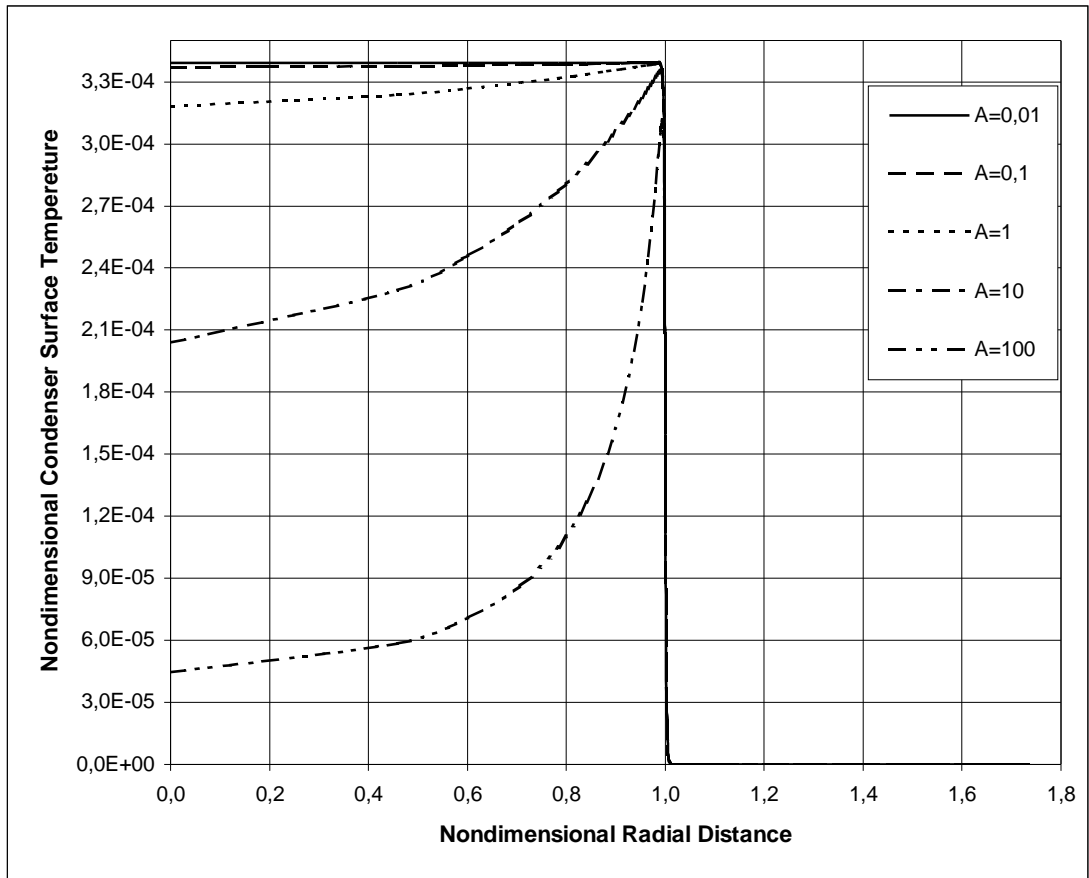


Figure E.7 Variation of nondimensional temperature as a function of nondimensional radial distance at nondimensional axial distance $\tilde{z} = 0$ for $B=10$

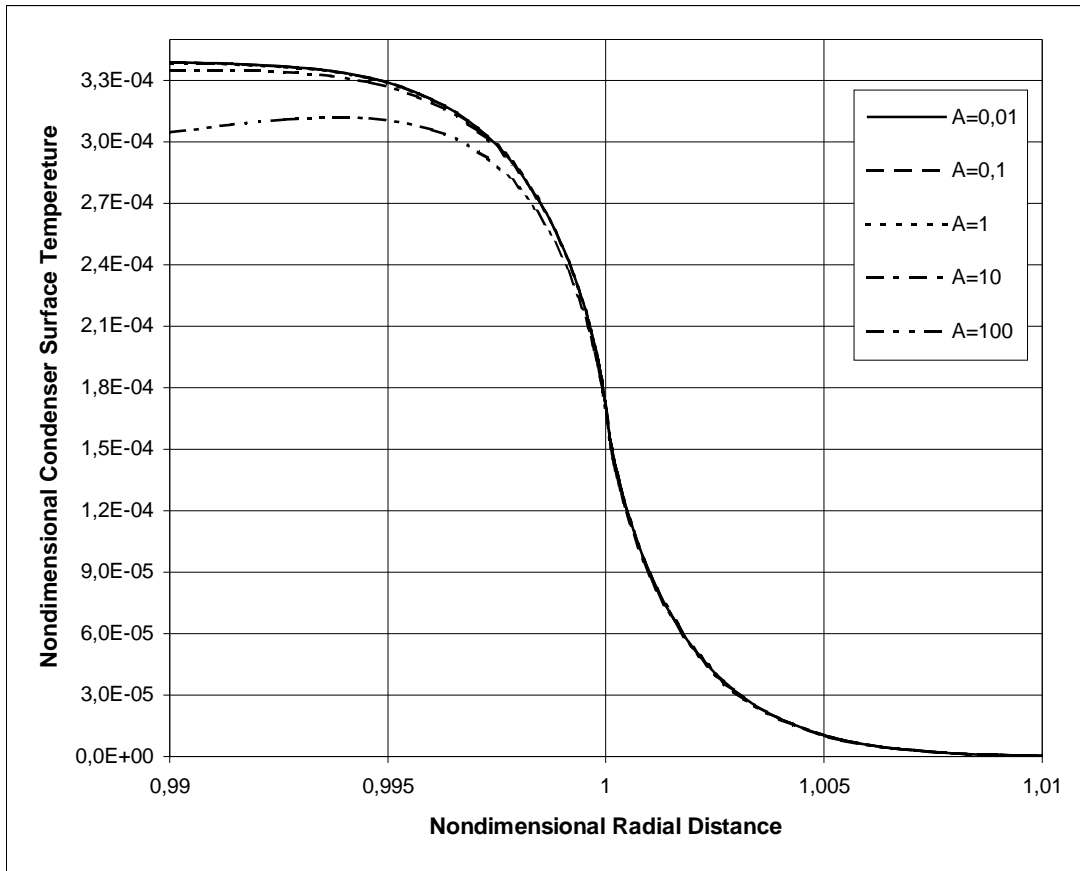


Figure E.8 Variation of nondimensional temperature as a function of nondimensional radial distance at nondimensional axial distance $\tilde{z} = 0$ for $B=10$

E.7 Variation of temperature at $\tilde{z} = 0$ for $B=100$

The variation of temperature at surface of the substrate for $B=100$ is shown in Figure E.9 and Figure E.10.

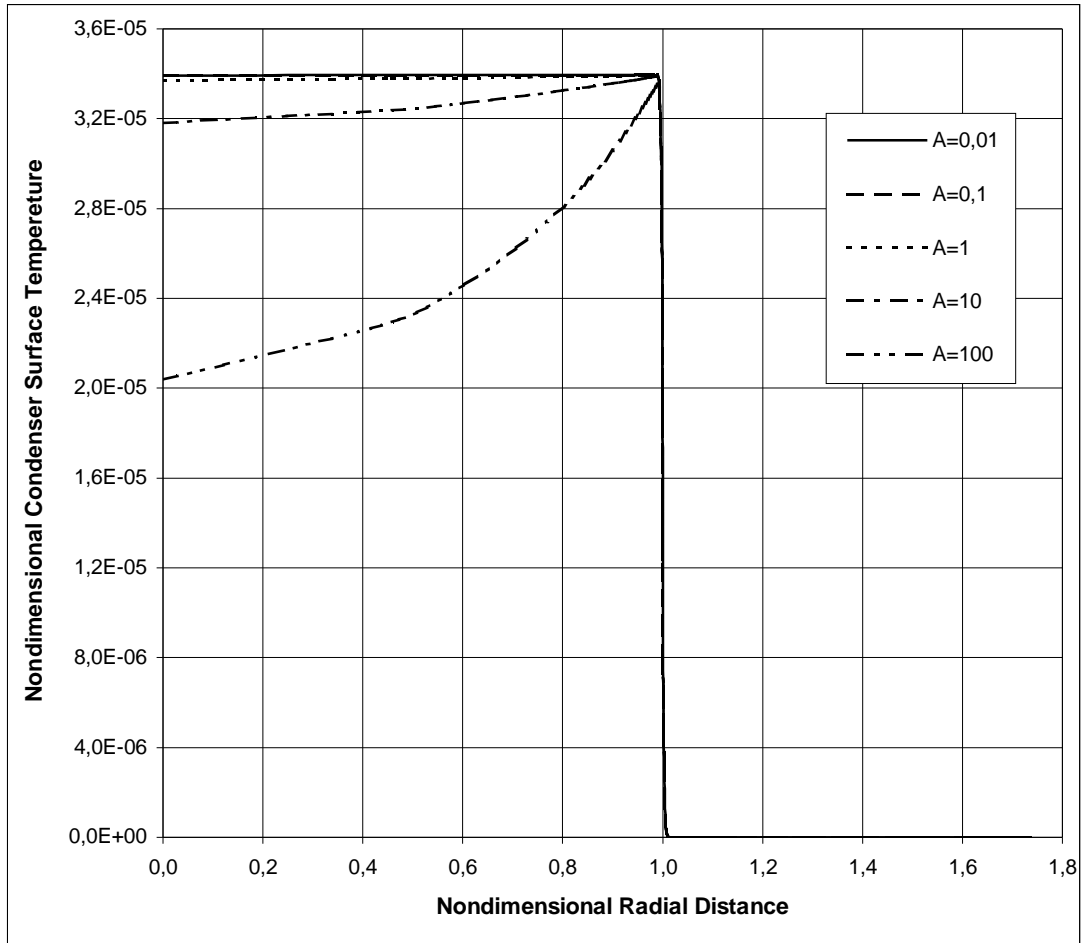


Figure E.9 Variation of nondimensional temperature as a function of nondimensional radial distance at nondimensional axial distance $\tilde{z} = 0$ for $B=100$

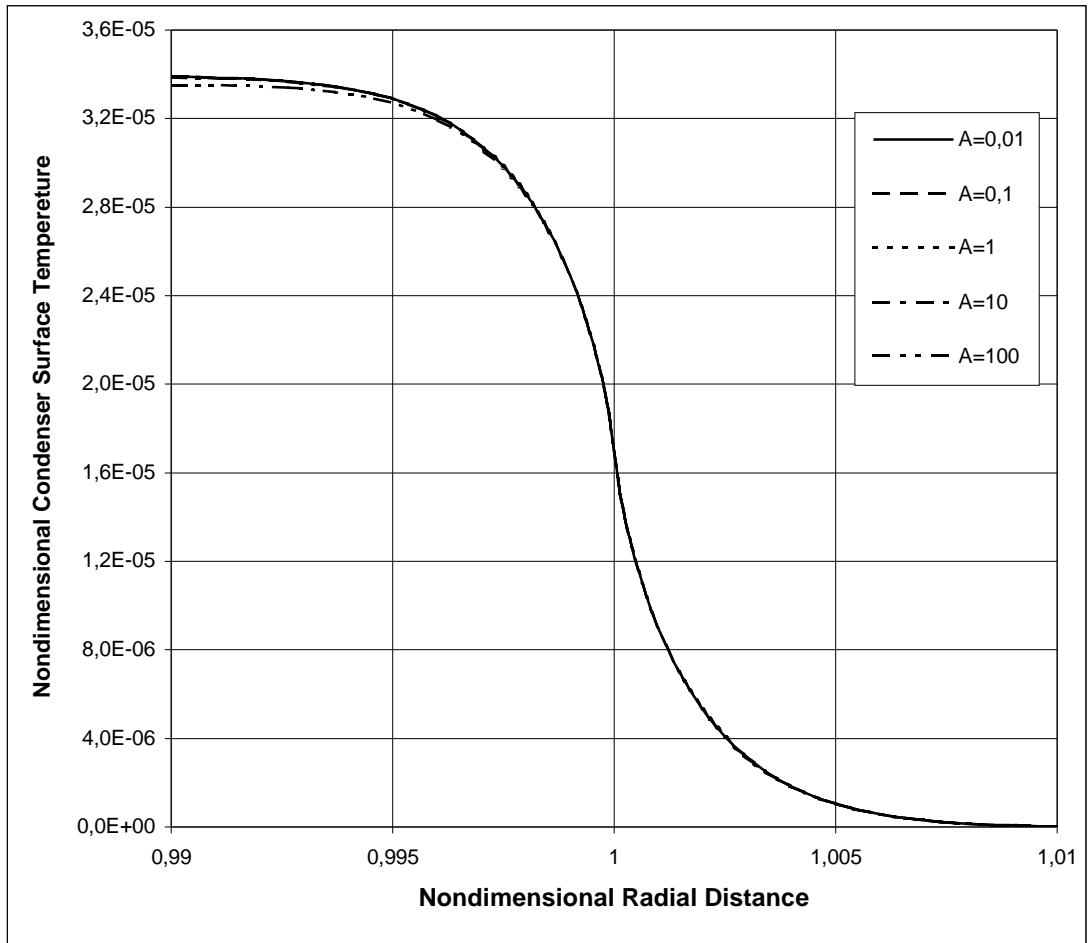


Figure E.10 Variation of nondimensional temperature as a function of nondimensional radial distance at nondimensional axial distance $\tilde{z} = 0$ for B=100

E.8 The data of average temperature

Table E.3 The data of average temperature

B	A	r (mm)	r (m)	\tilde{T}_{av}
0.001	0.01	4.22066E-04	4.22066E-07	5.11304E-01
0.0013	0.01	3.24666E-04	3.24666E-07	4.91463E-01
0.0016	0.01	2.63791E-04	2.63791E-07	4.72242E-01
0.002	0.01	2.11033E-04	2.11033E-07	4.48222E-01
0.004	0.01	1.05517E-04	1.05517E-07	3.55036E-01
0.006	0.01	7.03444E-05	7.03444E-08	2.93293E-01
0.008	0.01	5.27583E-05	5.27583E-08	2.49794E-01
0.01	0.01	4.22066E-05	4.22066E-08	2.17541E-01
0.1	0.01	4.22066E-06	4.22066E-09	3.20628E-02
1	0.01	4.22066E-07	4.22066E-10	3.36844E-03
10	0.01	4.22066E-08	4.22066E-11	3.38566E-04
100	0.01	4.22066E-09	4.22066E-12	3.38742E-05
0.001	0.1	4.22066E-03	4.22066E-06	1.55351E-01
0.0013	0.1	3.24666E-03	3.24666E-06	1.53035E-01
0.0016	0.1	2.63791E-03	2.63791E-06	1.50392E-01
0.002	0.1	2.11033E-03	2.11033E-06	1.46752E-01
0.004	0.1	1.05517E-03	1.05517E-06	1.30368E-01
0.006	0.1	7.03444E-04	7.03444E-07	1.17706E-01
0.008	0.1	5.27583E-04	5.27583E-07	1.07723E-01
0.01	0.1	4.22066E-04	4.22066E-07	9.95985E-02
0.1	0.1	4.22066E-05	4.22066E-08	2.60900E-02
1	0.1	4.22066E-06	4.22066E-09	3.28297E-03
10	0.1	4.22066E-07	4.22066E-10	3.37672E-04
100	0.1	4.22066E-08	4.22066E-11	3.38652E-05
0.001	1	4.22066E-02	4.22066E-05	2.79299E-02
0.0013	1	3.24666E-02	3.24666E-05	2.78007E-02
0.0016	1	2.63791E-02	2.63791E-05	2.75924E-02
0.002	1	2.11033E-02	2.11033E-05	2.72685E-02
0.004	1	1.05517E-02	1.05517E-05	2.56462E-02
0.006	1	7.03444E-03	7.03444E-06	2.43094E-02
0.008	1	5.27583E-03	5.27583E-06	2.32130E-02
0.01	1	4.22066E-03	4.22066E-06	2.22895E-02
0.1	1	4.22066E-04	4.22066E-07	1.10563E-02
1	1	4.22066E-05	4.22066E-08	2.66074E-03
10	1	4.22066E-06	4.22066E-09	3.29083E-04
100	1	4.22066E-07	4.22066E-10	3.37759E-05

Table E.3 Continued

0.001	10	4.22066E-01	4.22066E-04	3.95484E-03
0.0013	10	3.24666E-01	3.24666E-04	3.93876E-03
0.0016	10	2.63791E-01	2.63791E-04	3.91659E-03
0.002	10	2.11033E-01	2.11033E-04	3.88417E-03
0.004	10	1.05517E-01	1.05517E-04	3.73326E-03
0.006	10	7.03444E-02	7.03444E-05	3.61439E-03
0.008	10	5.27583E-02	5.27583E-05	3.51810E-03
0.01	10	4.22066E-02	4.22066E-05	3.43710E-03
0.1	10	4.22066E-03	4.22066E-06	2.35543E-03
1	10	4.22066E-04	4.22066E-07	1.11805E-03
10	10	4.22066E-05	4.22066E-08	2.66603E-04
100	10	4.22066E-06	4.22066E-09	3.29167E-05
0.001	20	8.44132E-01	8.44132E-04	2.15283E-03
0.0013	20	6.49332E-01	6.49332E-04	2.13604E-03
0.0016	20	5.27583E-01	5.27583E-04	2.11995E-03
0.002	20	4.22066E-01	4.22066E-04	2.09997E-03
0.004	20	2.11033E-01	2.11033E-04	2.02053E-03
0.006	20	1.40689E-01	1.40689E-04	1.96244E-03
0.008	20	1.05517E-01	1.05517E-04	1.91635E-03
0.01	20	8.44132E-02	8.44132E-05	1.87795E-03
0.1	20	8.44132E-03	8.44132E-06	1.36623E-03
1	20	8.44132E-04	8.44132E-07	7.39698E-04
10	20	8.44132E-05	8.44132E-08	2.24383E-04
100	20	8.44132E-06	8.44132E-09	3.20279E-05
0.001	50	2.11033E+00	2.11033E-03	9.86604E-04
0.0013	50	1.62333E+00	1.62333E-03	9.64385E-04
0.0016	50	1.31896E+00	1.31896E-03	9.48419E-04
0.002	50	1.05517E+00	1.05517E-03	9.32517E-04
0.004	50	5.27583E-01	5.27583E-04	8.87801E-04
0.006	50	3.51722E-01	3.51722E-04	8.62404E-04
0.008	50	2.63791E-01	2.63791E-04	8.43873E-04
0.01	50	2.11033E-01	2.11033E-04	8.29008E-04
0.1	50	2.11033E-02	2.11033E-05	6.40791E-04
1	50	2.11033E-03	2.11033E-06	3.96817E-04
10	50	2.11033E-04	2.11033E-07	1.58746E-04
100	50	2.11033E-05	2.11033E-08	2.97045E-05

Table E.3 Continued

0.001	70	2.95446E+00	2.95446E-03	7.54305E-04
0.0013	70	2.27266E+00	2.27266E-03	7.30049E-04
0.0016	70	1.84654E+00	1.84654E-03	7.13303E-04
0.002	70	1.47723E+00	1.47723E-03	6.97333E-04
0.004	70	7.38616E-01	7.38616E-04	6.56889E-04
0.006	70	4.92410E-01	4.92410E-04	6.36622E-04
0.008	70	3.69308E-01	3.69308E-04	6.22672E-04
0.01	70	2.95446E-01	2.95446E-04	6.11819E-04
0.1	70	2.95446E-02	2.95446E-05	4.81013E-04
1	70	2.95446E-03	2.95446E-06	3.10225E-04
10	70	2.95446E-04	2.95446E-07	1.35160E-04
100	70	2.95446E-05	2.95446E-08	2.83843E-05
0.001	100	4.22066E+00	4.22066E-03	5.77478E-04
0.0013	100	3.24666E+00	3.24666E-03	5.51346E-04
0.0016	100	2.63791E+00	2.63791E-03	5.33722E-04
0.002	100	2.11033E+00	2.11033E-03	5.17365E-04
0.004	100	1.05517E+00	1.05517E-03	4.79031E-04
0.006	100	7.03444E-01	7.03444E-04	4.62020E-04
0.008	100	5.27583E-01	5.27583E-04	4.51138E-04
0.01	100	4.22066E-01	4.22066E-04	4.43038E-04
0.1	100	4.22066E-02	4.22066E-05	3.53363E-04
1	100	4.22066E-03	4.22066E-06	2.36932E-04
10	100	4.22066E-04	4.22066E-07	1.11931E-04
100	100	4.22066E-05	4.22066E-08	2.66654E-05

E.9 Variation of average temperature for A=1

The variation of average nondimensional condenser surface temperature under the droplet for the substrate A=1 is shown in Figure E.11.

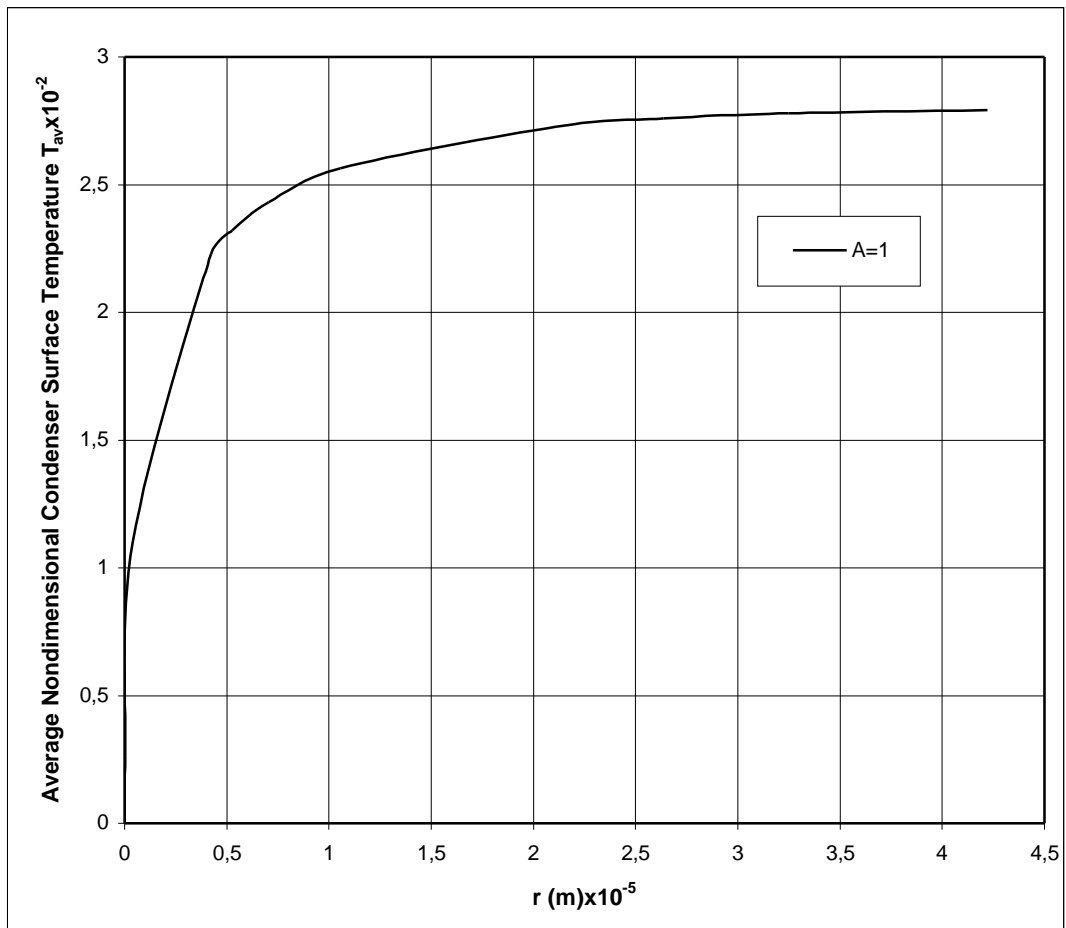


Figure E.11 Variation of average nondimensional condenser surface temperature at the drop base area as a function of drop radius for A=1

E.10 Variation of average temperature for A=0.01

The variation of average nondimensional condenser surface temperature under the droplet for the substrate A=0.01 is shown in Figure E.12.

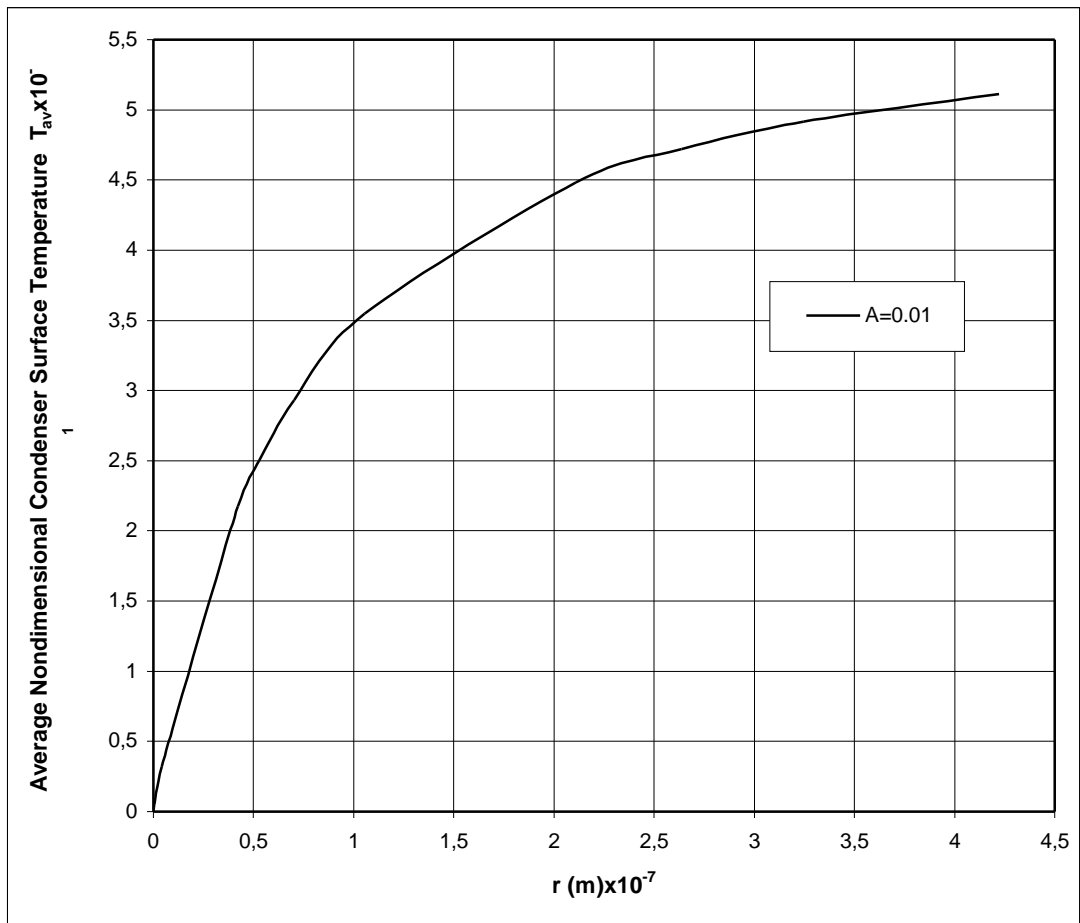


Figure E.12 Variation of average nondimensional condenser surface temperature at the drop base area as a function of drop radius for A=0.01

APPENDIX F

RESULTS FOR HEAT TRANSFER AND HEAT FLUX

F.1 The data and results of heat transfer and heat flux

Table F.1 The data and results of heat transfer and heat flux

B	A	r(m)	Q (W)	Q'' (W/m²)
0.001	0.01	4.22066E-07	1.17029E-04	2.09121E+08
0.0013	0.01	3.24666E-07	8.62193E-05	2.60364E+08
0.0016	0.01	2.63791E-07	6.73424E-05	3.08047E+08
0.002	0.01	2.11033E-07	5.12893E-05	3.66586E+08
0.004	0.01	1.05517E-07	2.07299E-05	5.92661E+08
0.006	0.01	7.03444E-08	1.15878E-05	7.45406E+08
0.008	0.01	5.27583E-08	7.47826E-06	8.55204E+08
0.01	0.01	4.22066E-08	5.24898E-06	9.37916E+08
0.1	0.01	4.22066E-09	8.04513E-08	1.43755E+09
1	0.01	4.22066E-10	8.49955E-10	1.51875E+09
10	0.01	4.22066E-11	8.54789E-12	1.52738E+09
100	0.01	4.22066E-12	8.55275E-14	1.52825E+09
0.001	0.1	4.22066E-06	3.91765E-03	7.00027E+07
0.0013	0.1	3.24666E-06	2.93780E-03	8.87151E+07
0.0016	0.1	2.63791E-06	2.33231E-03	1.06688E+08
0.002	0.1	2.11033E-06	1.81320E-03	1.29597E+08
0.004	0.1	1.05517E-06	8.02713E-04	2.29493E+08
0.006	0.1	7.03444E-07	4.84076E-04	3.11390E+08
0.008	0.1	5.27583E-07	3.32956E-04	3.80764E+08
0.01	0.1	4.22066E-07	2.46716E-04	4.40846E+08
0.1	0.1	4.22066E-08	6.55726E-06	1.17169E+09
1	0.1	4.22066E-09	8.28440E-08	1.48030E+09
10	0.1	4.22066E-10	8.52540E-10	1.52336E+09
100	0.1	4.22066E-11	8.55050E-12	1.52785E+09

Table F.1 Continued

0.001	1	4.22066E-05	7.63545E-02	1.36434E+07
0.0013	1	3.24666E-05	5.75401E-02	1.73759E+07
0.0016	1	2.63791E-05	4.59237E-02	2.10071E+07
0.002	1	2.11033E-05	3.59723E-02	2.57109E+07
0.004	1	1.05517E-05	1.65841E-02	4.74134E+07
0.006	1	7.03444E-06	1.04044E-02	6.69281E+07
0.008	1	5.27583E-06	7.42300E-03	8.48884E+07
0.01	1	4.22066E-06	5.68856E-03	1.01646E+08
0.1	1	4.22066E-07	2.79429E-04	4.99300E+08
1	1	4.22066E-08	6.71788E-06	1.20039E+09
10	1	4.22066E-09	8.30895E-08	1.48469E+09
100	1	4.22066E-10	8.52799E-10	1.52383E+09
0.001	10	4.22066E-04	1.26607	2.26228E+06
0.0013	10	3.24666E-04	9.40480E-01	2.84005E+06
0.0016	10	2.63791E-04	7.44040E-01	3.40350E+06
0.002	10	2.11033E-04	5.78737E-01	4.13647E+06
0.004	10	1.05517E-04	2.65166E-01	7.58101E+06
0.006	10	7.03444E-05	1.67568E-01	1.07791E+07
0.008	10	5.27583E-05	1.20763E-01	1.38103E+07
0.01	10	4.22066E-05	9.35421E-02	1.67146E+07
0.1	10	4.22066E-06	6.05973E-03	1.08279E+08
1	10	4.22066E-07	2.83212E-04	5.06059E+08
10	10	4.22066E-08	6.73430E-06	1.20332E+09
100	10	4.22066E-09	8.31142E-08	1.48513E+09
0.001	20	8.44132E-04	3.00230	1.34117E+06
0.0013	20	6.49332E-04	2.19769	1.65913E+06
0.0016	20	5.27583E-04	1.72241	1.96973E+06
0.002	20	4.22066E-04	1.32894	2.37462E+06
0.004	20	2.11033E-04	6.00005E-01	4.28849E+06
0.006	20	1.40689E-04	3.77956E-01	6.07817E+06
0.008	20	1.05517E-04	2.72249E-01	7.78351E+06
0.01	20	8.44132E-05	2.10980E-01	9.42476E+06
0.1	20	8.44132E-06	1.42272E-02	6.35548E+07
1	20	8.44132E-07	7.51447E-04	3.35682E+08
10	20	8.44132E-08	2.26811E-05	1.01320E+09
100	20	8.44132E-09	3.23497E-07	1.44511E+09

Table F.1 Continued

0.001	50	2.11033E-03	10.19946	7.28998E+05
0.0013	50	1.62333E-03	7.19997	8.69694E+05
0.0016	50	1.31896E-03	5.50426	1.00714E+06
0.002	50	1.05517E-03	4.15095	1.18674E+06
0.004	50	5.27583E-04	1.78767	2.04436E+06
0.006	50	3.51722E-04	1.11016	2.85652E+06
0.008	50	2.63791E-04	7.95035E-01	3.63677E+06
0.01	50	2.11033E-04	6.14513E-01	4.39218E+06
0.1	50	2.11033E-05	4.26789E-02	3.05044E+07
1	50	2.11033E-06	2.53489E-03	1.81179E+08
10	50	2.11033E-07	1.00400E-04	7.17601E+08
100	50	2.11033E-08	1.87547E-06	1.34048E+09
0.001	70	2.95446E-03	16.59215	6.05056E+05
0.0013	70	2.27266E-03	11.50315	7.08919E+05
0.0016	70	1.84654E-03	8.67836	8.10159E+05
0.002	70	1.47723E-03	6.46079	9.42407E+05
0.004	70	7.38616E-04	2.70063	1.57572E+06
0.006	70	4.92410E-04	1.65955	2.17864E+06
0.008	70	3.69308E-04	1.18262	2.76006E+06
0.01	70	2.95446E-04	9.11648E-01	3.32445E+06
0.1	70	2.95446E-05	6.34776E-02	2.31480E+07
1	70	2.95446E-06	3.89724E-03	1.42118E+08
10	70	2.95446E-07	1.67654E-04	6.11374E+08
100	70	2.95446E-08	3.51289E-06	1.28103E+09
0.001	100	4.22066E-03	28.55229	5.10188E+05
0.0013	100	3.24666E-03	19.38997	5.85535E+05
0.0016	100	2.63791E-03	14.39876	6.58649E+05
0.002	100	2.11033E-03	10.54893	7.53976E+05
0.004	100	1.05517E-03	4.23600	1.21106E+06
0.006	100	7.03444E-04	2.56260	1.64844E+06
0.008	100	5.27583E-04	1.81185	2.07201E+06
0.01	100	4.22066E-04	1.390438	2.48451E+06
0.1	100	4.22066E-05	9.64120E-02	1.72274E+07
1	100	4.22066E-06	6.10133E-03	1.09022E+08
10	100	4.22066E-07	2.83596E-04	5.06745E+08
100	100	4.22066E-08	6.73595E-06	1.20362E+09

F.2 Variation of heat transfer and heat flux for A=0.01

The variation of heat transfer and heat flux under the droplet for the substrate A=0.01 is shown in Figure F.1 and Figure F.2, respectively.

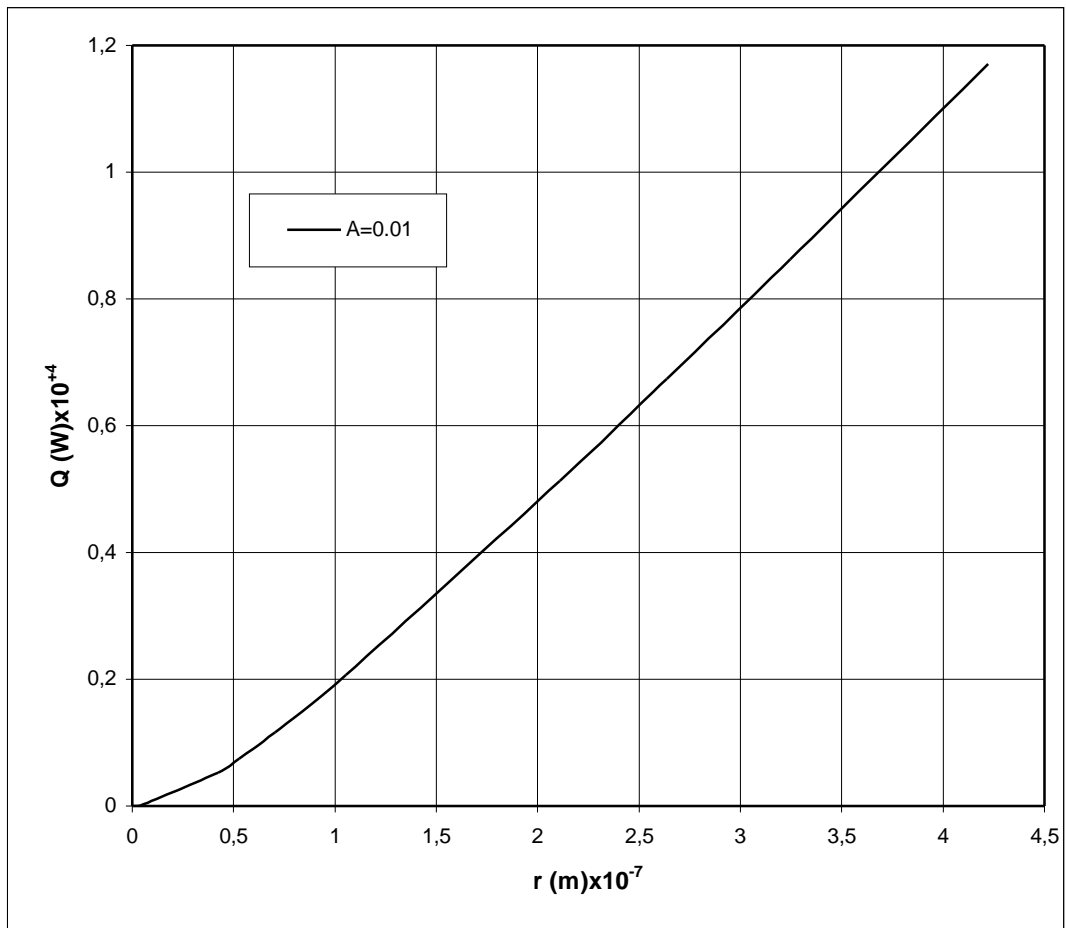


Figure F.1 Variation of heat transfer with drop radius for A=0.01

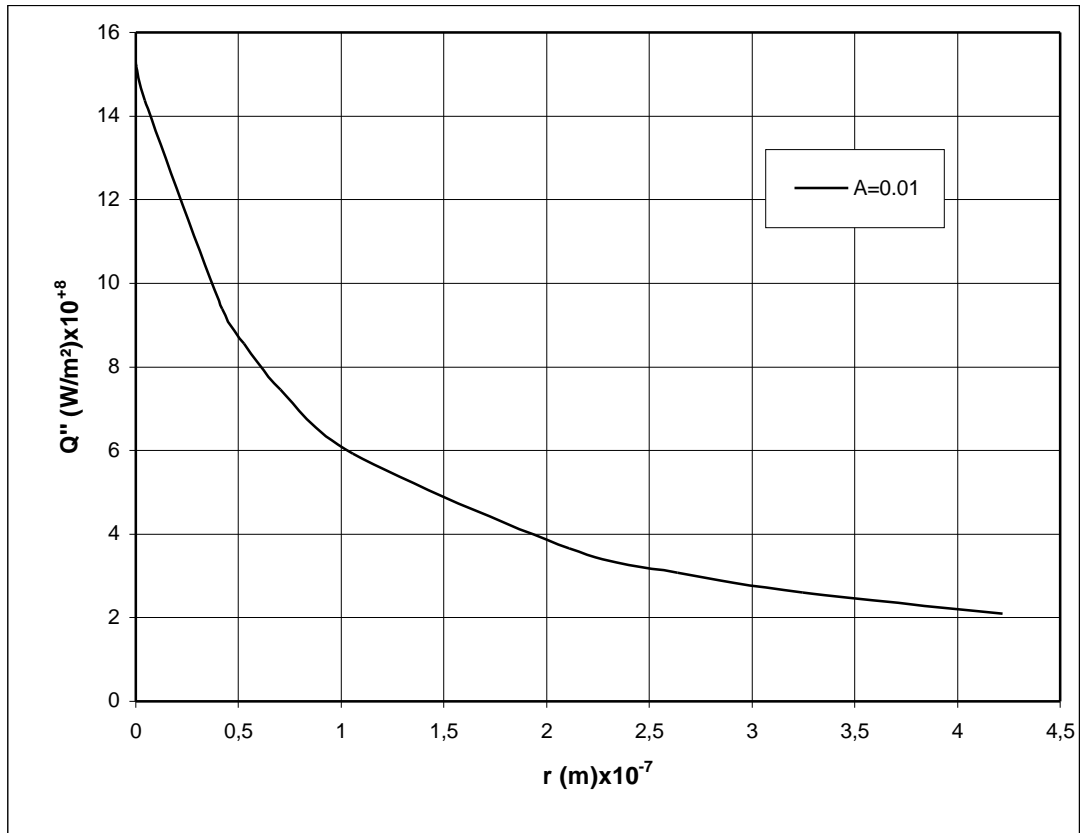


Figure F.2 Variation of heat flux with drop radius for $A=0.01$

F.3 Variation of heat transfer and heat flux for A=100

The variation of heat transfer and heat flux under the droplet for the substrate A=100 is shown in Figure F.3 and Figure F.4, respectively.

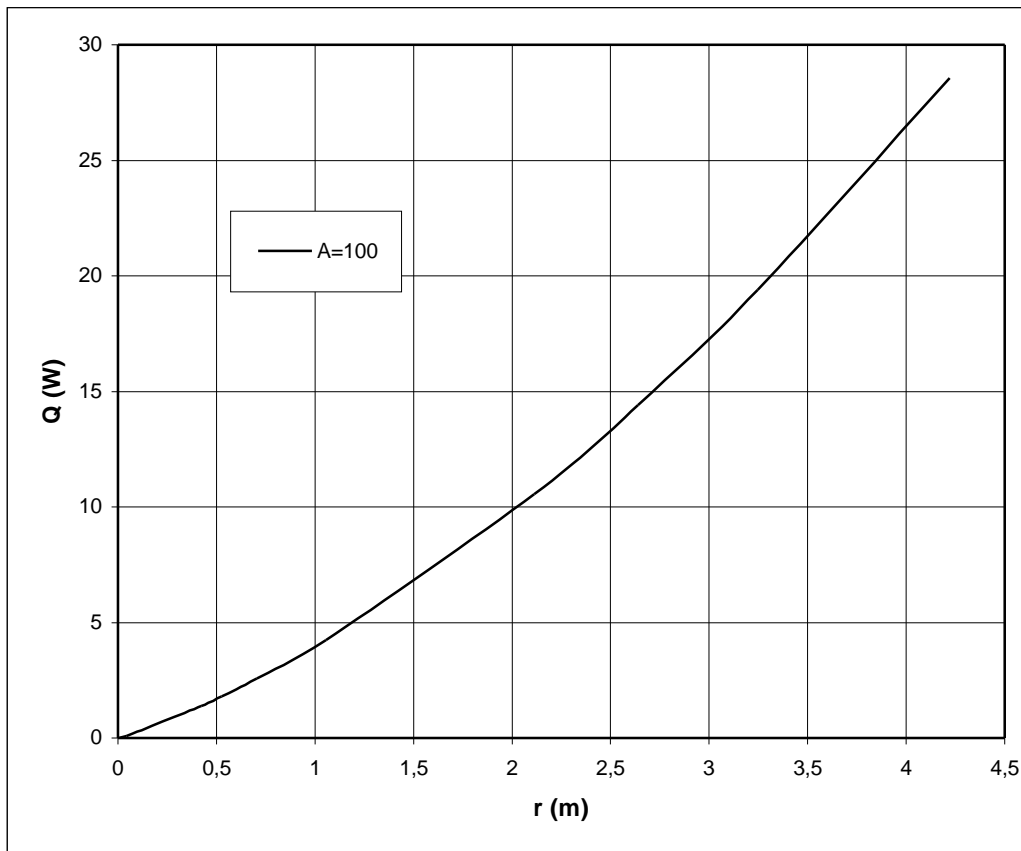


Figure F.3 Variation of heat transfer with drop radius for A=100

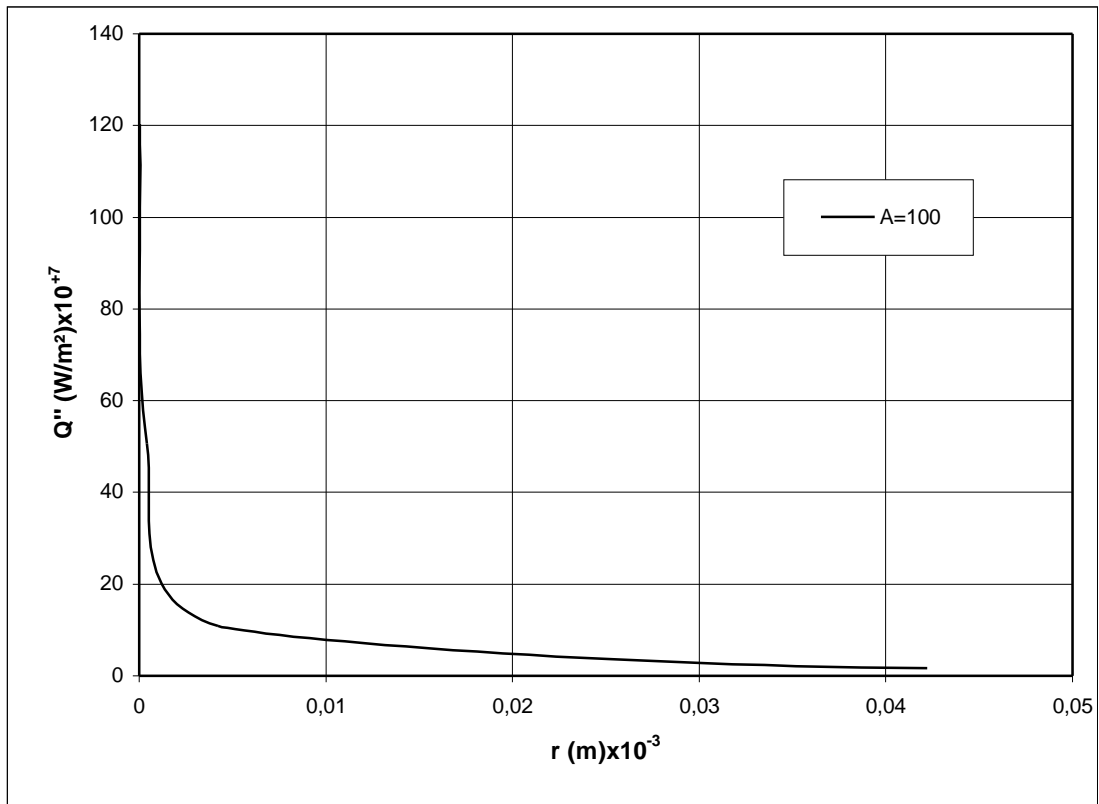


Figure F.4 Variation of heat flux with drop radius for A=100

F.4 The data and results of nondimensional heat transfer (Q_{nd})

Table F.2 The data and results of nondimensional heat transfer (Q_{nd})

B	A	r(mm)	r(m)	Q_{nd}
0.001	0.01	4.22066E-04	4.22066E-07	4.29901
0.001	0.1	4.22066E-03	4.22066E-06	14.39082
0.001	1	4.22066E-02	4.22066E-05	28.04752
0.001	10	4.22066E-01	4.22066E-04	46.50722
0.001	20	8.44132E-01	8.44132E-04	55.14280
0.001	50	2.11033E+00	2.11033E-03	74.93275
0.001	70	2.95446E+00	2.95446E-03	87.07002
0.001	100	4.22066E+00	4.22066E-03	104.88283
0.0013	0.01	3.24666E-04	3.24666E-07	4.11725
0.0013	0.1	3.24666E-03	3.24666E-06	14.02895
0.0013	1	3.24666E-02	3.24666E-05	27.47730
0.0013	10	3.24666E-01	3.24666E-04	44.91099
0.0013	20	6.49332E-01	6.49332E-04	52.47334
0.0013	50	1.62333E+00	1.62333E-03	68.76438
0.0013	70	2.27266E+00	2.27266E-03	78.47326
0.0013	100	3.24666E+00	3.24666E-03	92.59346
0.0016	0.01	2.63791E-04	2.63791E-07	3.95793
0.0016	0.1	2.63791E-03	2.63791E-06	13.70773
0.0016	1	2.63791E-02	2.63791E-05	26.99088
0.0016	10	2.63791E-01	2.63791E-04	43.72964
0.0016	20	5.27583E-01	5.27583E-04	50.61589
0.0016	50	1.31896E+00	1.31896E-03	64.70069
0.0016	70	1.84654E+00	1.84654E-03	72.86503
0.0016	100	2.63791E+00	2.63791E-03	84.62621
0.002	0.01	2.11033E-04	2.11033E-07	3.76805
0.002	0.1	2.11033E-03	2.11033E-06	13.32094
0.002	1	2.11033E-02	2.11033E-05	26.42762
0.002	10	2.11033E-01	2.11033E-04	42.51785
0.002	20	4.22066E-01	4.22066E-04	48.81623
0.002	50	1.05517E+00	1.05517E-03	60.99117
0.002	70	1.47723E+00	1.47723E-03	67.80746
0.002	100	2.11033E+00	2.11033E-03	77.49935

Table F.2 Continued

0.004	0.01	1.05517E-04	1.05517E-07	3.04591
0.004	0.1	1.05517E-03	1.05517E-06	11.79452
0.004	1	1.05517E-02	1.05517E-05	24.36751
0.004	10	1.05517E-01	1.05517E-04	38.96170
0.004	20	2.11033E-01	2.11033E-04	44.08032
0.004	50	5.27583E-01	5.27583E-04	52.53357
0.004	70	7.38616E-01	7.38616E-04	56.68751
0.004	100	1.05517E+00	1.05517E-03	62.24092
0.006	0.01	7.03444E-05	7.03444E-08	2.55394
0.006	0.1	7.03444E-04	7.03444E-07	10.66903
0.006	1	7.03444E-03	7.03444E-06	22.93132
0.006	10	7.03444E-02	7.03444E-05	36.93197
0.006	20	1.40689E-01	1.40689E-04	41.65068
0.006	50	3.51722E-01	3.51722E-04	48.93589
0.006	70	4.92410E-01	4.92410E-04	52.25211
0.006	100	7.03444E-01	7.03444E-04	56.47965
0.008	0.01	5.27583E-05	5.27583E-08	2.19761
0.008	0.1	5.27583E-04	5.27583E-07	9.78445
0.008	1	5.27583E-03	5.27583E-06	21.81368
0.008	10	5.27583E-02	5.27583E-05	35.48820
0.008	20	1.05517E-01	1.05517E-04	40.00239
0.008	50	2.63791E-01	2.63791E-04	46.72682
0.008	70	3.69308E-01	3.69308E-04	49.64724
0.008	100	5.27583E-01	5.27583E-04	53.24417
0.01	0.01	4.22066E-05	4.22066E-08	1.92812
0.01	0.1	4.22066E-04	4.22066E-07	9.06269
0.01	1	4.22066E-03	4.22066E-06	20.89593
0.01	10	4.22066E-02	4.22066E-05	34.36111
0.01	20	8.44132E-02	8.44132E-05	38.74996
0.01	50	2.11033E-01	2.11033E-04	45.14638
0.01	70	2.95446E-01	2.95446E-04	47.84006
0.01	100	4.22066E-01	4.22066E-04	51.07577

Table F.2 Continued

0.1	0.01	4.22066E-06	4.22066E-09	0.29552
0.1	0.1	4.22066E-05	4.22066E-08	2.40870
0.1	1	4.22066E-04	4.22066E-07	10.26436
0.1	10	4.22066E-03	4.22066E-06	22.25938
0.1	20	8.44132E-03	8.44132E-06	26.13053
0.1	50	2.11033E-02	2.11033E-05	31.35470
0.1	70	2.95446E-02	2.95446E-05	33.31060
0.1	100	4.22066E-02	4.22066E-05	35.41532
1	0.01	4.22066E-07	4.22066E-10	0.03122
1	0.1	4.22066E-06	4.22066E-09	0.30431
1	1	4.22066E-05	4.22066E-08	2.46770
1	10	4.22066E-04	4.22066E-07	10.40331
1	20	8.44132E-04	8.44132E-07	13.80156
1	50	2.11033E-03	2.11033E-06	18.62299
1	70	2.95446E-03	2.95446E-06	20.45123
1	100	4.22066E-03	4.22066E-06	22.41218
10	0.01	4.22066E-08	4.22066E-11	0.00314
10	0.1	4.22066E-07	4.22066E-10	0.03132
10	1	4.22066E-06	4.22066E-09	0.30522
10	10	4.22066E-05	4.22066E-08	2.47373
10	20	8.44132E-05	8.44132E-08	4.16576
10	50	2.11033E-04	2.11033E-07	7.37601
10	70	2.95446E-04	2.95446E-07	8.79783
10	100	4.22066E-04	4.22066E-07	10.41742
100	0.01	4.22066E-09	4.22066E-12	0.00031
100	0.1	4.22066E-08	4.22066E-11	0.00314
100	1	4.22066E-07	4.22066E-10	0.03133
100	10	4.22066E-06	4.22066E-09	0.30531
100	20	8.44132E-06	8.44132E-09	0.59416
100	50	2.11033E-05	2.11033E-08	1.37785
100	70	2.95446E-05	2.95446E-08	1.84343
100	100	4.22066E-05	4.22066E-08	2.47434

F.5 Variation of nondimensional heat transfer (Q_{nd}) and dimensional heat transfer (Q) for $B=0.01, 0.1, 1, 10, 100$

Variation of nondimensional heat transfer (Q_{nd}) and dimensional heat transfer (Q) for $B=0.01$ is shown in Figure F.5 and Figure F.6, respectively.

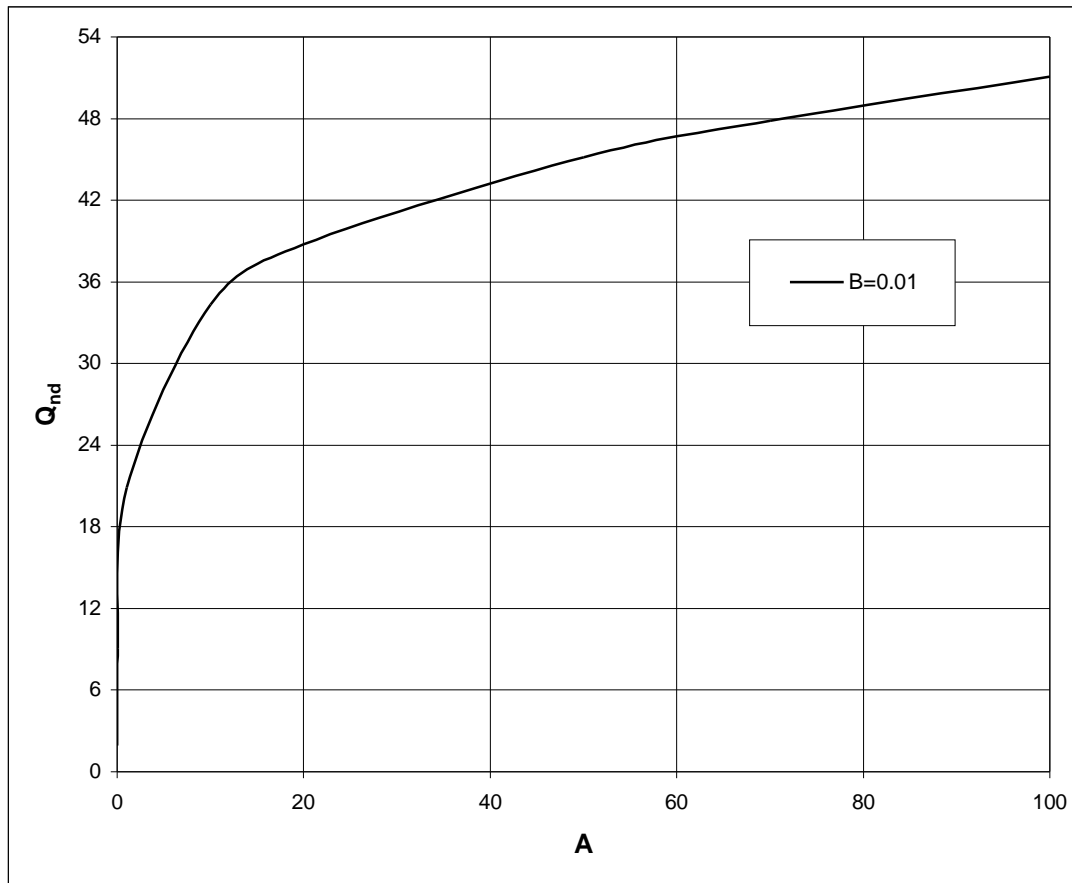


Figure F.5 Variation of Q_{nd} with A for $B=0.01$

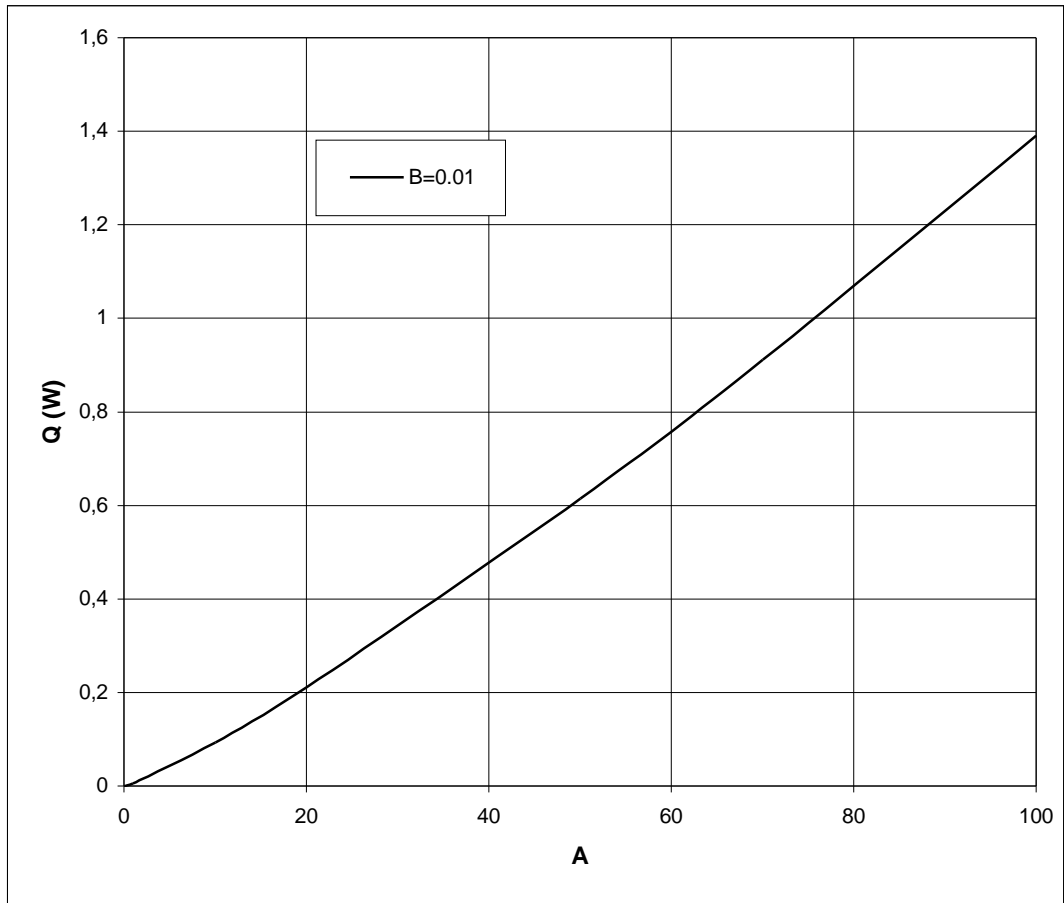


Figure F.6 Variation of Q with A for B=0.01

Variation of nondimensional heat transfer (Q_{nd}) and dimensional heat transfer (Q) for $B=0.1$ is shown in Figure F.7 and Figure F.8, respectively.

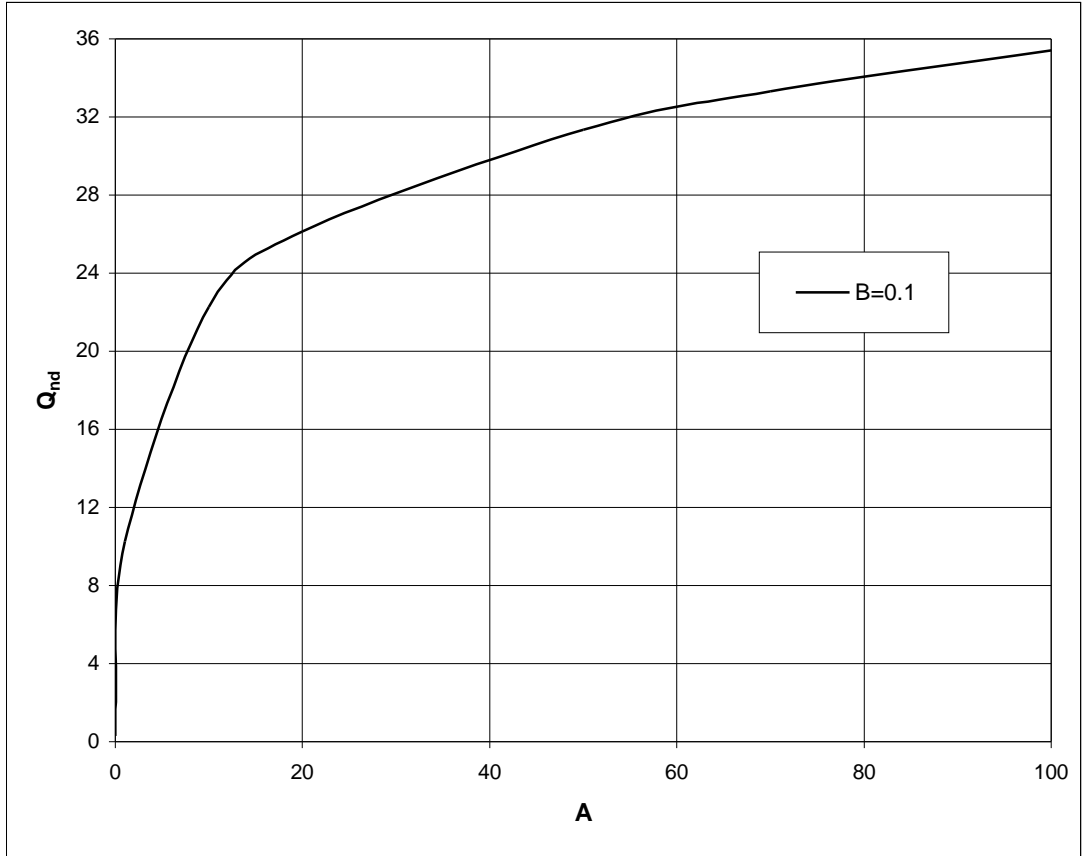


Figure F.7 Variation of Q_{nd} with A for $B=0.1$

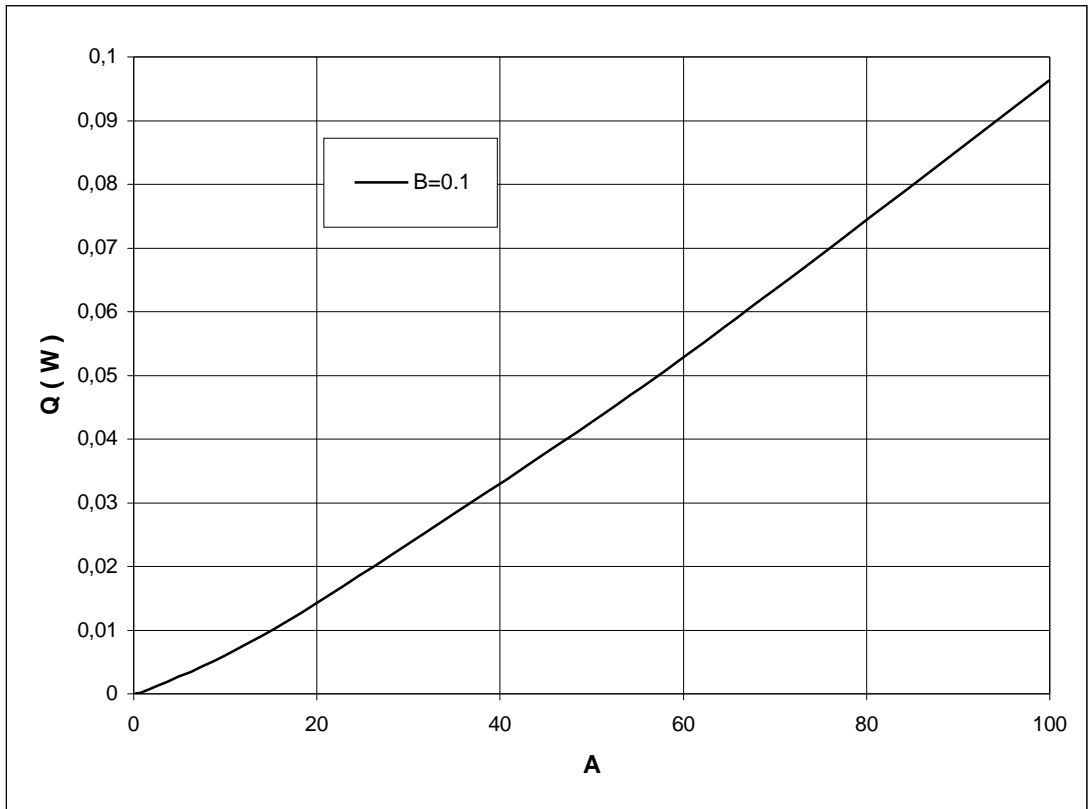


Figure F.8 Variation of Q with A for B=0.1

Variation of nondimensional heat transfer (Q_{nd}) and dimensional heat transfer (Q) for $B=1$ is shown in Figure F.9 and Figure F.10, respectively.

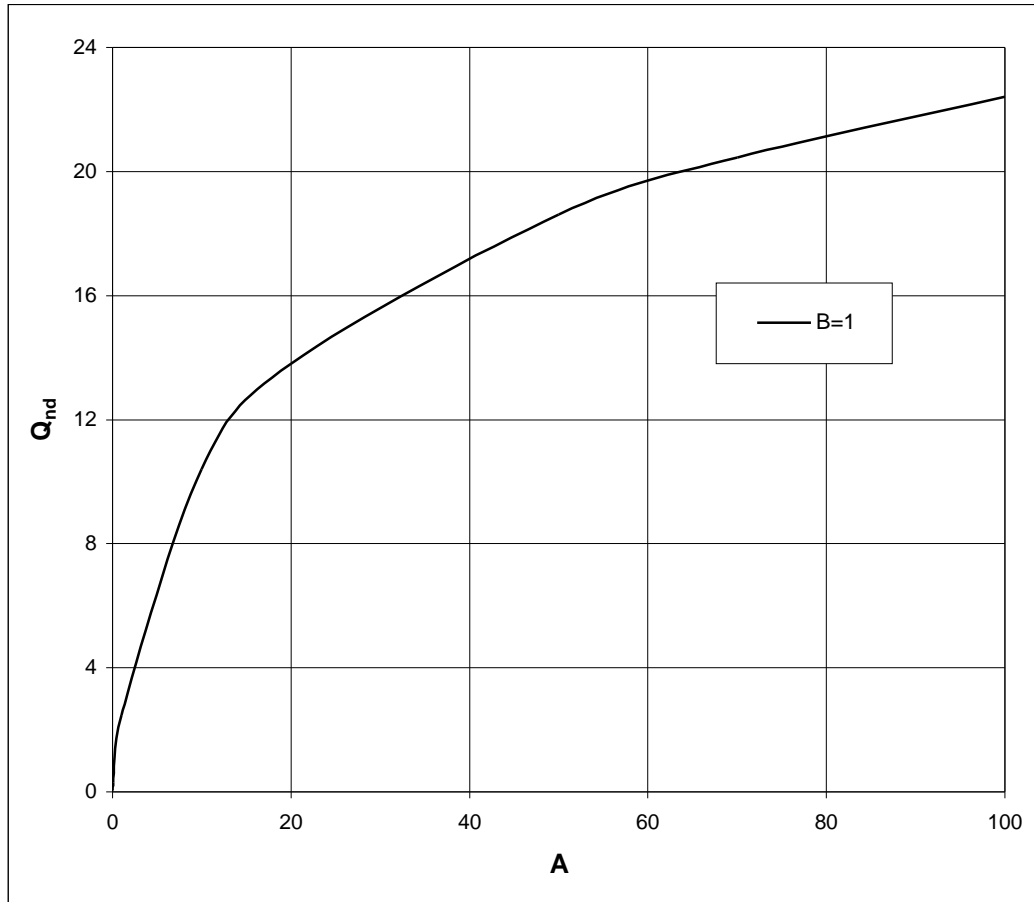


Figure F.9 Variation of Q_{nd} with A for $B=1$

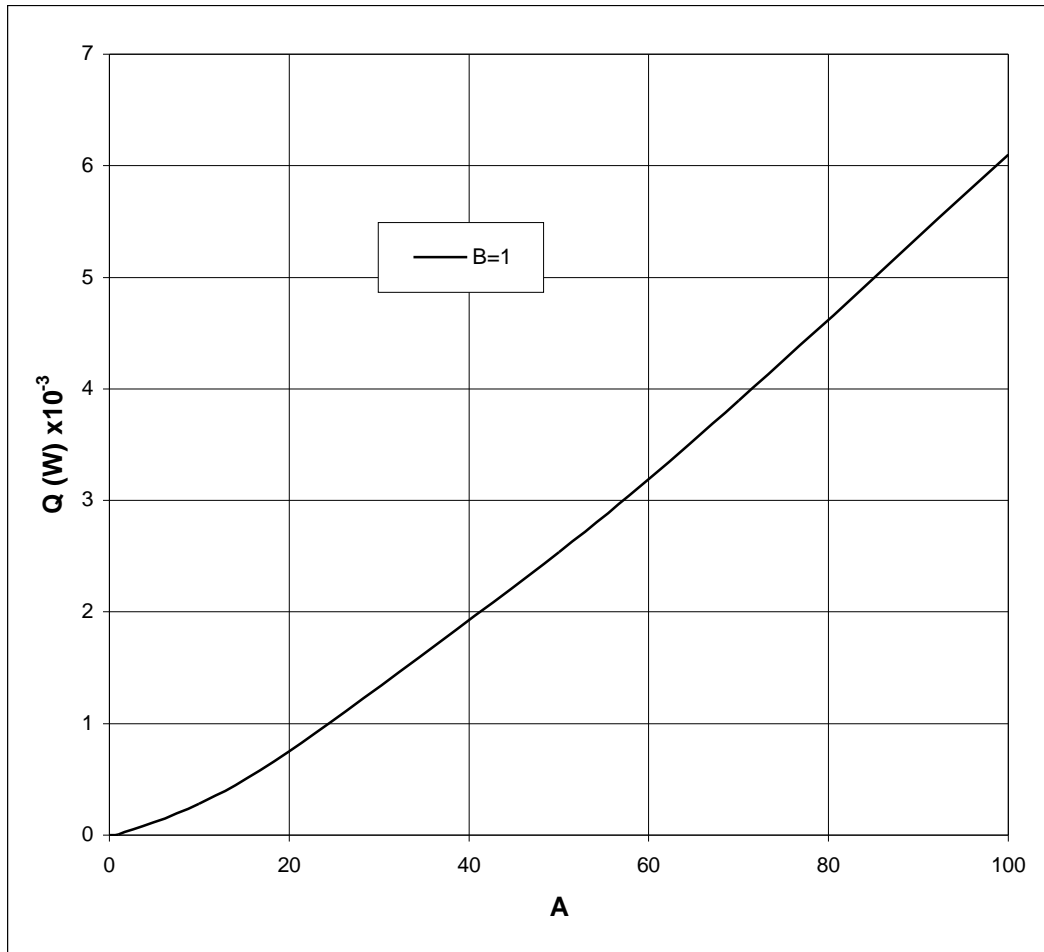


Figure F.10 Variation of Q with A for B=1

Variation of nondimensional heat transfer (Q_{nd}) and dimensional heat transfer (Q) for $B=10$ is shown in Figure F.11 and Figure F.12, respectively.

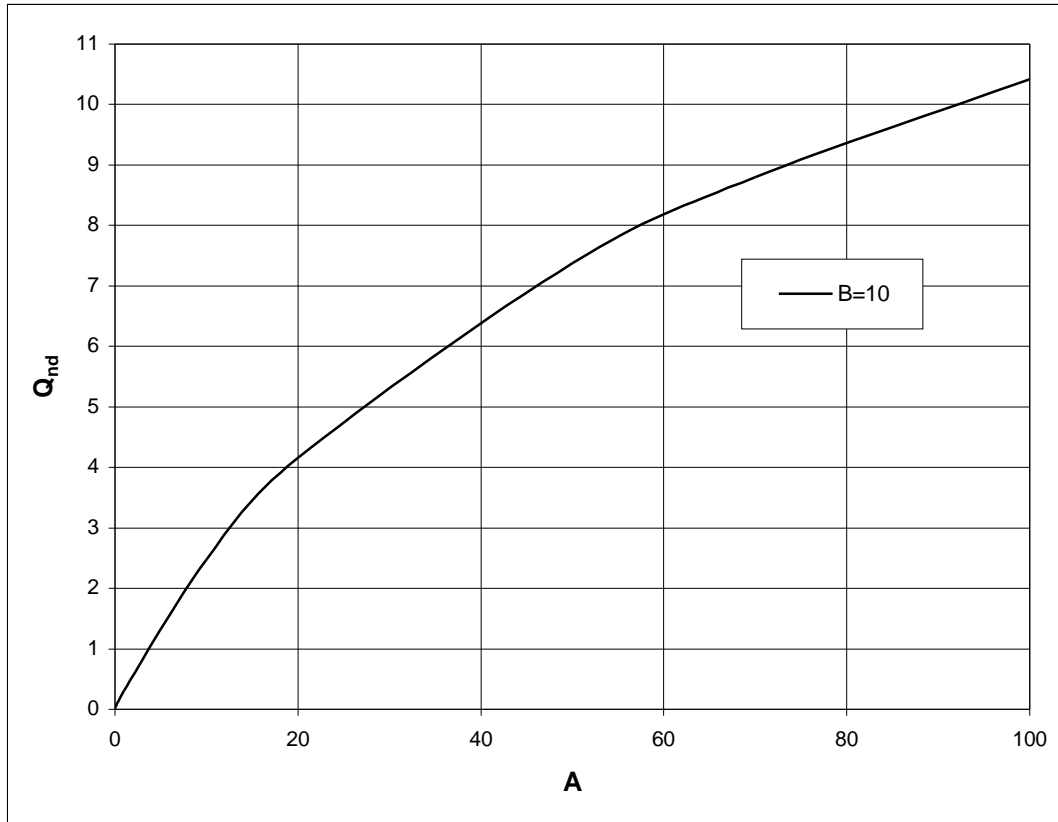


Figure F.11 Variation of Q_{nd} with A for $B=10$

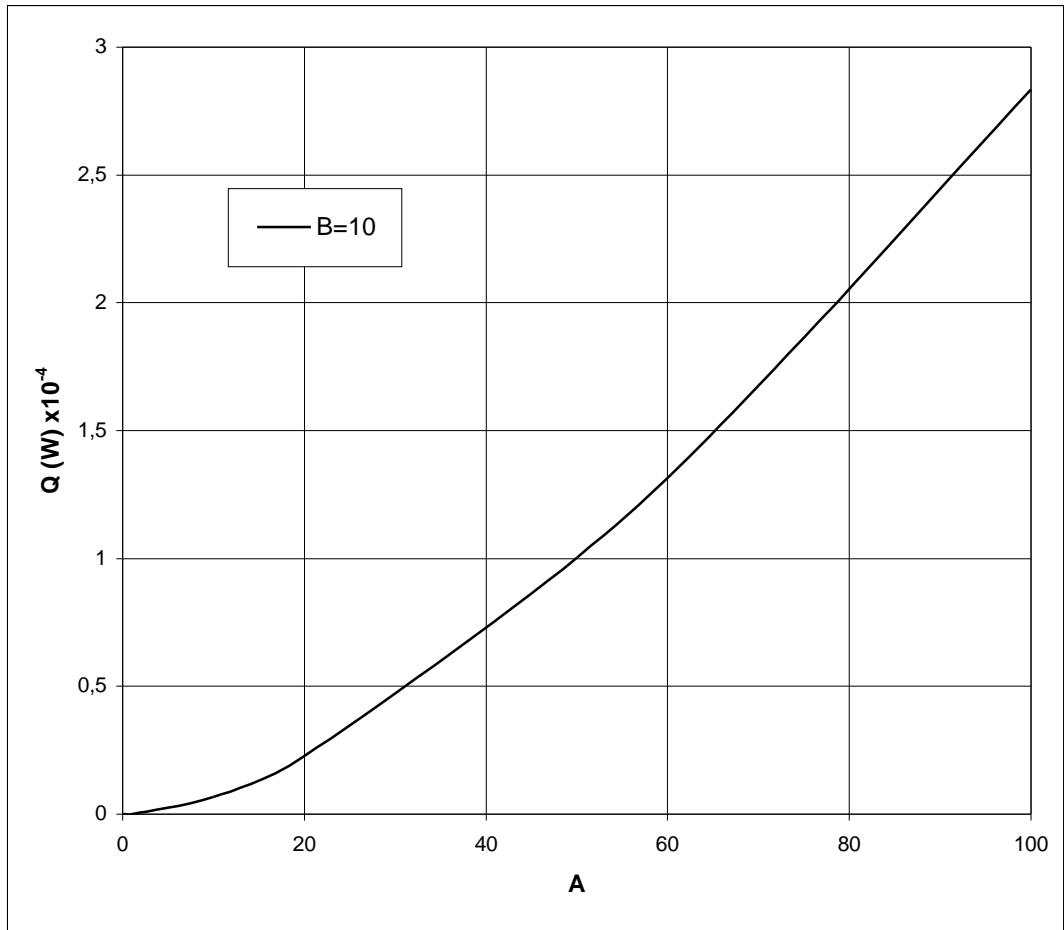


Figure F.12 Variation of Q with A for B=10

Variation of nondimensional heat transfer (Q_{nd}) and dimensional heat transfer (Q) for $B=100$ is shown in Figure F.13 and Figure F.14, respectively.

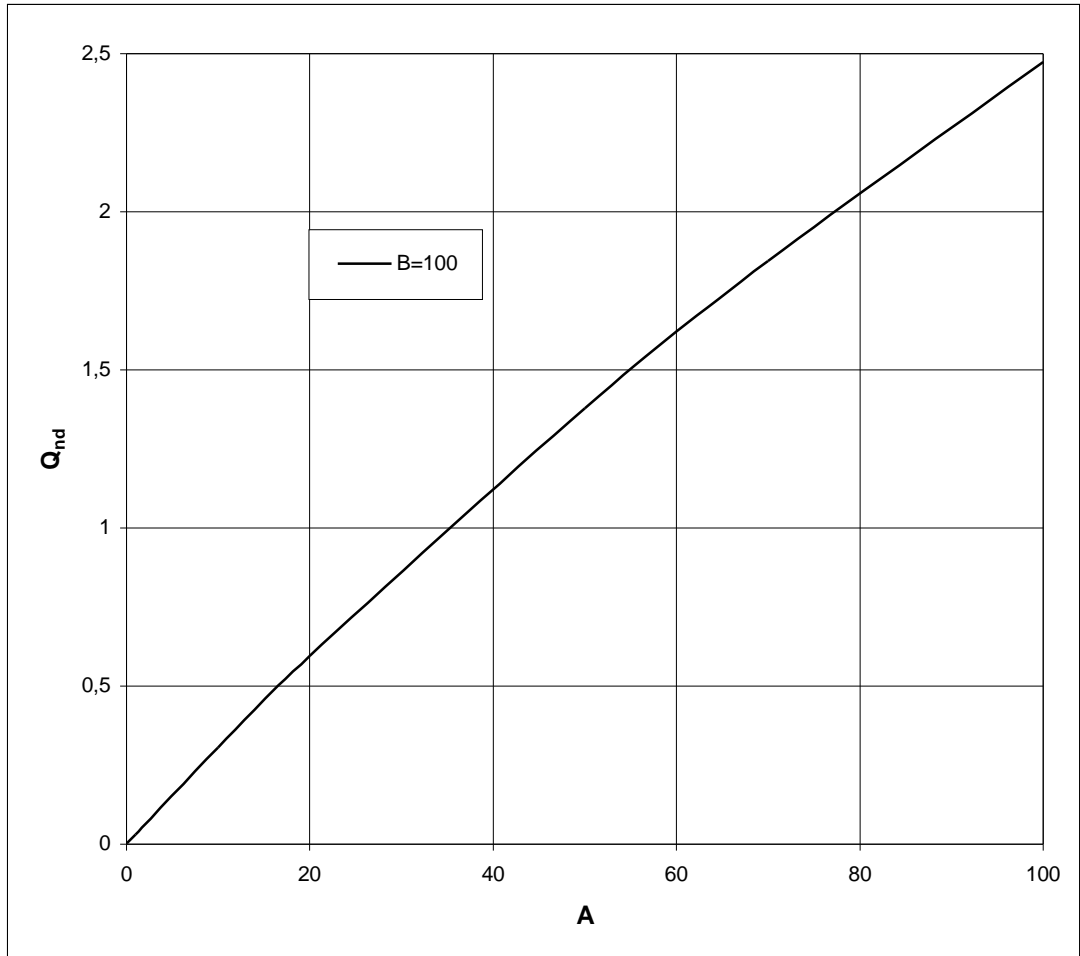


Figure F.13 Variation of Q_{nd} with A for $B=100$

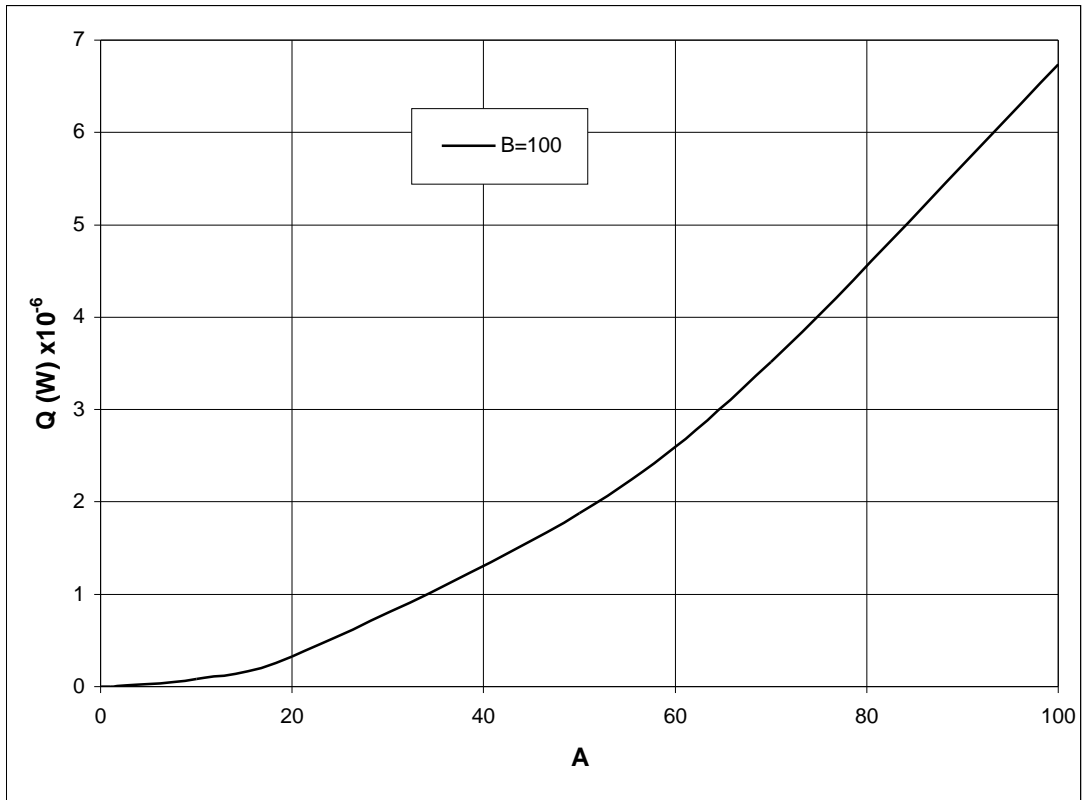


Figure F.14 Variation of Q with A for B=100

F.6 Variation of nondimensional drop resistance for B=0.001 and A=1

The variation of nondimensional drop resistance for B=0.001 and A=1 is given in Table F.3.

Table F.3 Variation of nondimensional drop resistance for B=0.001 and A=1

i	F_r
1	1.503384
2	2.079615
3	2.628648
4	3.39832
5	4.457397
6	5.902899
7	7.867437
8	10.52983
9	14.12915
10	18.98219
11	25.50465
12	34.23413
13	45.85363
14	61.20789
15	81.30518
16	107.2838
17	140.3291
18	181.5126
19	231.5603
20	290.5285
21	357.5433
22	430.6468
23	506.9167
24	582.8731
25	655.1416
26	720.8043
27	778.2587
28	826.7162
29	866.3265
30	898.1007
31	1000

F.7 Variation of heat transfer and heat flux with A for $r=4.22 \times 10^{-6}$ m

Variation of heat transfer and heat flux with A for $r=4.22 \times 10^{-6}$ m is shown in Figure F.15 and Figure F.16, respectively.

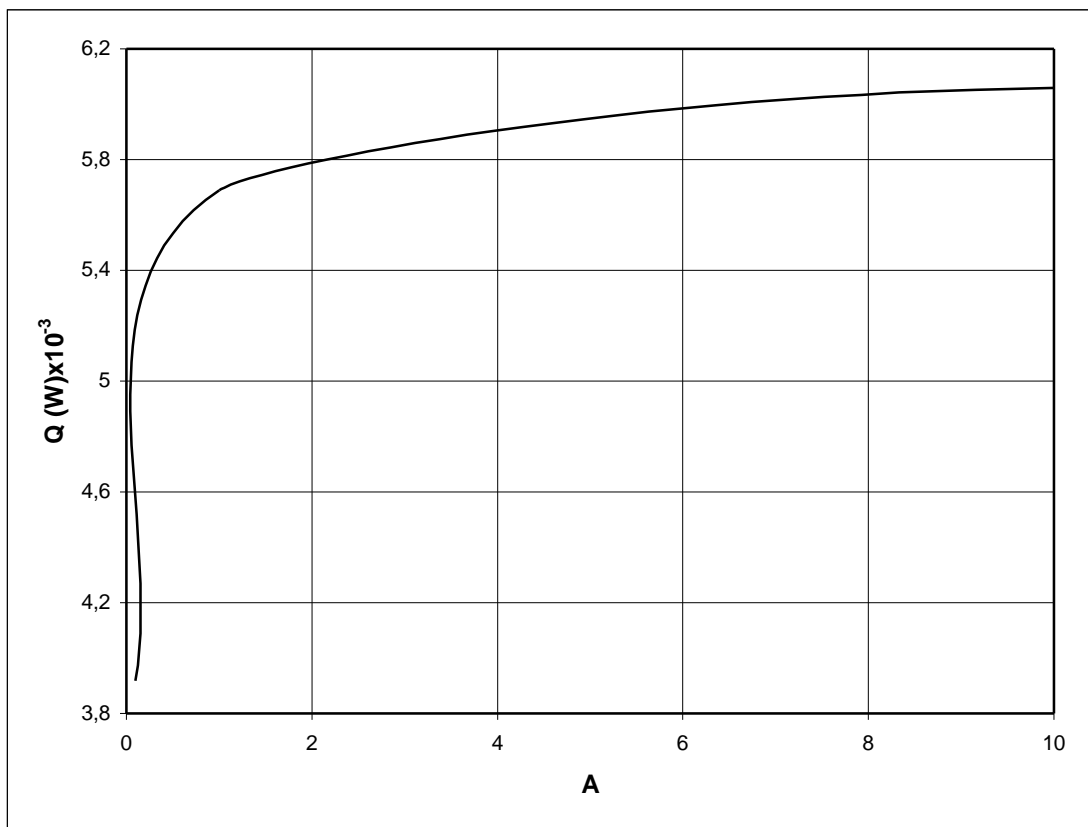


Figure F.15 Variation of heat transfer with A for $r=4.22 \times 10^{-6}$ m

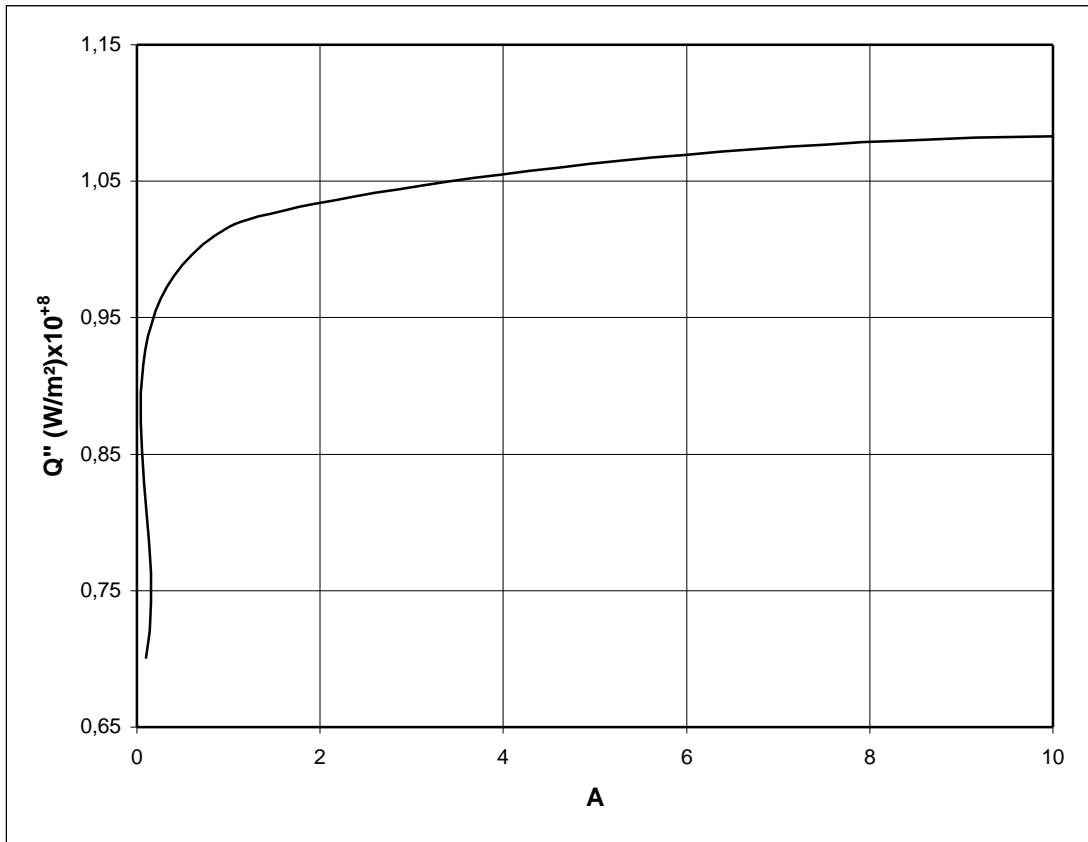


Figure F.16 Variation of heat flux with A for $r=4.22 \times 10^{-6}$ m